



ENERGY 2019

The Ninth International Conference on Smart Grids, Green Communications and
IT Energy-aware Technologies

ISBN: 978-1-61208-713-9

June 2 - 6, 2019

Athens, Greece

ENERGY 2019 Editors

Michael Negnevitsky, University of Tasmania, Australia

Vivian Sultan, California State University, Los Angeles

ENERGY 2019

Forward

The Ninth International Conference on Smart Grids, Green Communications and IT Energy-aware Technologies (ENERGY 2019), held between June 02, 2019 to June 06, 2019 - Athens, Greece, continued the event considering Green approaches for Smart Grids and IT-aware technologies. It addresses fundamentals, technologies, hardware and software needed support, and applications and challenges.

There is a perceived need for a fundamental transformation in IP communications, energy-aware technologies and the way all energy sources are integrated. This is accelerated by the complexity of smart devices, the need for special interfaces for an easy and remote access, and the new achievements in energy production. Smart Grid technologies promote ways to enhance efficiency and reliability of the electric grid, while addressing increasing demand and incorporating more renewable and distributed electricity generation. The adoption of data centers, penetration of new energy resources, large dissemination of smart sensing and control devices, including smart home, and new vehicular energy approaches demand a new position for distributed communications, energy storage, and integration of various sources of energy.

We welcomed academic, research and industry contributions. The conference had the following tracks:

- Energy efficiency planning
- Smart Grids management and control
- Trends in energy fields
- Green communications

We take here the opportunity to warmly thank all the members of the ENERGY 2019 technical program committee, as well as all the reviewers. The creation of such a high quality conference program would not have been possible without their involvement. We also kindly thank all the authors who dedicated much of their time and effort to contribute to ENERGY 2019. We truly believe that, thanks to all these efforts, the final conference program consisted of top quality contributions.

We also thank the members of the ENERGY 2019 organizing committee for their help in handling the logistics and for their work that made this professional meeting a success.

We hope that ENERGY 2019 was a successful international forum for the exchange of ideas and results between academia and industry and to promote further progress in the areas of smart grids, green communications and IT energy-aware technologies. We also hope that Athens, Greece provided a pleasant environment during the conference and everyone saved some time to enjoy the historic charm of the city.

ENERGY 2019 Chairs

ENERGY Steering Committee

Steffen Fries, Siemens, Germany

Akhtar Kalam, Victoria University, Australia
Vincenzo Gulisano, Chalmers University of Technology, Sweden
Marco Lützenberger, Technische Universität Berlin, Germany
Evangelos Pournaras, ETH Zurich, Switzerland
Angela Russo, Politecnico di Torino, Italy
Chun-Hsi Huang, University of Connecticut, USA
Mark Apperley, University of Waikato, New Zealand
Magnus Almgren, Chalmers University of Technology, Sweden

ENERGY Industry/Research Advisory Committee

Hongbo Sun, Mitsubishi Electric Research Laboratories, USA
Daisuke Mashima, Advanced Digital Sciences Center, Singapore
Sambaran Bandyopadhyay, IBM Research, India
Eric MSP Veith, OFFIS e.V. - Oldenburg, Germany
Dragan Obradovic, Siemens - Corporate Technology, Munich, Germany
Chresten Træholt, Center for Electric Power and Energy - CEE | Technical University of Denmark
- DTU, Denmark

ENERGY 2019 Committee

ENERGY Steering Committee

Steffen Fries, Siemens, Germany
Akhtar Kalam, Victoria University, Australia
Vincenzo Gulisano, Chalmers University of Technology, Sweden
Marco Lützenberger, Technische Universität Berlin, Germany
Evangelos Pournaras, ETH Zurich, Switzerland
Angela Russo, Politecnico di Torino, Italy
Chun-Hsi Huang, University of Connecticut, USA
Mark Apperley, University of Waikato, New Zealand
Magnus Almgren, Chalmers University of Technology, Sweden

ENERGY Industry/Research Advisory Committee

Hongbo Sun, Mitsubishi Electric Research Laboratories, USA
Daisuke Mashima, Advanced Digital Sciences Center, Singapore
Sambaran Bandyopadhyay, IBM Research, India
Eric MSP Veith, OFFIS e.V. - Oldenburg, Germany
Dragan Obradovic, Siemens - Corporate Technology, Munich, Germany
Chresten Træholt, Center for Electric Power and Energy - CEE | Technical University of Denmark
- DTU, Denmark

ENERGY 2019 Technical Program Committee

Cristinel Ababei, Marquette University, USA
Kouzou Abdellah, Djelfa University, Algeria
Hatim G. Abood, The University of Western Australia, Australia
A. Abu-Siada, Curtin University, Australia
Baris Aksanli, San Diego State University, USA
Kamal Al-Haddad, École de technologie supérieure (ETS), Montréal, Québec, Canada
Nizar Al-Holou, University of Detroit Mercy, USA
Ahmed Al-Salaymeh, University of Jordan, Jordan
Magnus Almgren, Chalmers University of Technology, Sweden
Mark Apperley, University of Waikato, New Zealand
Ali Arefi, Murdoch University, Australia
Sambaran Bandyopadhyay, IBM Research, India
Chakib Bekara, University of Tlemcen, Algeria
Rachid Benchrifa, Mohammed V University, Morocco
Andreas Berl, Technische Hochschule Deggendorf, Germany
Andrea Bonfiglio, University of Genoa, Italy
Massimo Brignone, University of Genoa, Italy
Concettina Buccella, University of L'Aquila, Italy

Erik Buchmann, Hochschule für Telekommunikation Leipzig (University of Applied Sciences)
Leipzig, Germany

Vito Calderaro, University of Salerno, Italy

Umit Cali, The University of North Carolina at Charlotte, USA

Davide Careglio, Universitat Politècnica de Catalunya, Spain

Sara Carcangiu, University of Cagliari, Italy

Hsi-Ya Chang, National Center for High-performance Computing, Taiwan

Antonin Chazalet, Orange, France

Ali Cheknane, Amar Telidji University of Laghouat, Algeria

Luigi Costanzo, Università degli Studi della Campania Luigi Vanvitelli, Italy

Narottam Das, University of Southern Queensland Toowoomba, Australia

Margot Deruyck, iMinds - Ghent University - INTEC - WAVES, Belgium

Vincenzo Di Dio, University of Palermo, Italy

Efrén Díez Jiménez, Universidad de Alcalá, Spain

Rekioua Djamil, University of Bejaia, Algeria

Rolf Egert, Technische Universität Darmstadt, Germany

Tullio Facchinetti, University of Pavia, Italy

Daniel Freund, Distributed Artificial Intelligence Lab (DAI-Lab), Berlin, Germany

Steffen Fries, Siemens, Germany

Rong Ge, Clemson University, USA

Joern Geisbuesch, KIT - Institute for Technical Physics (ITEP), Germany

Anandha Gopalan, Imperial College London, UK

Vincenzo Gulisano, Chalmers University of Technology, Sweden

Anwar Ul Haq, Technische Universität München (TUM), Germany

Chun-Hsi Huang, University of Connecticut, USA

Zhiyi Huang, University of Otago, New Zealand

Dan M. Ionel, University of Kentucky, USA

Philip Johnson, University of Hawaii, USA

Akhtar Kalam, Victoria University, Australia

György Kálmán, Norwegian University of Science and Technology (NTNU)/mnemonic AS,
Research Group on Critical Infrastructure Protection, Norway

Eleni Kaplani, University of East Anglia-Norwich Research Park, UK

Essam E. Khalil, Cairo University, Egypt

Tobias Küster, Technische Universität Berlin (TU Berlin), Germany

Elias Kyriakides, KIOS Research Center | University of Cyprus, Cyprus

Stephen Lee, UMass, Amherst, USA

Yiu-Wing Leung, Hong Kong Baptist University, Kowloon Tong, Hong Kong

Zhenhua Liu, Stony Brook University, USA

Abraham Lomi, National Institute of Technology, Malang, Indonesia

Marco Lützenberger, Technische Universität Berlin, Germany

Thair Mahmoud, Edith Cowan University, Australia

Apel Mahmud, Deakin University, Australia

Daisuke Mashima, Advanced Digital Sciences Center, Singapore

Rafael Mayo-García, CIEMAT, Spain

Amer Mesanovic, Siemens, Germany
Marilena Minou, Athens University of Economics & Business, Greece
Hemanta Kumar Mondal, CNRS Lab-STICC - UMR 6285 | Université Bretagne Sud (UBS), France
Hugo Morais, ISEP/IPP, Portugal
Fabio Mottola, University of Naples Federico II, Italy
Gero Mühl, Universitaet Rostock, Germany
Masayuki Murata, Osaka University Suita, Japan
Md Mustafizur Rahman, Universiti Malaysia Pahang, Malaysia
Michael Negnevitsky, University of Tasmania, Australia
Rajiv Nishtala, Barcelona Supercomputing Center, Spain
Bruce Nordman, LBNL, USA
Dragan Obradovic, Siemens - Corporate Technology, Munich, Germany
Thanasis Papaioannou, Athens University of Economics and Business, Greece
Marina Papatriantafilou, Chalmers University of Technology, Sweden
Jonathan Pastor, DAPI - IMT Atlantique, France
Massimo Poncino, Politecnico di Torino, Italy
Evangelos Pournaras, ETH Zurich, Switzerland
Manuel Prieto-Matias, Complutense University of Madrid, Spain
Renato Procopio, University of Genoa, Italy
Marco Pruckner, University of Erlangen-Nürnberg, Germany
Jan Richling, South Westphalia University of Applied Sciences, Germany
Jon Robinson, Nottingham Trent University, UK
Angela Russo, Politecnico di Torino, Italy
Mischa Schmidt, NEC Laboratories Europe, Heidelberg, Germany
Kenneth Schmitz, German Research Center for Artificial Intelligence - DFKI GmbH, Germany
Harald Schrom, Institut für Datentechnik und Kommunikationsnetze - TU Braunschweig, Germany
Pierluigi Siano, University of Salerno, Italy
Vivian Sultan, California State University, Los Angeles, USA
Hongbo Sun, Mitsubishi Electric Research Laboratories, USA
Lavinia Chiara Tagliabue, University of Brescia, Italy
Saurav Talukdar, University of Minnesota, USA
Chresten Træholt, Center for Electric Power and Energy - CEE | Technical University of Denmark - DTU, Denmark
Pietro Varilone, Università di Cassino e del Lazio Meridionale, Italy
Eric MSP Veith, OFFIS e.V. - Oldenburg, Germany
Massimo Vitelli, Università degli Studi della Campania Luigi Vanvitelli, Italy
Matthias Vodel, Technische Universitaet Chemnitz, Germany
Florian Volk, Technische Universität Darmstadt, Germany
Anke Weidlich, Albert-Ludwigs-Universität Freiburg, Germany

Copyright Information

For your reference, this is the text governing the copyright release for material published by IARIA.

The copyright release is a transfer of publication rights, which allows IARIA and its partners to drive the dissemination of the published material. This allows IARIA to give articles increased visibility via distribution, inclusion in libraries, and arrangements for submission to indexes.

I, the undersigned, declare that the article is original, and that I represent the authors of this article in the copyright release matters. If this work has been done as work-for-hire, I have obtained all necessary clearances to execute a copyright release. I hereby irrevocably transfer exclusive copyright for this material to IARIA. I give IARIA permission to reproduce the work in any media format such as, but not limited to, print, digital, or electronic. I give IARIA permission to distribute the materials without restriction to any institutions or individuals. I give IARIA permission to submit the work for inclusion in article repositories as IARIA sees fit.

I, the undersigned, declare that to the best of my knowledge, the article does not contain libelous or otherwise unlawful contents or invading the right of privacy or infringing on a proprietary right.

Following the copyright release, any circulated version of the article must bear the copyright notice and any header and footer information that IARIA applies to the published article.

IARIA grants royalty-free permission to the authors to disseminate the work, under the above provisions, for any academic, commercial, or industrial use. IARIA grants royalty-free permission to any individuals or institutions to make the article available electronically, online, or in print.

IARIA acknowledges that rights to any algorithm, process, procedure, apparatus, or articles of manufacture remain with the authors and their employers.

I, the undersigned, understand that IARIA will not be liable, in contract, tort (including, without limitation, negligence), pre-contract or other representations (other than fraudulent misrepresentations) or otherwise in connection with the publication of my work.

Exception to the above is made for work-for-hire performed while employed by the government. In that case, copyright to the material remains with the said government. The rightful owners (authors and government entity) grant unlimited and unrestricted permission to IARIA, IARIA's contractors, and IARIA's partners to further distribute the work.

Table of Contents

Integration of Wireless Sensor Networks with Building Energy Management Systems <i>Nikoleta Pontikakou, Panagiotis Trakadas, Theodore Zahariadis, Panagiotis Gonis, Stamatis Voliotis, and Dimitrios Bargiotas</i>	1
A Study of Solar Irradiance Prediction Error Impact on a Home Energy Management System <i>Mallek Mziou SALLAMI, Rim Kaddah, and Amira Ben Hamida</i>	7
Modelling Fractal-Structured Smart Microgrids: Exploring signals and protocols <i>Mark Apperley</i>	13
Is Power Outage Associated With Population Density? <i>Vivian Sultan and Brian Hilton</i>	18
Adversarial Resilience Learning — Towards Systematic Vulnerability Analysis for Large and Complex Systems <i>Lars Fischer, Jan-Menno Memmen, Eric MSP Veith, and Martin Troschel</i>	24
A Transient Classification System Implementation on an Open Source Distributed Power Quality Network <i>Charles Dickens, Anthony Christe, and Philip Johnson</i>	33
An Empirical Study of Power Characterization Approaches for Servers <i>Yewan Wang, David Nortershauser, Stephane Le Masson, and Jean-Marc Menaud</i>	38
Where Should a Utility Improve Tree Cutting to Reduce the Risk of Vegetation Coming into Contact with Power Lines? <i>Vivian Sultan and Brian Hilton</i>	44

Integration of Wireless Sensor Networks with Building Energy Management Systems

Nikoleta Pontikakou, Panagiotis Trakadas, Theodore
Zahariadis, Panagiotis Gkonis, Stamatis Voliotis
Department of Electrical Engineering
Technological Educational Institute of Sterea Ellada
Chalkida, Greece
e-mails:

{npontikakou|ptrakadas|zahariad|pgonis|svoliotis}@teiste.gr

Dimitrios Bargiotas

Department of Electrical and Computer Engineering
University of Thessaly
Volos, Greece
e-mail: bargiotas@e-ce.uth.gr

Abstract— Reducing energy consumption within buildings has been an active area of research. Energy usage both in commercial and residential buildings represents a significant portion of overall energy consumption. The viability of Wireless Sensor Network (WSN) technologies can be integrated with Building Energy Management Systems (BEMS) in order to reduce energy consumption within buildings. This paper targets the description of a generic architecture and classification of WSN-based BEMS.

Keywords - *Wireless Sensor Networks; Smart buildings; Building Energy Management Systems.*

I. INTRODUCTION

The use of electricity in commercial and residential buildings represents a significant portion of overall energy consumption. Effective energy conservation within buildings will result in a significant decrease in energy demand. This demands that customers be provided with accurate and detailed information concerning their energy usage in real time. Such information is a prerequisite for effective feedback provision as well as for enabling the deployment of remote intelligent autonomous energy control systems. Recent advances in wireless communications, low-power integrated circuits, sensor design, and energy storage technologies have enabled the effective deployment of Wireless Sensor networks (WSNs) in a range of real-world application domains [1]-[3]. WSNs can be used by environmental and event monitoring systems, such as Building Energy Management Systems (BEMS). BEMS harness WSNs to harvest detailed information concerning energy consumption within buildings, as well as the prevailing context under which such consumption occurs. BEMS are an integral part of so-called intelligent or smart buildings. In this article, a classification of the WSNs based BEMS for smart buildings is presented. In this context, the rest of this article is organized as follows: An overall presentation of WSN technology is provided in Section II, while Section III describes BEMS and a generic BEMS architecture is provided in Section IV. Then, in Sections V-VII, energy monitoring, energy feedback and control systems are presented. Finally, Section VIII list some of BEMS challenges and Section IX states the conclusions.

II. WSN TECHNOLOGY

A. Characteristic Features of WSNs

A WSN can be seen as a node network that gathers information from the surrounding environment, thus enabling interactions in predefined cases. WSNs usually include sensor nodes, actuator nodes, gateways and clients. A large number of sensor nodes are deployed randomly inside of or near the monitoring area (sensor field), form networks through self-organization. During the transmission process, the monitored data are processed and forwarded by multiple nodes to finally reach the gateway node. The cost of WSN equipment has dropped dramatically and WSN applications are gradually expanding to industrial and commercial fields.

B. Sensor Nodes

The sensor node is one of the main parts of a WSN. Hardware implementation of sensor nodes typically includes four parts: the power and power management module, a sensor, a microcontroller, and a wireless transceiver. The power module is responsible for the provision of the appropriate power (i.e., in terms of frequency and nominal voltage value) for secure and reliable operation. The sensor module is responsible for data acquisition from the surrounding environment. A sensor is in charge of collecting and transforming the signals, such as light, vibration and chemical signals, into electrical signals and then transferring them to the microcontroller. The latter receives data from the sensor and processes them according to predefined operations. The Wireless Transceiver module transmits data to other wireless nodes, mobile devices, or control centers. At this point, it should be noted that all parts of a WSN node consider the WSN node features should be of tiny size and limited power [4].

C. Topology

In general, a WSN consists of a number of sensor nodes and a gateway for the connection to the Internet. The general deployment process of a WSN can be described as follows: first, the sensor network nodes broadcast their status to the surroundings and receive the corresponding status from other nodes to detect each other. Afterwards, the sensor network nodes are organized into a connected network, according to a predefined topology. After the

establishment of the network topology, optimal paths are computed for transmitting the sensing data. The power of sensor network nodes is usually provided by batteries, in order to keep transmission distance of WSN nodes in a short range. The transmission distance can be up to 800-1000 meters in the open outdoor environment under line of sight. However, in the case of indoor environments, this distance can be significantly reduced. In such situations, the coverage of a network can be extended by the use of multi-hop transmission mode. In these cases, the sensor network nodes act both as transmitters and receivers. The source node sends data to its preferred node within its range (called parent node) based on predefined metrics. The next node, again, forwards the data to one of its nearby nodes along the path towards the gateway. The forwarding is repeated until the data arrives at the gateway, the destination. All protocols and some implementation techniques of WSNs can be adapted to the mature architecture and technologies of wireless and wired computer networks.

D. Low-cost IP interconnection technology

The choice during the design of the first sensor networks was to use private addresses to manage the sensor network nodes. Due to its relatively short length, the address was suitable for implementing in low-power embedded sensor nodes. However, the management of private addresses increased the difficulty of interaction between the sensor network nodes and the traditional IP network nodes. Therefore, there is a need to resolve the connectivity problem of WSN and IP network. As it is known, IPv4 addresses have been gradually depleted, and the new IPv6 addressing scheme is suitable for a wide range of sensor network deployment, providing each sensor node with its unique, public IPv6 address. As a result, 6LoWPAN low-power wireless technology based on IPv6 has emerged. The 6LoWPAN has generally implemented a simplified IPv6 protocol above the link layer of the IEEE 802.15.4 protocol [5]. Header compression and packet fragmentation reloading is implemented by adding an adaptation layer between the IP layer and the link layer, which is a reliable method to achieve protocol adaptation between the IPv6 network and the sensor network.

III. BUILDING ENERGY MANAGEMENT SYSTEMS

The advent of Building Management Systems (BMS) is sometimes also referred to as Building Automation Systems (BAS). Though energy control systems were becoming progressively more sophisticated, an increased awareness of the importance of consumption feedback to consumers as an instrument of affecting positive behavior change was emerging. Initial studies, mainly conducted by psychologists, demonstrated the potential of feedback to reduce wasteful energy usage and save on energy cost. Energy consumption feedback has been studied as a mechanism for affecting behavior change in energy conservation within residential buildings. In the 1990's

thermostats, many with dead zones, were harnessed extensively to control temperature within buildings; this technology was subsequently improved by using Proportional-Integral-Derivative (PID) controllers. The potential of Artificial Intelligence (AI) techniques was also considered. Environmental parameters served as input in the control of Heating Ventilation and Air-Conditioning (HVAC) systems. Due to the invisible nature of energy consumption in residential and commercial buildings, a major challenge faced by early researchers concerned the collection of real-time and detailed information on energy consumed by individual electrical devices within a building. To enable energy disaggregation at the appliance level, researchers formulated Nonintrusive Load Monitoring (NILM) or Nonintrusive Appliance Load Monitoring (NIALM). NILM enables per-appliance energy consumption by identifying changes in energy usage data, as recorded by a meter. A new generation of BEMS emerged with the introduction of WSN technologies [6]. Acquiring information on energy usage at different levels, such as appliance, building, or circuit, was made possible through the aid of WSNs. In recent years, wireless smart meters and smart plugs have been developed that can be installed inside the circuit-breaker box and on outlets close to individual appliances. Such devices integrate traditional metering systems with communication interfaces to deliver detailed information on resource consumption in real time, as well as to offer additional features, such as remote actuation. Thus, smart meters are a fundamental component of the current generation of BEMS. In addition, the concept of Internet of Things (IoT) integration in BMS is a challenging research field, as it allows the interconnection of various diverse functions in the concept of smart cities (i.e., energy demand and consumption of various components) to be integrated in order to maximize energy efficiency [7].

IV. GENERIC BEMS ARCHITECTURE

A. Key components

A generic architecture for such a BEMS is presented in Figure 1. Conceptually, it can be considered as comprising of three key components, namely Sensor Layer, Computation Layer, and Application Layer.

a) Sensor Layer

Buildings, and the electrical devices and appliances within them, are monitored by a sensor configuration that collects data on energy usage and temporal contextual environmental parameters. This information is made available to the computation layer for further data processing and analysis. The sensor layer is a physical-level configuration composed of a suite of sensor nodes deployed inside a building that periodically measure relevant phenomena and forward measurements to the computation layer for further analysis and storage [8]. This component can be seen as comprising three subcomponents:

- *energy sensing*: consists of a smart meter (sensor) deployment that monitors energy usage within and throughout a building.
- *environmental sensing*: consists of an array of sensors that collect information on prevailing environmental factors, such as luminance level, temperature, relative humidity, carbon dioxide level, and so on.
- *human sensing*: addresses the monitoring of occupant presence and behavior and the development of behavior models for a given environment.

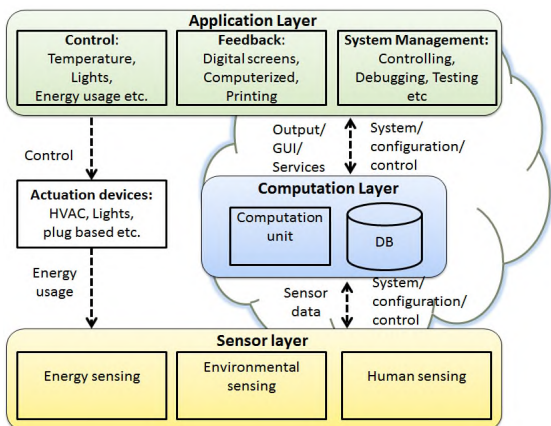


Figure 1. Architecture of BEMS.

b) *Computation Layer*

The function of the computation layer is to analyse all information collected by the sensor layer using algorithmic calculations and statistical analysis. It comprises two components:

- The *computation software* and
- The *database* that records all data, including real time and event driven, such as energy usage comparisons, and historical calculations.

c) *Application Layer*

What analysis occurs, and what tools to adopt, for example, logical reasoning, data mining, and so on, will be driven by the needs of the application layer. This layer can be further categorized into two application subcategories: appliance control and the provision of user feedback across a range of modalities. Implicit within this layer is a management component allowing for system testing. BEMS functionality is realized in the application layer. Two categories of functionality may be identified:

- *Energy feedback* systems provide building services, in inhabitants, and any other interested party with information concerning energy consumption. Such systems can present both real-time and historical energy usage information. Ambient displays, mobile devices, or Web portals may be harnessed for visualisation purposes.
- *Energy control* systems control devices and appliances within the building in accordance with policies and preferences defined by consumers. Preferences may be defined using intuitive user interfaces; likewise, control can be exercised via a range of digital displays.

Computational intelligence techniques may be harnessed for enabling autonomous behavior.

In each of the two categories, an interface and control component for system management activities is necessary.

B. *Cloud-enabled BEMS*

Local computational capabilities may prove insufficient to represent and manage data of BEMS using WSN. One possible solution may involve the harnessing and integration of cloud computing with BEMS [9]. They will initially be realised as cloud services in the commercial context. A service-oriented paradigm may evolve where a wide range of services is hosted on the cloud, but consumers access them on a subscription basis, as their needs dictate. For example, domestic consumers may be driven by a simple need to save money.

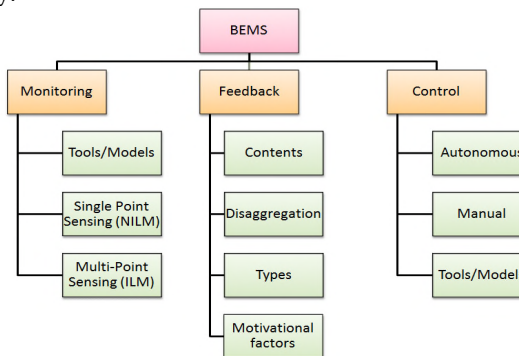


Figure 2. Classification of BEMS

In contrast, industrial and business users may perceive cloud services as an appropriate solution for legislative adherence, insurance provision, as well as enabling contractual fulfilment. BEMS can be classified in three categories, namely monitoring, feedback, and control (see Figure 2) [6].

V. ENERGY MONITORING TOOLS AND TECHNIQUES

A. *Approaches*

Traditionally, meters installed in buildings between the baseline and the external power line fail to provide sufficiently detailed data on energy usage, nor do they offer a communication interface by which one could obtain such data in real time. Research has proposed WSN-based solutions that include energy usage monitoring using smart meters/outlets and distributed approaches for appliance activity monitoring. These are advanced energy monitoring systems that measure energy consumption and provide communication interfaces by which to transmit data in real time. There are two major approaches being harnessed to monitor energy usage and in the literature are referred to as single-point monitoring and distributed monitoring:

- *single-point monitoring (NILM)*: they use a single metering device installed at the fuse box to monitor the entire building energy usage. To identify energy consumption at the appliance level, the data is then analyzed using estimation algorithms to identify the

different load usage patterns generated by various appliances when in use.

- distributed monitoring (ILM): this approach is used for monitoring appliance-level energy consumption. It harnesses either smart plugs/outlets or various types of sensors for each individual appliance.

B. Single-Point Monitoring (NILM)

A smart clip-on meter is installed at the main electrical panel outside the building and it meters the entire building energy usage in real time and reports this to a PC via a gateway. This data is sometimes referred to as the aggregated energy usage measurement of a building. The next step is to disaggregate appliance-specific information from this measurement. Appliance signatures are created by turning appliances on/off during the training phase and appropriately annotating the dataset. These signatures are then used by machine learning algorithms to disaggregate energy data. Appliances that have different energy usage patterns (or signatures) are easily identifiable but those with similar patterns are harder to distinguish. Some examples of smart metering and WSN-based systems are the following:

a) Direct Energy Monitoring

Direct energy monitoring systems require an in-line installation of the metering component to measure energy usage. Most of the systems surveyed provide broadly similar functionality, however, each of them uses varying sensor types and is designed using different hardware/software techniques, such as circuit-panel meter and energy consumption display.

b) Indirect Energy Monitoring.

Instead of an in-line installation of a clip-on meter, this method uses a plugin sensor to capture electrical noise generated on power lines by the running of appliances. This approach is used to capture appliance activity information. Electrical Noise Sensing is an approach to identifying appliance status is pre-sented. The system uses a single plugin sensor to detect electrical noise on power lines created by electrical appliances when they are switched on. Different appliances generate different electrical noise signals. This technique computationally expensive and also requires a complex and time-consuming training process compared to other NILM techniques.

C. Distributed Monitoring (ILM)

In the case of distributed sensing, each appliance in a monitored environment typically has one or more sensors allocated to it. These sensors measure a range of activities from energy usage to appliance state activity. Distributed sensing can be considered as the most accurate approach for appliance-level monitoring but it is very expensive. This type of sensing consists of using either smart meters/outlets to measure appliance level energy usage or various types of sensors to infer appliance-specific activities [10].

a) Direct Energy Monitoring

The installation of smart metering systems usually occurs inside the circuit breaker box and, due to safety concerns,

may require an electrician for installation. To ease installation, a range of smart outlets have been developed and used. Smart outlets are installed between AC plugs of appliances and the standard wall power sockets. Using a gateway, the data is acquired by a PC and is then visualized on a variety of media. Such systems are straightforward, provide accurate appliance-level metering, but provide limited functionality regarding data aggregation, analysis, and visualization.

b) Indirect Energy Monitoring

While smart power outlets and meters are appropriate for appliances that provide standard AC plugs, they cannot be easily installed to operate with major energy consuming devices, such as HVAC systems, ceiling lights, and electric boilers because these devices are typically connected directly to the main power line. To address such issues, various types of sensors for indirect energy usage monitoring have been used. Most of these techniques are used to obtain fine-grained appliance activity information within buildings and differ from each other on the basis of the hardware (sensor nodes) they have adopted and software implementation. The main approaches follow:

- *Electromagnetic Sensing.*

It is an indirect and detailed power monitoring system in which wireless sensors are used to report appliance state information. The system provides detailed feedback on appliance-level electricity consumption using a collaboration between sensor nodes placed in close proximity to appliances and the main power meter that reports overall electricity usage. It uses three types of sensors: magnetic, sound, and light sensors. Magnetic sensors, placed near an appliance or a power line, can sense magnetic field variations when the current flows in the power line.

- *Environmental Sensing*

It is an environmental sensing approach that harnesses various types of sensors to infer appliance state activities based on measured environmental parameters. A sound sensor records the sounds produced by appliances and a light sensor obtains information regarding light status when switched on/off. All sensors transmit their data to a PC that processes the data and visualizes power usage per appliance. In order to automate the NILM training process, a temporary deployment of wireless sensors to each appliance is done and then appliance activity information is inferred based on the data reported by these sensors. Systems have been developed to reduce the energy consumption of meeting rooms by identifying waste. Placing various types of sensors close to appliances increases overall accuracy level but also increases system complexity. Such approaches demand more time for deployment while increasing installation and maintenance cost as compared to other indirect sensing techniques [4].

- *Thermal Sensing*

Systems that disaggregate total power usage into appliance-level consumption by observing the heat patterns generated by appliances have been developed and used. A power meter to obtain overall energy usage and one thermal

camera to observe heat patterns on the appliance surface have been also used.

D. Monitoring Subsystem

The monitoring subsystem, is composed of a number of electricity sensors, measuring the power consumption of each single electrical appliance in the building. In addition to electricity sensors, the monitoring subsystem also includes environmental sensors for monitoring parameters, such as temperature, light intensity, human presence, and so on. Such information will be used by the energy manager application to minimize energy wastes, according to energy conservation strategies defined by the user(s). Data collected by both electricity and environmental sensors are communicated wirelessly to a base station located on the same floor (there is at least one base station per floor) and, then, conveyed to a central server. The communication between base stations and the central server typically occurs through a wired LAN (e.g., Ethernet) [4]. The central server has the responsibility to collect and process data. It provides users with real-time and/or periodic reports on energy consumption and costs. The server also sends alert messages to notify of specific events (e.g., a device being in active mode when it is supposed to be in inactive mode) suggesting possible actions to save energy.

VI. ENERGY FEEDBACK SYSTEMS

The content of feedback given to users may contain different reporting units, such as energy consumption and cost, appliance-state information, or environmental impacts (for example, carbon emissions). These units, when displayed, have different impacts on motivating users to reduce energy consumption. A classification of these systems follows:

- *Energy Consumption and Cost*

Usually, feedback systems provide information on energy consumptions and the cost of energy used to help users make financial savings.

- *Appliance-State Information*

Some feedback systems provide information on appliance state, whether active or otherwise. With this information, consumers can understand where energy is being wasted inside a building and, as a result, they can turn appliances off if they are not needed. Systems with high accuracy use either smart outlets or various types of wireless sensors to obtain appliance-state information.

- *Environmental Impacts*

One of the motivational factors of energy conservation is to lower carbon emissions to further the goal of a greener environment.

- *Feedback Disaggregation*

Providing disaggregated feedback results in more energy conservation. There are five major types of disaggregation to help users understand their energy usage in detail: space-specific, user-specific, appliance-specific, time-specific, and service-specific. Space-specific disaggregation is achieved

by dividing a building into smaller areas. Division can be based on rooms, circuit breakers, or appliance types. Appliance-Specific disaggregated information is considered as highly enriched feedback targeting energy estimation at appliance level. Time-Specific Disaggregation, feedback on different time-scales, past, present, and future is given to help users know when and over what timescale energy was consumed and wasted. User-Specific Disaggregation or personalized feedback can help individuals in a building to keep track of their own energy usage. Service-Specific Disaggregation supports energy conservation based upon a broader perspective through the possible reconfigurations of services.

- *Feedback Presentation*

The information on energy consumption should be displayed using a medium that can capture attention, such as digital screens, smart TVs, mobile phones, and in written form; it should also be delivered in a way that is inter-active using graphs, figures, and easily understandable numerical data is preferred.

- *Motivational Factors*

Apart from motivational factors described in the previous sections, there are several other approaches to motivation, such as using comparisons, goal settings, media campaigns, and rewards has led to reduced energy usage.

VII. ENERGY CONTROL SYSTEMS

A. Architecture

A variety of building automation and control systems use WSNs to conserve energy. These systems usually adopt a three-tier architecture:

- a network of sensor nodes, that report energy usage, occupant behaviour, and environmental conditions;
- a central control server; and
- a set of intelligent plugs and relays that control electric appliances within a building.

The first layer provides information to the control server. The control server performs computation on information received from the sensors as well as information obtained from other sources, such as weather conditions/forecast using the Internet. The data is then harnessed by intelligent algorithms to control energy by switching off electric appliances, turning off lights, reducing HVAC parameters, and so forth. Based on the techniques and implementation details, the energy control systems consist of three major categories: autonomous energy control systems, manual energy control systems, and energy forecast/modelling systems [10].

B. Autonomous Energy Control

Autonomous energy control systems, once configured, can reduce energy consumption within a building by controlling electrical appliances, such as HVAC and lights

without requiring continuous user interaction. Such systems primarily target HVAC and lighting systems that consume a significant portion of overall energy consumption within commercial buildings. A combination of different sensor nodes, such as temperature, PIR (Passive Infrared for occupancy detection), ambient light, and sound sensors inform the control server about the monitored environment. The control server can then make decisions and send signals to actuators. The overall goal is to switch off (or lower) HVAC, lights, and other loads in the building when not needed.

C. Manual Energy Control

Manual energy control systems provide user functionalities to monitor and control electric appliances remotely. BEMS provide GUIs that visualize energy consumption per appliance (mostly HVAC and lights) and provides control options for these devices. Manual energy control systems use smart outlets for plug-based appliances and standard actuation devices for HVAC and ceiling-light control.

D. Energy Modeling Systems

The use of software tools for energy management within buildings has become quite popular. These tools enable users to estimate the energy consumption of buildings as well as provide energy control features. Energy modelling tools offer a number of functionalities regarding energy consumption auditing, prediction, and design and evaluation of energy control systems. Such tools are helpful in motivating users to improve building energy consumption by enabling them to understand the spectrum of energy usage within buildings, especially when there are limited resources and many technical challenges to face.

VIII. CHALLENGES OF MANAGING BUILDING ENERGY INFRASTRUCTURE

In building energy management, a number of challenges can be identified:

- Installing resource monitoring can prove demanding in terms of the required technical knowledge and associated deployment time, both for single-sensor and distributed approaches.
- Monitoring energy consumption demands sensing the environment as to patterns of movement, potential activities within, and occupancy levels.
- Engineering and sustaining behavior change is fundamental and core to the success of building energy management systems. User feedback is the instrument through which behaviour change may be achieved.
- Building energy management systems is extremely heterogeneous and there is a need for the development

tools to support the rapid prototyping of standards-compliant BEMS.

IX. CONCLUSIONS AND FUTURE WORK

With increasing demand and costs in energy production and limited supply of energy resources, energy conservation has emerged as a critical environmental issue. Much of this attention has been directed to the use of energy in the buildings, as energy consumption in commercial and residential buildings, and there is a need to examine ways in which energy consumption may be reduced.

This article presents energy monitoring, feedback, and control strategies aimed at energy conservation within the built environment. Also, a generic architecture for BEMS incorporating WSNs has been given to achieve such a solution. Finally, a classification of BEMS has also been presented.

Future work includes the implementation of the proposed architecture and its extended testing and comparison with existing architectures and approaches.

REFERENCES

- [1] M. Alahmad, P. Wheeler, A. Schwer, J. Eiden, and A. Brumbaugh, "A comparative study of three feedback devices for residential real-time energy monitoring", *IEEE Trans. On Industr. Electron.*, issue 59, no. 4, 2011, pp. 2002–2013.
- [2] X. Chen, T. Wei, and S. Hu, "Uncertainty-aware household appliance scheduling considering dynamic electricity pricing in smart home", *IEEE Trans. on Smart Grid*, issue 4, no. 2, 2013, pp. 932–941.
- [3] S. Park, H. Kim, H. Moon, J. Heo, and S. Yoon, "Concurrent simulation platform for energy-aware smart metering systems", *IEEE Trans. On Consumer Electron.* issue 56, no. 3, 2010, pp. 1918–1926.
- [4] L-W Yeh, Y-C Wang, and Y-C Tseng, "iPower: an energy conservation system for intelligent buildings by wireless sensor networks", 2009, White Paper, available at <http://citeseerx.ist.psu.edu/viewdoc/download?doi=10.1.1.470.9793&rep=rep1&type=pdf> [retrieved: March, 2019]
- [5] F. Corucci, G. Anastasi, and F. Marcelloni, "A wsn-based testbed for energy efficiency in buildings", *Proceedings of the IEEE Symposium on Computers and Communications*, 2011 (ISCC'11), pp. 990–993.
- [6] J.-J. Chang, P.-C. Hsiu, and K. Tei-Wei, "Search-oriented deployment strategies for wireless sensor networks", *Proceedings of the 10th IEEE International Symposium on Object and Component-Oriented Real-Time Distributed Computing*, 2007 (ISORC'07), pp. 164–171.
- [7] D. Minoli, K. Sohrawy and B. Occhiogrosso, "IoT considerations, requirements, and architectures for smart buildings—energy optimization and next-generation building management systems, *IEEE Internet of Things Journal*, vol. 4, no. 1, 2017.
- [8] A. H. Kazmi, M. J. O' Grady, D. T. Delaney, A. G. Ruzzelli and G. M. P. O' Hare, "A review of wireless-sensor-network-enabled building energy management systems", *ACM Transactions on Sensor Networks (TOSN)*, vol. 10, Issue 4, June 2014, Article No. 66
- [9] W. Kurschl and W. Beer, "Combining cloud computing and wireless sensor networks", *Proceedings of the 11th International Conference on Information Integration and Web-based Applications and Services*, 2009 (iiWAS'09), ACM Press, New York, pp. 512–518.
- [10] A. Marchiori and Q. Han, "Distributed wireless control for building energy management", in *Proceedings of the 2nd ACM Workshop on Embedded Sensing Systems for Energy-Efficiency in Building*, 2010 (BuildSys'10), ACM Press, New York, pp. 37–42.

A Study of Solar Irradiance Prediction Error Impact on a Home Energy Management System

Mallek Sallami Mziou
IRT SystemX
Palaiseau, France
e-mail: mallek.mziou-sallami@irt-systemx.fr

Rim Kaddah
IRT SystemX
Palaiseau, France
e-mail: rim.kaddah@irt-systemx.fr

Amira Ben Hamida
IRT SystemX
Palaiseau, France
e-mail: amira.benhamida@irt-systemx.fr

Abstract— Nowadays, Energy Management Systems (EMS) are accessible for homes and buildings to optimize energy consumption especially when solar panels and batteries are installed. The intelligence of existing systems is often based on environmental or exogenous information like the weather, energy prices, and endogenous information like user consumption behavior and activity. The solutions aim to adapt a consumption profile to the produced energy in order to reduce costs. In the case of a perfect prediction of all variables, system performance can be controlled. In this article, we study the impact of generation prediction error on the daily energy cost. For this, we consider the energy management system as a black-box and we simulate multiple scenarios with different prediction errors using the quasi-random Monte Carlo method. We observe the global sensitivity of the system by measuring the Sobol indices in order to identify errors that impact more the daily energy cost. The analyses are based on French consumption data and on irradiance data for Carpentras, France. Results show that findings are aligned with battery charge and discharge strategies.

Keywords— home energy optimization; renewable energies; irradiance prediction; sensitivity study; Sobol indices.

I. INTRODUCTION

With the current environmental issues, several solar energy-based technologies have been proposed as a partial solution to reach environmental goals. In the context of smart homes, the benefit of using green energy can be both environmental and economic. However, due to the solar resource high variability and depending on the energy purchase and selling schemes, forecasting algorithms can be important to better plan with respect to incoming solar production. Using forecasting information, flexible energy devices functioning can be optimized with respect to local generation and by taking into consideration the wear of the equipment. So, a measure of performance is required. Indeed, a better understanding of uncertainty in the netload (consumption – generation) allows to better maintain grid stability and develop adequate real-time control mechanisms. This can have the positive effect of keeping down the costs.

Furthermore, the topic of coping with uncertainty for complex systems is not new [1]. In addition, researchers have developed systems to simulate buildings thermal and energy behavior as black-box functions including many parameters. Due to the complexity of buildings energy

model, only few important parameters are taken into account.

In this paper, we study the impact of forecasting errors on the total daily system cost. For this, we analyze the sensitivity of irradiance prediction errors on this total cost.

To perform a Sensitivity Analysis (SA), several approaches and categorization were proposed in the literature. According to [2], SA methods may be classified into three approaches: the mathematical approach, the statistical approach and graphical assessment. The major difference between these methods relates to the number of input parameters. For instance, in the statistical sensitivity analysis, a large enough number of inputs has to be (randomly) generated.

Heiselberg et al. [3] proposed to group Sensitivity Analysis methods into three classes, which are: the local sensitivity methods, the global sensitivity methods, and the screening methods. In the local sensitivity methods, one can study the variation of system output under the variation of one parameter. In global methods, the sensitivity to one input is computed by varying simultaneously many other inputs (i.e., input is represented by a vector). Screening methods compute the sensitivity indices as an average of derivative with respect to the different inputs. In the context of the building energy models, the choice of the most suitable SA method depends on the assumptions one can make on the model output and mainly on the linearity of the function linking inputs to the output.

A similar SA analysis has been conducted by authors in [4]. The authors present a performance comparison of sensitivity analysis methods for building energy model in terms of time and computation. However, the interpretability of the sensitivity indices is lacking. In addition, their analysis is solely related to physical endogenous variables of the house and does not take into account exogenous variables that may affect energy management system decisions.

In this work, we focus on a global SA for the assessment of the Energy-Efficient Smart Home solutions. To conduct this analysis, we use a hybrid modular simulator separating the user input, optimization module and physical simulation module. The cited components are connected thanks to a loosely-coupled architecture that enables communication exchanges.

For the SA analysis, we use the Sobol method [5] [6] for evaluating the system's behavior by performing a functional

analysis of the variance (ANOVA). To generate the scenarios to be evaluated, many strategies were proposed like Sobol sequence [6], Fast method [7], etc. It is also possible to generate a sequence of randomly distributed points of inputs using the Monte Carlo method. In practice, it is common to substitute random sequences with low discrepancy sequences to improve the efficiency of the estimators. This method is known as the quasi-Monte Carlo method. It is less expensive than Monte Carlo, but no evaluation of the error is made. The third one is quasi-Monte Carlo randomized (intermediate cost between the two previous methods and evaluation of the error). In this study, we use the Saltelli's sampling scheme, which is based on quasi-random Monte Carlo [12].

The remainder of this paper is structured as follows: in Section II, we describe our system: the software system architecture and simulation modules. We also describe the home energy model with a specific highlight on the optimization and the sensitivity analysis procedure considered. In Section III, we present the sensitivity study results and analyze the correlation between the daily total cost and the forecast error. Finally, we conclude in Section IV.

II. SYSTEM

We aim at building a system capable of analyzing the impact of prediction errors on an energy management system. In particular, we are interested in studying the impact of irradiance prediction errors on household electricity bills. We focus on a residential house equipped with solar panels and a storage device (see Figure 1.). This house can have varying buying and selling prices.

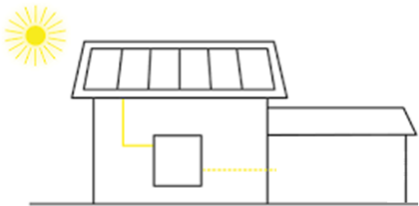


Figure 1. Smart Home with solar panels and a storage device

A. Smart Home architecture

To assess the impact on a realistic house, we build a user-friendly Smart Home simulator. It is designed as a modular platform: each component of the platform represents a different function and can be replaced and/or developed independently. It contains three main components:

1. *The User Interface (UI) component*: allows the user to enter all the required inputs and initiate the simulation. It helps to select the equipment of the Smart Home. Finally, the UI renders the results of the study in a summarized report.
2. *The Optimization component*: calculates and finds the best planning for controllable devices in the Smart Home taking into account the constraints of electric

equipment, buying and selling price and local generation of renewables.

3. *The Simulation component*: simulates the physical response of the house taking into account the equipment used and the planning generated by the optimization component. Our model is built using Phisim library [8].

To ensure the communication, we implement messaging between each of the previously mentioned components. For this, we use the Websocket technology and nodejs language. In Figure 2. , we present the platform including all the components. Grey boxes represent different distant machines. In our analysis, the user is an automated script that launches scenarios corresponding to the conducted sensitivity analysis.

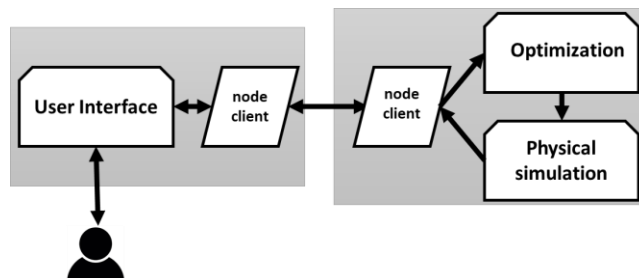


Figure 2. Smart Home simulator structure

B. Context and assumptions

We consider an energy management system that works as follows: each day, the system produces a charge and discharge planning for each hour of the next day. This case allows to decide energy trading decisions on day-ahead market coupled with having the possibility to sell at a feed-in tariffs. In this paper, we do not consider intra-day control mechanisms but we aim at understanding the uncertainty that can occur when we are planning ahead of time.

The energy management system decides to auto-consume or sell the energy produced by the solar panels. This is done based on a house consumption and energy production forecast. The system does not change the house consumption habits (no demand management is considered for our analysis). In addition, the use of battery is restricted to fulfilling house consumption needs (i.e., the energy stored in the battery cannot be sold to the grid).

C. Optimization model

Based on solar irradiance forecasts, the system solves a cost minimization problem formalized as a Mixed Integer Linear Problem (MILP):

$$\min \sum_{h=1..24} (Q_h P_{buy}(h) - p_h P(h) P_{sell}(h)) \quad (1a)$$

Such that:

$$Q_h = Y(h) + B_h - (1 - p_h) P(h) \quad (1b)$$

$$p_h \in [0, 1] \quad (1c)$$

$$Q_h \geq 0 \quad (1d)$$

$$B_h \in [-B_{maxDischarge}, B_{maxCharge}] \quad (1e)$$

where h is an hour of a day ($h=1,\dots,24$), Q_h is the amount of energy bought at hour h at the price $P_{\text{buy}}(h)$, p_h is the fraction of the power produced $P(h)$ by solar panels at hour h . This power can be sold at the price $P_{\text{sell}}(h)$. $Y(h)$ denotes the consumption forecast at hour h . The battery charge or discharge rate at hour h is denoted by B_h . It takes values between a maximum discharge rate $-B_{\text{maxDischarge}}$ and a maximum charge rate $B_{\text{maxCharge}}$. The evolution of the energy content of the battery E_h at hour h is given by:

$$E_h = \begin{cases} E_{h-1} + \eta B_h & \text{if } B_h \geq 0 \\ E_{h-1} - B_h & \text{Otherwise} \end{cases} \quad (2)$$

This energy content is a positive value smaller than the considered battery capacity. η represents the battery charging efficiency.

The optimization system is linear. To make a realistic assessment of the house response, we run the optimized planning in a physical simulator, which tries to imitate the real energetic behavior using Phisim library [8].

D. Sensitivity analysis model

There are many approaches to perform sensitivity analysis. Since we do not want any restriction on the energy management system model, we use a black-box method consisting in running simulations and observing the effect on the output.

In addition to the nature of the analysis technique, the choice of the method also depends on the variables dependencies. We can study the impact of variables separately. This is called a local sensitivity analysis. Or, we can analyze the impact by varying variables simultaneously. This is called a global sensitivity analysis. In our case, since we are interested in analyzing the impact of solar generation on costs, variables are naturally related. Indeed, we can expect three main causes of differences between predicted and real irradiance, namely a shift with respect to prediction, a change in the amplitude on the whole irradiance curve or unexpected local (hourly) changes (e.g., caused by clouds). For this reason, we argue that a global analysis method is more appropriate.

The global sensitivity is often measured by a numeric value called the global sensitivity index. This index can be of three orders (see Figure 3. for illustration):

- **First-order index:** measures the contribution of a single model input (alone) to the output variance.
- **Second-order index:** measures the contribution of the interaction of two model inputs to the output variance.
- **Total-order index:** measures the contribution to the output variance of a model input, including both its first-order effects (the input varying alone) and all higher-order interactions.

Suppose a model denoted by G and its d input variables denoted by X_1, X_2, \dots, X_d . The output Y can be described by:

$$Y = G(X_1, X_2, \dots, X_d) \quad (3)$$

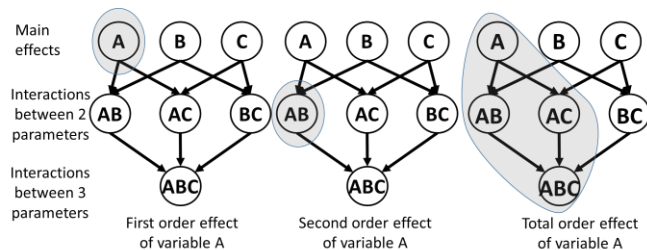


Figure 3. Different orders of sensitivity indices

To estimate the sensitivity indices, several methods exist in the literature. We compute sensitivity indices obtained through a variance decomposition of G (see [9] for details). They satisfy:

$$1 = \sum_{i=1..d} SI_i + \sum_{i<j} SI_{i,j} + \dots + SI_{1,2,\dots,d} \quad (4)$$

where SI_i is the principal (First order) sensitivity index of variable X_i , $SI_{i,j}$ is the second order index of variables X_i and X_j . The total sensitivity indices are defined based on the first order indices with these equations:

$$SI_i = \text{Var}(E(Y/X_i)) / \text{Var}(Y) \quad (5)$$

$$SI_i^T = \sum_{I \subset \{1, \dots, d\}, i \in I} SI_I \quad (6)$$

where SI_i^T measures the contribution of X_i to the output variance including the variance caused by its interactions with the other input variables. Estimating these indices can be costly in time and computation [10] [11]. In this paper, we use the method described in [12]. It is based on the Saltelli's sampling scheme, which is based on quasi-random Monte Carlo.

III. APPLICATION

In this section, we propose to conduct the sensitivity analysis on the proposed home energy management system. In our model, the intelligence of the smart home management relies on the optimization results. The performance of these results depends on the accuracy of solar irradiation prediction. However, there is always a difference between the predicted and the real irradiation.

A. Objectives

The aim of this work is to take advantage of the knowledge of the energy management system strategy in order to assess the interpretability of the sensitivity analysis results. For this, we assume that prediction error can occur at any of the 24 hours and we measure the impact of the prediction error on the total cost at the end of the day. Since, the optimization controls the battery charge and discharge, we include the electric storage capacity as an additional parameter that may impact sensitivity. Therefore, different sizes of the battery and prediction error have to be studied.

B. Model simplification

Simulator inputs can be grouped into three categories:

- Installed equipment in the house, with their characteristics and limitations (electric power, flexibility, etc.).

- The forecasted environmental and market variables: temperature, irradiance, wind speed, electricity buying prices, electricity selling prices.
- The occupation scenario of the different equipment based on user activity, or an expected behavior of consumption devices.

Conducting sensitivity analysis of all these variables can be very costly in time and is not in the scope of the present paper. In order to reduce the complexity of our system, we fix the parameters representing hourly electricity prices and energy consumption profile.

To select our model input for the house consumption, we use the results of the analysis in [13], which identifies four typical consumption profiles for houses in France represented by four periods: summer week, summer weekend, winter week and winter weekend. This is built based on consumption data collected from 149 houses and 36 multiple-unit dwellings of different characteristics in 2010. Since we are interested in studying solar generation, we consider the summer profile of a weekday.

To ease the interpretation of the sensitivity analysis results, we use simple pricing models for energy purchase and selling. Indeed, we consider a fixed buying price at 0.2977€/kWh and a selling price at 0.1231€/kWh. This pricing scheme is very similar to the actual German pricing for feed-in-tariff and energy purchase (selling price lower than the buying price). It incentivizes to auto-consume PhotoVoltaic (PV) power. Average solar irradiance is calculated using data from Carpentras station (France) for 2011 to 2013 during summer. We use average generation values of a solar panel with a performance ratio of 15%.

The fixed daily scenario considered with respect to energy price, consumption and generation profiles, is represented in Figure 4.

We consider four classes for battery capacity (kWh):

- First class: ranges from 5 to 8,
- Second class: ranges from 9 to 12,
- Third class: ranges from 15 to 20,
- Fourth class: ranges from 30 to 40.

First and second class correspond to battery capacities that are lower than 12933Wh (the total consumption after 4pm that cannot be satisfied by the mean predicted PV generation). Third and fourth classes correspond to batteries larger than the needed power storage.

In this study, we use the Saltelli's sampling scheme to generate the scenarios for irradiance variables and battery capacity. In order to validate our observations, we conduct the study also by shifting the generation curve to the left (i.e., the generation peak is earlier) and to the right (i.e., the generation peak is later).

C. Results and interpretations

To analyze the sensitivity of the model with respect to irradiance and battery capacity, a $N(2d+2)$ sample matrix is generated where d is the number of parameters (related with hours and capacity) and N is a number of scenarios (i.e. each row of the matrix is a sample vector). Since irradiance is very close to zero during night hours, we only consider the irradiance parameters from 5am.

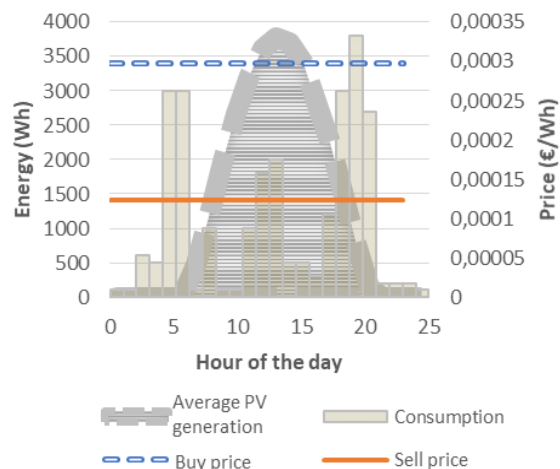


Figure 4. Power and prices profiles for each hour of the day

7pm. This will make the number of parameters describing irradiance equal to 15. With the battery capacity, the total number of inputs for our sensitivity analysis will equal 16. If we choose to set N equal to 1000 and the number of model inputs d is 16, we need to run the model on a 34000 sample matrix. Then, we can estimate the sensitivity indices based on the outputs of all run scenarios.

Results are shown in Tables I and II for first order and second order indices, respectively. Indices are highlighted with more intensified color when the value of the index is higher. The values in Table I are very similar to those of first order indices. This can be checked since first order indices sum to 1 for each row of the table. This observation suggests that there is little interaction between variables in this case. In Table I, in addition to testing for the different capacity classes, we also test cases where we shift left or right the generation curve for some hours with respect to Figure 4 (a.k.a. "No change" case) in order to have an earlier or later generation peak respectively. Table II only shows results for the "No change" case and illustrates the effect of pure interaction between any pair of input variables.

Looking at first order indices and for the different classes of battery capacities, we notice a change in the impact of battery capacity variable. Indeed, if we compute the positive netload at the end of the day (since we know the optimization strategy in this case), this will give us the battery capacity required and used to the fullest. These values are for each of the shifting cases:

- Left shift of 2: 17479.5 Wh
- Left shift of 1: 15479.5 Wh
- No change: 12932.9 Wh
- Right shift of 1: 9142.7 Wh
- Right shift of 2: 5346.8 Wh

We can see that, depending on the capacity range and how it compares to previously presented values, the impact of the capacity value changes drastically. This can be explained by the usage of the whole capacity when capacity is lower than the needed usage of a specific case: capacity variation has an important effect on the total cost since it reflects how much energy can be actually stored.

TABLE I. TOTAL ORDER SENSITIVITY INDICES

Changes in average PV generation (in hours)	Capacity range (Wh)	5am	6am	7am	8am	9am	10am	11am	12pm	1pm	2pm	3pm	4pm	5pm	6pm	7pm	capacity
Left shift of 2	5000 to 8000	0.0361	0.0172	0.0724	0.0434	0.0548	0.0695	0.0591	0.0488	0.0341	0.0228	0.0097	0.0147	0.0005	0.0000	0.0000	0.5495
Left shift of 2	9000 to 12000	0.0277	0.0725	0.1332	0.0334	0.0422	0.0468	0.0465	0.0376	0.0263	0.0175	0.0075	0.0113	0.0004	0.0000	0.0000	0.5129
Left shift of 2	15000 to 20000	0.0278	0.0730	0.1337	0.1955	0.1875	0.0460	0.0466	0.0377	0.0263	0.0176	0.0075	0.0114	0.0004	0.0000	0.0000	0.2126
Left shift of 2	30000 to 40000	0.0321	0.0842	0.1542	0.2283	0.2857	0.0530	0.0526	0.0435	0.0304	0.0203	0.0087	0.0131	0.0004	0.0000	0.0000	0.0000
Left shift of 1	5000 to 8000	0.0048	0.0303	0.0823	0.0258	0.0379	0.0477	0.0539	0.0496	0.0429	0.0313	0.0188	0.0085	0.0131	0.0004	0.0000	0.5644
Left shift of 1	9000 to 12000	0.0049	0.0319	0.0839	0.0472	0.0388	0.0486	0.0549	0.0508	0.0437	0.0319	0.0192	0.0087	0.0134	0.0004	0.0000	0.5381
Left shift of 1	15000 to 20000	0.0083	0.0416	0.1095	0.2008	0.2934	0.0634	0.0716	0.0660	0.0571	0.0418	0.0250	0.0113	0.0174	0.0005	0.0000	0.0024
Left shift of 1	30000 to 40000	0.0093	0.0416	0.1094	0.2005	0.2945	0.0633	0.0716	0.0660	0.0570	0.0418	0.0250	0.0113	0.0174	0.0005	0.0000	0.0000
No change	5000 to 8000	0.0000	0.0047	0.0311	0.0149	0.0257	0.0376	0.0492	0.0516	0.0498	0.0449	0.0295	0.0188	0.0508	0.0128	0.0004	0.5962
No change	9000 to 12000	0.0000	0.0063	0.0360	0.0520	0.0521	0.1155	0.0554	0.0681	0.0590	0.0505	0.0332	0.0211	0.0589	0.0144	0.0004	0.3897
No change	15000 to 20000	0.0000	0.0060	0.0394	0.1037	0.1903	0.2783	0.0623	0.0654	0.0630	0.0569	0.0373	0.0238	0.0641	0.0162	0.0005	0.0000
No change	30000 to 40000	0.0000	0.0060	0.0394	0.1037	0.1903	0.2783	0.0623	0.0654	0.0630	0.0569	0.0373	0.0238	0.0641	0.0162	0.0005	0.0000
Right shift of 1	5000 to 8000	0.0000	0.0000	0.0048	0.0306	0.0152	0.0561	0.0396	0.0481	0.0528	0.0531	0.0431	0.0300	0.1137	0.0502	0.0129	0.4543
Right shift of 1	9000 to 12000	0.0000	0.0000	0.0067	0.0443	0.1162	0.2130	0.0607	0.0674	0.0740	0.0745	0.0604	0.0420	0.1595	0.0703	0.0180	0.0001
Right shift of 1	15000 to 20000	0.0000	0.0000	0.0067	0.0443	0.1165	0.2129	0.0603	0.0674	0.0739	0.0744	0.0604	0.0420	0.1594	0.0703	0.0180	0.0000
Right shift of 1	30000 to 40000	0.0000	0.0000	0.0067	0.0443	0.1165	0.2129	0.0603	0.0674	0.0739	0.0744	0.0604	0.0420	0.1594	0.0703	0.0180	0.0000
Right shift of 2	5000 to 8000	0.0000	0.0000	0.0000	0.0057	0.0368	0.0994	0.1682	0.0457	0.0581	0.0668	0.0603	0.0519	0.2149	0.1324	0.0598	0.0028
Right shift of 2	9000 to 12000	0.0000	0.0000	0.0000	0.0058	0.0381	0.0999	0.1697	0.0480	0.0584	0.0670	0.0606	0.0522	0.2180	0.1341	0.0601	0.0000
Right shift of 2	15000 to 20000	0.0000	0.0000	0.0000	0.0058	0.0381	0.0999	0.1697	0.0480	0.0584	0.0670	0.0606	0.0522	0.2180	0.1341	0.0601	0.0000
Right shift of 2	30000 to 40000	0.0000	0.0000	0.0000	0.0058	0.0381	0.0999	0.1697	0.0480	0.0584	0.0670	0.0606	0.0522	0.2180	0.1341	0.0601	0.0000

TABLE II. SECOND ORDER SENSITIVITY INDICES

	5am	6am	7am	8am	9am	10am	11am	12pm	1pm	2pm	3pm	4pm	5pm	6pm	7pm	capacity
5am	0.0000	0.0000	0.0000	0.0000	0.0000	0.0000	0.0000	0.0000	0.0000	0.0000	0.0000	0.0000	0.0000	0.0000	0.0000	0.0000
6am	0.0000	0.0000	0.0015	0.0012	0.0017	0.0014	0.0020	0.0020	0.0015	0.0014	0.0015	0.0014	0.0014	0.0015	0.0014	0.0010
7am	0.0000	0.0015	0.0000	-0.0043	-0.0040	-0.0039	-0.0043	-0.0046	-0.0044	-0.0046	-0.0042	-0.0044	-0.0042	-0.0044	-0.0041	-0.0004
8am	0.0000	0.0012	-0.0043	0.0000	0.0009	0.0013	0.0007	0.0017	0.0017	0.0014	0.0013	0.0010	0.0008	0.0011	0.0012	0.0010
9am	0.0000	0.0017	-0.0040	0.0009	0.0000	0.0028	0.0022	0.0026	0.0028	0.0028	0.0029	0.0023	0.0023	0.0032	0.0025	0.0028
10am	0.0000	0.0014	-0.0039	0.0013	0.0028	0.0000	-0.0001	-0.0001	0.0001	-0.0003	-0.0001	0.0002	-0.0001	0.0000	-0.0001	-0.0004
11am	0.0000	0.0020	-0.0043	0.0007	0.0022	-0.0001	0.0000	0.0013	0.0018	0.0008	0.0021	0.0014	0.0014	0.0014	0.0012	0.0037
12pm	0.0000	0.0020	-0.0046	0.0017	0.0029	-0.0001	0.0013	0.0000	0.0019	0.0032	0.0016	0.0026	0.0026	0.0011	0.0024	0.0048
1pm	0.0000	0.0015	-0.0044	0.0017	0.0028	0.0001	0.0018	0.0019	0.0000	-0.0034	-0.0037	-0.0037	-0.0058	-0.0040	-0.0038	-0.0038
2pm	0.0000	0.0014	-0.0046	0.0014	0.0028	-0.0003	0.0008	0.0032	-0.0034	0.0000	-0.0013	-0.0009	-0.0012	-0.0011	-0.0013	-0.0018
3pm	0.0000	0.0015	-0.0042	0.0013	0.0029	-0.0001	0.0021	0.0016	-0.0037	-0.0013	0.0000	-0.0025	-0.0044	-0.0028	-0.0028	-0.0033
4pm	0.0000	0.0014	-0.0044	0.0010	0.0023	0.0002	0.0014	0.0026	-0.0037	-0.0009	-0.0025	0.0000	0.0001	0.0004	0.0003	0.0003
5pm	0.0000	0.0014	-0.0042	0.0008	0.0023	-0.0001	0.0014	0.0026	-0.0037	-0.0012	-0.0044	0.0001	0.0000	-0.0030	-0.0030	-0.0100
6pm	0.0000	0.0015	-0.0044	0.0011	0.0032	0.0000	0.0014	0.0011	-0.0040	-0.0011	-0.0026	0.0004	-0.0090	0.0000	0.0000	0.0010
7pm	0.0000	0.0014	-0.0041	0.0012	0.0025	-0.0001	0.0012	0.0024	-0.0038	-0.0013	-0.0026	0.0003	-0.0090	0.0000	0.0000	-0.0001
capa city	0.0000	0.0010	-0.0004	0.0010	0.0028	-0.0004	0.0037	0.0048	-0.0038	-0.0018	-0.0033	0.0003	-0.0160	0.0010	-0.0001	0.0000

Capacity range 5000 to 8000 W

5am	0.0000	0.0000	0.0000	0.0000	0.0000	0.0000	0.0000	0.0000	0.0000	0.0000	0.0000	0.0000	0.0000	0.0000	0.0000	0.0000
6am	0.0000	0.0000	0.0022	0.0017	0.0024	0.0019	0.0027	0.0027	0.0022	0.0020	0.0021	0.0021	0.0021	0.0021	0.0021	0.0011
7am	0.0000	0.0022	0.0000	-0.0030	-0.0021	-0.0022	-0.0026	-0.0030	-0.0028	-0.0029	-0.0025	-0.0027	-0.0025	-0.0028	-0.0024	0.0009
8am	0.0000	0.0017	-0.0030	0.0000	0.0047	0.0059	0.0037	0.0060	0.0067	0.0062	0.0065	0.0062	0.0044	0.0051	0.0055	0.0058
9am	0.0000	0.0024	-0.0021	0.0047	0.0000	0.0049	0.0052	0.0051	0.0055	0.0054	0.0058	0.0045	0.0047	0.0060	0.0051	0.0153
10am	0.0000	0.0019	-0.0022	0.0059	0.0049	0.0000	-0.0041	-0.0044	-0.0037	-0.0045	-0.0033	-0.0031	-0.0029	-0.0036	-0.0038	0.0108
11am	0.0000	0.0027	-0.0026	0.0037	0.0052	-0.0041	0.0000	0.0007	0.0012	0.0011	0.0015	0.0007	0.0008	0.0008	0.0006	0.0030
12pm	0.0000	0.0027	-0.0030	0.0060	0.0051	-0.0044	0.0007	0.0000	0.0012	0.0026	0.0009	0.0019	0.0020	0.0003	0.0017	0.0048
1pm	0.0000	0.0022	-0.0028	0.0067	0.0055	-0.0037	0.0012	0.0012	0.0000	-0.0060	-0.0063	-0.0064	-0.0068	-0.0067	-0.0065	-0.0061
2pm	0.0000	0.0020	-0.0029	0.0062	0.0054	-0.0045	0.0001	0.0026	-0.0060	0.0000	-0.0008	-0.0004	-0.0006	-0.0005	-0.0008	-0.0005
3pm	0.0000	0.0021	-0.0025	0.0055	0.0058	-0.0033	0.0015	0.0009	-0.0063	-0.0008	0.0000	-0.0049	-0.0009	-0.0050	-0.0050	-0.0025
4pm	0.0000	0.0021	-0.0027	0.0052	0.0045	-0.0031	0.0007	0.0019	-0.0064	-0.0004	-0.0049	0.0000	-0.0003	0.0001	0.0000	-0.0003
5pm	0.0000	0.0021	-0.0025	0.0044	0.0047	-0.0029	0.0008	0.0020	-0.0068	-0.0006	-0.0071	-0.0003	0.0000	-0.0066	-0.0066	-0.0129
6pm	0.0000	0.0021	-0.0028	0.0051	0.0060	-0.0036	0.0008	0.0003	-0.0067	-0.0005	-0.0050	0.0001	-0.0066	0.0000	-0.0017	-0.0016
7pm	0.0000	0.0021	-0.0024	0.0055	0.0051	-0.0038	0.0006	0.0017	-0.0065	-0.0008	-0.0050	0.0000	-0.0066	-0.0017	0.0000	0.0001
capa city	0.0000	0.0011	0.0009	0.0058	0.0153	0.0108	0.0030	0.0048	-0.0061	-0.0005	-0.0025	-0.0003	-0.0129	-0.0016	0.0001	0.0000

Capacity range 9000 to 12000 W

5am	0.0000	0.0000	0.0000	0.0000	0.0000	0.0000	0.0000	0.0000	0.0000	0.0000	0.0000	0.0000	0.0000	0.0000	0.0000	0.0000
6am	0.0000	0.0000	0.0015	0.0009	0.0022	0.0013	0.0021	0.0021	0.0015	0.0013	0.0015	0.0014	0.0014	0.0014	0.0014	0.0014
7am	0.0000	0.0015	0.0000	0.00												

When the capacity class becomes higher, the index will drop to zero. Hence, in this study, the sensitivity analysis can allow us to identify the “best” capacity class with respect to our energy management system. Indeed, the second class batteries seem to best fit storage needs based on the “No change” test case.

When battery capacity has a significant sensitivity index, the earliest hours with the highest netload value are the most impacting (i.e., hours 7am-9am). This suggests that day-ahead planning of charging is taking place during these hours.

Looking at the hour for irradiance, we can see that the sensitivity index is proportional to the irradiance value. At 10am and 11am, the prediction error has the highest impact on the estimated total cost and optimization results.

For second order indices in Table II, we can observe a change in results depending on the capacity class. The first class of capacity presents a high sensitivity to irradiance at 9pm, 11am and 12pm coupled with the subsequent hours of each as well as capacity. 9am represents the hour at which the battery will be fully charged. So, the state will be impacted in subsequent hours with respect to discharge possibilities. 11am and 12pm are hours during which the netload is very low. Then, variability of generation affects cost significantly.

The second class of capacity has a sensitivity that is the most significant for hours 8am and 9am coupled with variables representing subsequent hours and capacity. This is unexpected since usually hours at which the battery is fully charged are the most impacting in combination with subsequent hours and the capacity (1pm for this capacity class). However, 8am and 9am are crucial hours for charging the battery and can affect decisions taken subsequently.

For large batteries (the third capacity class), the most important sensitivity from coupling variables is that of hours 9am and 12pm. In this case, 9am presents a peak in netload and 12pm represents the hour. In this study at which the battery might become the fullest (since charging is constrained by energy consumption in subsequent hours).

As a final observation, we can notice that second order sensitivity indices become more significant when the capacity is larger.

IV. CONCLUSION

In this paper, we analyze the sensitivity of radiation forecast on the total cost incurred in a home equipped with a flexible device and an energy management system. We use a black-box technique to conduct the sensitivity analysis. The chosen technique takes into account requirements of minimizing the time and computation required through quasi-random sampling. For the proposed energy management system based on day-ahead scheduling, the analysis results reflect well the charging strategy. The analysis also allows us to validate the use (or not) of the full battery capacity. Although we consider a simple scenario, our system allows to analyze more complex energy management systems and can integrate their interaction with different pricing schemes. As a perspective, it is possible to

study the impact of prediction error on a city. A decentralized and distributed solution can reduce the complexity of the sensitivity study such as proposed in [14] [15] to regularize the mismatches of supply and demand.

ACKNOWLEDGMENT

This research work has been carried out under the leadership of the Institute of Technological Research SystemX, within the scope of a joint collaboration with Sherpa Engineering (France) and Reuniwatt (France) in the Smart City Energy Analytics project.

REFERENCES

- [1] M. D. McKay, “Evaluating prediction uncertainty, Technical Report NUREG/CR-6311,” U.S. Nuclear Regulatory Commission and Los Alamos National Laboratory, 1995.
- [2] H. Frey, A. Mokhtari, and T. Danish, “Evaluation of selected sensitivity Analysis methods Based Upon Applications to two Food safety Process risk models,” Reigh-North Carolina, North Carolina State University, 2003.
- [3] P. Heiselberg et al., “Application in sensitivity Analysis in design of sustainable buildings,” *Renewable Energy*, pp. 2030-2036, 2009.
- [4] A.-T. Nguyen and S. Reiter, “A performance comparison of sensitivity analysis methods for building energy models,” *Research Article Building Thermal, Lighting, and Acoustics Modeling*, pp. 651-664, 2015.
- [5] I. M. Sobol, “Sensitivity estimates for nonlinear mathematical models,” *MMCE 1*, pp. 407-414, 1993.
- [6] I. M. Sobol, “Global sensitivity indices for nonlinear mathematical models and their Monte Carlo estimates,” *Mathematics and Computers in Simulation*, pp. 271-280, 2001.
- [7] R. I. Cukier, C. M. Fortuin, K. E. Shuler, A. G. Petschek, and J. H. Schaibly, “Study of the sensitivity of coupled reaction systems to uncertainties in rate coefficients I Theory,” *The Journal of Chemical Physics* 59, pp. 3873-3878, 2001.
- [8] Phisim library. [retrieved: April, 2019]. from <https://www.sherpa-eng.com/produits/phisim/>.
- [9] A. Saltelli, K. Chan, and E. M. Scott, “Sensitivity Analysis,” Chichester : Wiley Series in Probability and Statistics, 2000.
- [10] M. Ratto, S. Tarantola, and A. Saltelli, “Estimation of importance indicators for correlated inputs,” *ESREL2001*, 2001.
- [11] A. Saltelli, “Making best use of model evaluations to compute sensitivity indices,” *Computer Physics Communications*, pp. 280-297, 2002.
- [12] A. Saltelli et al., “Variance based sensitivity analysis of model output. Design and estimator for the total sensitivity index,” *Computer Physics Communications*, pp. 259-270, 2010.
- [13] A. Henry, M. Sinquin, and C. Boudesocque, “Prospective d'évolution de la consommation électrique domestique à l'horizon 2030,” INP Toulouse, ENSEEIHT, ENSIACET, 2011.
- [14] Pournaras, E., Pilgerstorfer, P. and Asikis, T., 2018. Decentralized collective learning for self-managed sharing economies. *ACM Transactions on Autonomous and Adaptive Systems (TAAS)*, 13(2), p.10.
- [15] Pournaras, E., Yao, M. and Helbing, D., 2017. Self-regulating supply-demand systems. *Future Generation Computer Systems*, 76, pp.73-91.

Modelling Fractal-Structured Smart Microgrids

Exploring signals and protocols

Mark Apperley

Computer Science Department

University of Waikato

Hamilton, New Zealand

email: mark.apperley@waikato.ac.nz

Abstract— This paper discusses some of the issues surrounding the interconnection of smart microgrids, with a focus on fractal structures, their implementation, management, operation, and potential effectiveness. It builds on a basic smart microgrid model which focuses on the property of localised energy balance, in order to mitigate the dependency on legacy-grid resources to accommodate short-term (hourly) and medium term (daily to monthly) imbalance. This model provides the basis for further development to allow connecting a group of such micro-grids into a network which externally presents identical structure and characteristics, so enabling the fractal-like interconnection of these micro-grids, or groups of microgrids. Such structures simplify the interconnection, management and operation of smart microgrids, and their connection to the legacy grid. They also intrinsically enable the notion of grid-edge trading. These characteristics have the potential not just to further enable and promote the effective utilisation of distributed generation and storage, but also to simplify and rationalise future backbone grid development.

Keywords-fractal micro-grid; legacy grid; backbone grid; grid edge trading; localised temporal energy balance; autonomous microgrid.

I. INTRODUCTION

The rapid development of new renewable energy sources, typically with non-deterministic patterns of generation, provides significant challenges for the traditional, or *legacy*, grid [1]–[3]. Coupled with similarly rapidly developing storage technologies [4][5], and automation systems which enable effective and tolerable load matching and shifting [6], these technologies can facilitate a significant degree of distribution. Concerns with long-distance hierarchal/radial energy transfer and real-time load following from centralized generating systems, grow less and less relevant and appropriate when microgrids, with their highly distributed generation, storage, and load management, become more prevalent [2][6]–[10].

While the integration of centralized renewables into the legacy grid has been the subject of much research, discussion and debate [11][12], they typically require significant energy storage capacity for their contribution to be effective. Although a range of storage concepts have been explored, including V2G (Vehicle-to-grid) [13], when utilized with centralized renewable generation, the distributed nature of

such storage in contrast to the generation, places increased energy transfer demands on the grid.

In this paper the microgrid concept is extended into networks of hierarchically interconnected microgrids, ultimately connected to the *backbone* grid, in a fractal-type structure [15]. The term *legacy grid* is well established, describing the centralized generation and distribution models of the past. Here, the term *backbone* is used to describe its evolution/successor where the centralized functionality begins to take on a new role, delegating aspects of control, balance and generation outwards from the center, depending to some extent on, and exploiting, the growth of localized balance, although elsewhere the term has been used to describe new major national and international transmission systems [8][14].

The protocols for the interconnection of the microgrids to the backbone grid, including potential grid-edge trading, are discussed, with an emphasis on overall system and communication simplicity, although there is no constraint on individual complexity within a single node [16]–[18]. This concept is not unlike that of the Internet, where the protocols are essentially simple, with any complexity residing in the individual terminal devices, and simple devices not ruled out [19].

This paper does focus on relatively small-scale consumption/generation nodes, typically those found in individual residential installations. However, the concepts could be extended to larger commercial or industrial nodes, although some aspects may not scale so well.

The remainder of the paper is structured as follows. In Section II, a model to describe the characteristics of a smart microgrid is developed, and then in Section III, this is extended to enable multiple microgrids to be interconnected in fractal-type structures. Section IV then explores the way in which energy, and relevant information, might be exchanged within, and to and from, these structures, and the overall effectiveness of the approach. Section V summarizes the paper, and concludes that these techniques can lead to more effective utilisation of distributed generation, and simplify future backbone grid development.

II. MODELLING SMART MICROGRIDS

The notion of localised temporal energy balance within a microgrid, as a significant advancement of the *Net-Zero Energy Balance* concept [20][21], is well developed [22][23]. To minimize or completely remove grid dependency, balance

conditions need to be calculated on a much shorter time scale than the annual balance used in the *Net-Zero* model. A household-level smart microgrid model, which enables these calculations, has been developed and is shown in Figure 1 [22] [23]. While the inclusion of the battery flows in both the *local consumption* and *local generation* totals may appear to account for the stored energy twice, this is necessary in order to examine flows over short time scales [22][23]. Typically, and usefully, balance calculations can be performed at hourly intervals over the year (as shown later in Figure 2).

For an example (New Zealand) household with an average daily consumption of 17.6 kWh, the energy balance plot of Figure 2 (taken from [22]) shows the actual hourly balance, based on the model of Figure 1, with solar PV chosen to exactly match the load over a year, and with 24 hours equivalent of battery storage (1.3 Tesla Powerwall 2s [5]). As can be seen, for this hourly energy balance plot, many of the 8760 hours lie on the diagonal, showing perfect balance.

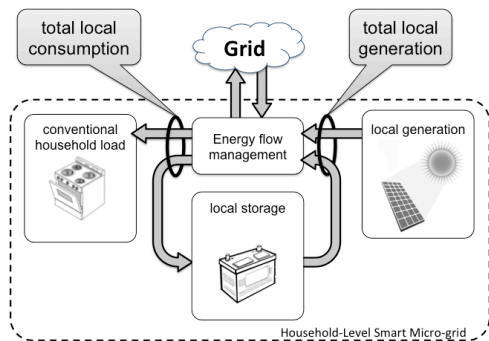


Figure 1. Energy flows within the smart microgrid, and the contextual definitions of local generation and local consumption.

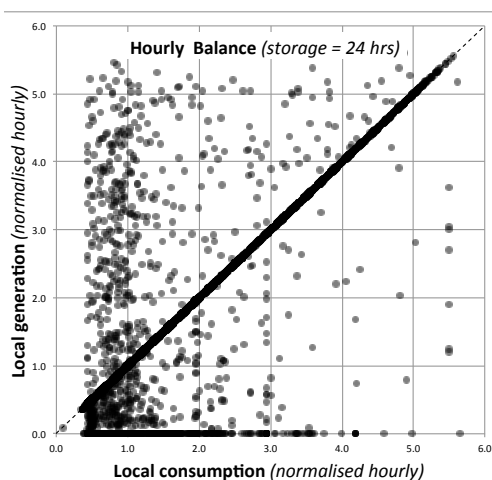


Figure 2. Energy balance at hourly intervals over a year for an example installation.

However, a substantial number fall below the diagonal, representing a net grid load for that interval, and a significant number lie above, representing excess generation. It is

interesting to note that the *Net-Zero Energy Balance* model for this configuration would describe it as in perfect balance, which it is only if you consider generated and consumed energy over a whole year. The vertical stack of points towards the left of the graph represents times of high solar generation, often with low day-time load, as is experienced in most residential installations.

III. A FRACTAL MODEL FOR NETWORKS OF SMART MICROGRIDS

The hourly balance plot of Figure 2 clearly shows the potential for networking such micro-grids, for example within a neighbourhood, to improve local energy balance. It is possible that when the example household of Figure 2 is in surplus, one of its neighbours may be in deficit, so providing the opportunity for local energy exchange, or grid-edge trading, and reducing the demand on the external backbone grid. Overall, this local exchange can only reduce the external demand, potentially reduce the network distribution capacity requirements, and make more effective local use of the distributed generation and storage, improving both the local and backbone efficiency.

The microgrid illustrated in Figure 1 represents just a single household. Several households in the same neighbourhood could be interconnected in a higher level microgrid, as suggested in Figure 3. Here, a number of households are connected to a higher level node, which bears very close resemblance to the household nodes themselves, and presents a similar face to the backbone/grid as the individual households previously did. In this model, the neighborhood node includes potential neighborhood load (e.g., community street lighting, electric vehicle charging), neighborhood storage, and neighborhood generation (perhaps in a school or other public building or space). A multi-level self-similar structure, such as this, can be defined as a fractal structure [15], and its utility in modelling and describing networks of smart-microgrids has been discussed [24].

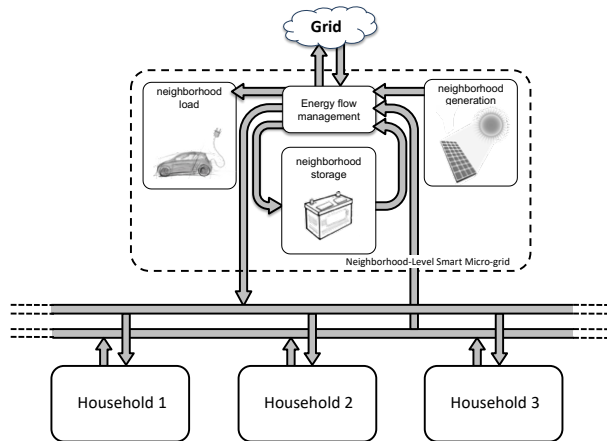


Figure 3. A collection of households grouped together in a neighborhood, using a fractal-like construction technique.

To support this fractal approach, closer examination of the neighbourhood grid of Figure 3, and the household grid of Figure 1, leads to the single generic microgrid model of Figure 4, which could represent a node at any level in a tree of microgrids; a household (leaf) node, or a neighbourhood, a suburb, or a township node, if appropriate. A leaf node would not have any connection to a lower level grid, and at any level, any component other than the energy flow management unit, could be omitted. In other words, some units could have no storage, some could have no generation, and some no load, or any combination of these.

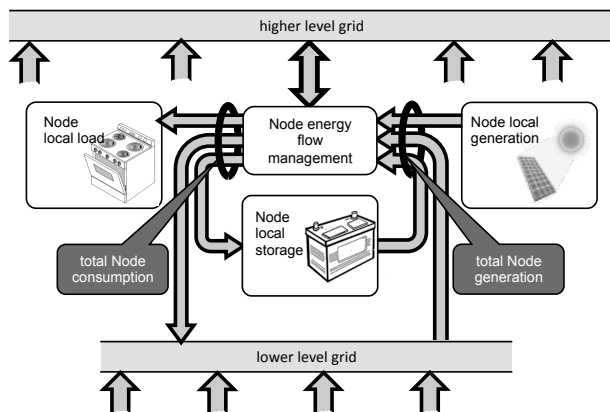


Figure 4. A fractal microgrid energy flow model.

IV. SIGNALS, PROTOCOLS, AND EFFECTIVENESS

For the purposes of this discussion, and our desire, alluded to in the introduction, to maintain simplicity in the communication between nodes, it is suggested that the only signal transmitted between nodes is one of price/need. This leads to the simplified generic node representation of Figure 5, with bidirectional energy flow and downward propagation of pricing signals. As suggested earlier, this simplicity is consistent with the end-to-end principle of smart system communication, fundamental, for example, to the Internet [19].

This simple model enables a non-smart (passive) node to pass on the incoming price signal downwards, to use/buy any available or offered energy it needs from above, and to propagate any surplus energy that it has upwards, to the higher level grid, if there is a demand for it. The more detailed model of Figure 4 implies that the lower level grid simply contributes additional load or additional generation.

Consider first a passive node such as this which is a leaf node, effectively more like the node of Figure 1. It would normally be in one of three possible states:

- *deficit*, when it is unable to meet its own demand from its own available generation and/or storage (i.e., when total node load exceeds total available node generation – Figure 1);
- *balance*, when it is able to provide for its own demand from local generation and/or storage, without any wasted generation (i.e., when total node generation can be adjusted to exactly meet total node load); and

- *surplus*, when it is unable to consume all of its available energy (i.e., when total node generation exceeds total node load, including battery charging – Figure 1)).

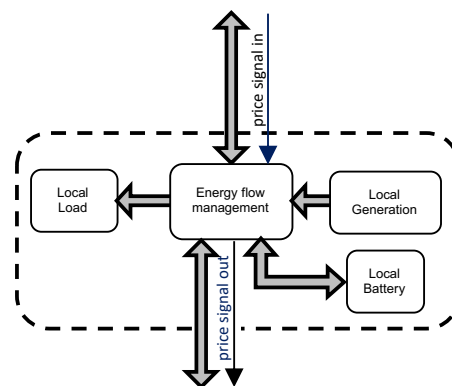


Figure 5. A simplified energy flow model for a fractal node.

For passive *non-leaf* nodes, consistent with the model of Figure 4, and for the purposes of the current discussion, the lower level grid is assumed to contribute to the node’s generation and load, as mentioned earlier and suggested in the figure.

These three states just described are deterministic, and can be readily established, even for a passive node. However, as the “smart” nature of a node increases, the nature of these states may be modified by the energy flow management system, particularly in the *balance* state. For example, in this *balance* state, a smart node may decide, on the basis of history, current charging levels, future prediction, and price, to sell or buy energy from the upper grid. This is an attribute of the smart node alone, and has no impact on the topology and signals proposed in Figure 4 and Figure 5.

An individual smart node could potentially have a quite complex policy, perhaps to always sell when the price offered is at least 10% above the norm, and the battery is more than 80% charged. But it could also utilize factors such as expected

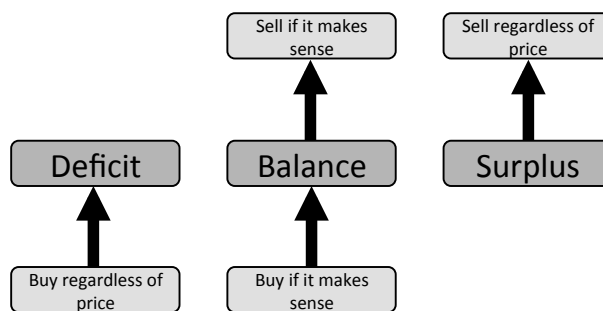


Figure 6. The three states of a fractal node such as Figure 5, with the addition of optional and imperative sell and buy.

or predicted generation and load over the next period. The model here enables such policies to be implemented at the node level, and for smart nodes such as this to co-exist, and be networked, with more passive nodes such as that previously described. Figure 6 shows the original 3 states with the addition of the buying and selling imperatives (deficit and surplus), and options (balance). In the balance state, the decision to buy or sell is totally dependent on the policy employed by the node, and the price signal.

In general terms, we can represent the possible policy based decisions that could take place within a smart node to determine the “if it makes sense” modifier of Figure 6, with the decision tree shown in Figure 7.

Figure 7 still hides specific detail, but enables it at varying levels of complexity. For example, decision 1 “is there enough to last until next charging” could exploit history of daily load, time of day and solar characteristics, weather conditions now, and for the remainder of the day, amongst other factors.

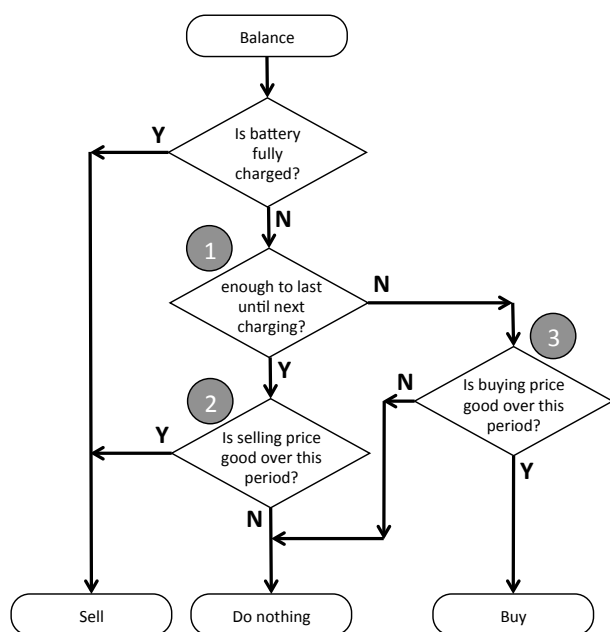


Figure 7. An energy flow management decision tree enabling flexible policy implementation, and levels of “smartness”, in any fractal node.

Decision 2, “is selling price good over this period”, suggests the node should look for the optimum time to sell during the time between now and the next charging. Decision 3, “is buying price good...” is really asking is the buying price likely to get lower before the battery runs out.

V. CONCLUSION

A model characterising a smart microgrid has been proposed, which allows for fractal structured interconnection. Individual nodes can be of any level of “smartness”, and totally passive nodes can be included without compromising the autonomy of others. The model is based on very simple signalling, consistent with the end-to-end approach

successfully utilised, for example, in the Internet, which totally supports these notions of autonomy and participatory variety [19]. Without attempting to provide any technical implementation detail, the paper has demonstrated the potential utility of the approach.

Internally, the networked smart microgrid is no different in its configuration and operation when a part of a neighbourhood fractal network, than it is when it is a stand-alone backbone-grid connected microgrid. It is totally autonomous in its operation. Non-leaf nodes still retain this autonomy, although obviously the load and generation of the lower level nodes passes through them. Network transparency simplifies and facilitates individual interconnection, management, and operation of these microgrids.

Technically, grid-edge trading is implicit in the structure, although it is not explicitly represented. Contracting, accounting, charging for this at any level is not different from the situation on a regular grid with multiple generators and multiple consumers, but as described, it does fall short of enabling peer-to-peer contracting [17].

These features all potentially contribute to the notion that semi-self-reliant microgrids, can, without internal compromise, be connected into neighbourhood and local grids, which maximise the local consumption of local generation, and provide a basis for future backbone grid development, in terms of both generation and distribution capacity.

The model presented here is based purely on energy flows, and does not take into consideration the practical physical details of electricity networks, including voltage transitions, security, stability, etc. However, with the growth in distributed renewable energy, electronic frequency control, and the gradual decline of rotating generators, many of these issues must be regarded as volatile, as we move from the legacy grid model to the backbone plus fractal smart microgrids discussed here.

There are aspects of the model which may still subject to debate. For example:

- Should non-leaf nodes be able to modify the pricing information they propagate downwards?
- Should lower level nodes be able to signal their own selling price upwards?

If not specifically answered by the analysis, it is suggested that these considerations have been shown to be of little consequence, and unnecessary for effective operation of autonomous microgrids, although the model used here is based on effective and efficient energy utilisation, rather than being motivated by business opportunity.

Simulation studies of this model, utilising real household and neighbourhood consumption data, are currently underway.

REFERENCES

- [1] G. Venkataramanan and C. Marnay, “A larger role for microgrids,” *IEEE Power and Energy M.*, vol. 6, no. 3, pp. 78-82, May-June 2008.
- [2] “Transmission Tomorrow,” 2016, [Online] <https://www.transpower.co.nz/resources/transmission-tomorrow-2016-0>. [Retrieved: Mar. 10, 2017].

- [3] T. Seba, Clean disruption of energy and transportation, Clean Planet Ventures: CA., 2014.
- [4] R. Hensley, J. Newman, and M. Rogers, "Battery technology charges ahead", McKinsey Quarterly, vol. 3, pp. 5-50, 2012.
- [5] Tesla, "Powerwall," 2017. [Online]. https://www.tesla.com/en_NZ/powerwall. [Retrieved: Mar. 01, 2017].
- [6] A. Ipakchi and F. Albuyeh, "Grid of the future," IEEE Power Energy M., vol. 7, no. 2, pp. 52-62, 2009.
- [7] J. P. Lopes, N. Hatzargyriou, J. Mutale, P. Djapic, and N. Jenkin, "Integrating distributed generation into electric power systems: A review of drivers, challenges and opportunities," Electr. Pow. Syst. Res., vol. 77, no. 9, pp. 1189-1203, 2007.
- [8] M. Amin, "The Case for Smart Grid: Funding a new infrastructure in an age of uncertainty," Public Utilities Fortnightly, March 2015, pp. 24-32.
- [9] D. Coll-Mayor, M. Paget, and E. Lightner, "Future intelligent power grids: analysis of the vision in the European Union and the United States", Energy Policy, vol. 35, pp. 2453-2465, 2007.
- [10] M. Lehtonen and S. Nye, "History of electricity network control and distributed generation in the UK and Western Denmark", Energy Policy, vol. 37, pp. 2338-2345, 2009.
- [11] Y. Riffonneau, S. Bacha, F. Barruel, and S. Ploix, "Optimal power flow management for grid connected PV systems with batteries", IEEE Trans. Sustain. Energy, vol. 2, no. 3, pp. 309-320, 2011.
- [12] J. von Appen, M. Braun, T. Stetz, K. Diwold, and D. Geibel, "Time in the sun: the challenge of high PV penetration in the German electric grid," IEEE Power and Energy M., vol. 11, no. 2, pp. 55-64, 2013.
- [13] P. Monigatti, M. Apperley, and B. Rogers, "Improved grid integration of intermittent electricity generation using electric vehicles for storage: A simulation study," In Proceedings of the 2012 International Green Computing Conference (IGCC), IEEE Press, pp. 1-10, 2012.
- [14] A. Hellemans, "Creating Europe's new backbone for efficient power distribution." [Online]. <http://www.youris.com/energy/energy-grid/creating-europes-new-backbone-for-efficient-power-distribution.kl> [Retrieved: Feb. 06, 2019].
- [15] B. B. Mandelbrot, Fractals: form, chance, and dimension, W. H. Freeman: San Francisco, CA., 1977.
- [16] Z. Fan *et al.*, "Smart Grid Communications: Overview of Research Challenges, Solutions, and Standardization Activities," IEEE Communications Surveys & Tutorials, vol. 15, no. 1, pp. 21-38, First Quarter 2013.
- [17] T. Morstyn, A. Teytelboym and M. D. McCulloch, "Bilateral Contract Networks for Peer-to-Peer Energy Trading," IEEE Transactions on Smart Grid, vol. 10, no. 2, pp. 2026-2035, March 2019.
- [18] C. Lo and N. Ansari, "The Progressive Smart Grid System from Both Power and Communications Aspects," IEEE Communications Surveys & Tutorials, vol. 14, no. 3, pp. 799-821, Third Quarter 2012.
- [19] J. H. Saltzer, D. P. Reed, and D. D. Clark, "End-to-End Arguments in System Design," ACM Transactions on Computer Systems, vol.2, no. 4, pp. 277-288, 1984.
- [20] J. Salom, J. Widén, J. Candanedo, I. Sartori, K. Voss, and A. Marzal, "Understanding net zero energy buildings: evaluation of load matching and grid interaction indicators," In Proceedings of Building Simulation, vol. 6, pp. 2514-2521, 2011.
- [21] P. Torcellini, S. Pless, M. Deru, and D. Crawley, Zero energy buildings: a critical look at the definition, National Renewable Energy Laboratory and Department of Energy, US. 2006.
- [22] M. Apperley, "Modelling energy balance and storage in the design of smart microgrids", In Proceedings of Energy 2017, Barcelona, pp. 40-45, 2017.
- [23] M. Apperley, P. Monigatti, and J. Suppers, "Grid-Lite: A network integrated semi-autonomous local area electricity system", In Proceedings of the 4th International Conference on Green IT Solutions (ICGreen 2015), Milan, Italy, SciTePress, pp. 27-33, 2015.
- [24] G. Florea, O. Chenaru, D. Popescu and R. Dobrescu, "A fractal model for power smart grids," In Proceedings of the 20th IEEE International Conference on Control Systems and Computer Science (CSCS), pp. 572-577, 2015.

Is Power Outage Associated With Population Density?

Vivian Sultan
 Claremont Graduate University
 Center For Information Systems & Technology
 Claremont, CA 91711
 Email: vivian.sultan@cgu.edu

Brian Hilton
 Claremont Graduate University
 Center For Information Systems & Technology
 Claremont, CA 91711
 Email: brian.hilton@cgu.edu

Abstract—The U.S. electric power infrastructure is in urgent need of renovation. Recent major power outages in California, New York, Texas, and Florida have drawn attention to the unreliability of the U.S. electric power system. The media discussed America’s aging power infrastructure and the Public Utilities Commission called for a comprehensive review of the causes of recent power outages. This study explores geographic information systems to identify a correlation between population density and power outages in Georgia. Initial investigation using ArcMap software as a visualization tool revealed areas where this association emerged.

Keywords—Power Outages; Electric Power Infrastructure; ArcMap; GIS.

I. INTRODUCTION & PROBLEM DEFINITION

In a short time, electrical power has become a necessity of modern life. Our work, healthcare, leisure, economy, and livelihood depend on the constant supply of electrical power. Even a temporary power outage can lead to relative chaos, financial setbacks, and possible loss of life. U.S. cities dangle on electricity and without the constant supply from the power grid, pandemonium would ensue. Power outages can be especially tragic when they endanger life-support systems in hospitals and nursing homes or systems in synchronization facilities such as in airports, train stations, and traffic control. In 2004, the economic cost of power interruptions to U.S. electricity consumers was \$79 billion annually in damages and lost economic activity [1]. In 2017, Lawrence Berkeley National Laboratory estimated power-interruption costs had increased more than 68% per year since their 2004 study [2].

Many reasons underlie current power failures. Among these reasons are severe weather, damage to electric transmission lines, shortage of circuits, and the aging of the power-grid infrastructure. Severe weather is the leading cause of power outages in the United States [3]. In 2018, weather events as a whole cost U.S. utilities \$306 billion: the highest figure ever recorded by the federal government [4].

The aging of the grid infrastructure is another noteworthy reason for power failures. In 2008, the American Society of Civil Engineers gave the U.S. power-grid infrastructure an unsatisfactory grade [5]. They stated in a report that the power-transmission system in the United States required immediate attention. Furthermore, the report mentioned that the U.S. electric-power grid is similar to those of third-world countries. According to the Electric Power Research Institute, equipment such as transformers

controlling power transmission need to be replaced, as they have exceeded their expected lifespan considering the materials’ original design [6].

Electrical outages have three main causes: (1) hardware and technical failures, (2) the environment, and (3) human error [7]. Hardware and technical failures are due to equipment overload, short circuits, brownouts, and blackouts, to name a few [8]–[10]. These failures are often attributed to unmet peak usage, outdated equipment, and malfunctioning back-up power systems. Environment-related causes for power outages comprise weather, wildlife, and trees that come into contact with power lines. Lightning, high winds, and ice are common weather-related power interruptions. Also, squirrels, snakes, and birds that come in contact with equipment such as transformers and fuses can cause equipment to momentarily fail or shut down completely [8]. As for the third main cause for electrical outages, human error, the Uptime Institute estimated that human error causes roughly 70% of the problems that plague data centers. Hacking can be included in the human-error category [11].

Analytics have been a popular topic in research and practice, particularly in the energy field. The use of analytics can help advance Smart Grid reliability by, for example, elucidating a root cause of power failure, defining a solution for a blackout through data, or implementing a solution with continuous monitoring and management. In this research paper, we aim to unveil the novel use of location analytics to investigate power-failure events and their association with population density. In this manuscript, we use ArcMap software to investigate U.S. power concerns and to answer the research question, “Is power outage associated with population density?” The rest of this paper is organized as follows. Section II presents the literature review and the research importance. Section III describes the process of data selection and acquisition. Section IV addresses research tools and methodology. In Section V, we discuss our findings.

II. LITERATURE REVIEW

The economic cost of power interruptions to U.S. electricity is \$79 billion annually [1]. The year 2018 was particularly onerous for outages with wildfires in California and a number of hurricanes that plagued Texas, the Southeast, and Puerto Rico [12]. When Hurricane Harvey struck the Gulf Coast in August 2017, about 280,000 people were without electricity at one point [13]. The report

specified that the storm took out six transmission lines, 91 circuits, and about 10,000 MW of generation.

When Hurricane Irma hit Florida in 2017, it impacted about 5 million customers in districts where Florida Power & Light operates [14]. Commenting on Hurricane Irma, energy journalist Peter Maloney stated, “Miami-Dade County was hit hardest. At one point, more than 815,000 people, or 80% of [Florida Power & Light] accounts in the county, were without power” [15]. According to Maloney, other jurisdictions in Florida, such as Palm Beach and Broward County, also lost power in 68–70% of their accounts due to the hurricane [15]. Figure 1 sketches the yearly total number of outages in the United States and people affected since February 16, 2008 [16, p. 3].

Year	Total number of outages	People affected
2008*	2,169	25.8 million
2009	2,840	13.5 million
2010	3,149	17.5 million
2011	3,071	41.8 million
2012	2,808	25.0 million
2013	3,236	14.0 million
2014	3,634	14.2 million
2015	3,571	13.2 million
2016	3,879	17.9 million
2017	3,526	36.7 million

Figure 1. Total U.S. Annual Outages and People Affected 2008–2017

In addition, the report offered the pie chart shown in Figure 2 to break down the 2017 reported power-outage incidents by cause [16]. In the annual report, power-outage incidents were grouped into one of eight possible causes. The number next to each pie piece in Figure 2 is the number of outages associated with that cause.

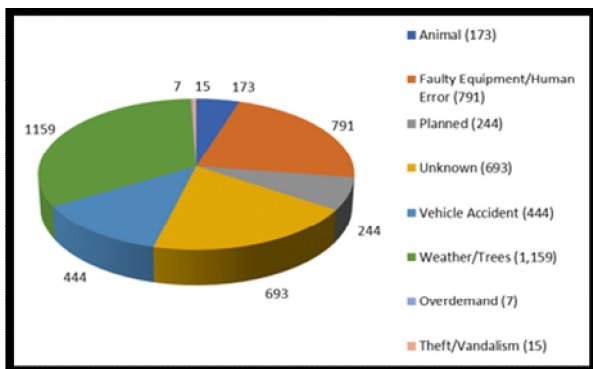


Figure 2. U.S. Reported Power Outages by Cause in 2017 [16]

Based on Eaton’s Blackout Tracker [16] and similar reports that investigate power-outage incidents, key factors behind these outages can be summarized as shown in Figure 3. In our framework (Figure 3), electrical outages have three main causes: (1) hardware and technical failures, (2) environment-related outages, and (3) operation-related failures.

Environment-related incidents comprise the largest portion of power-outage causes. Environment-related incidents can be classified into three distinct categories: weather, wildlife, and trees. In 2017, Wisconsin Public Service delineated the weather-related causes of power outages; a 2005 study by Davies Consulting for the Edison Electric Institute stated that 70% of power outages in the

United States are weather related [17][18]. In 2014, Kenward and Raja analyzed power-outage data over a 28-year period; between 2003 and 2012, 80% of all outages were caused by weather [19]. Similarly, in 2012, Campbell highlighted the damage to the electrical grid caused by seasonal storms, rain, and high winds [20].

Severe weather is the leading cause of power outages in the United States: “Between 2003 and 2012, an estimated 679 widespread power outages occurred due to severe weather” [3, p. 3]. Likewise, researchers showed that annual costs changed significantly and were increasingly greater due to major storms such as Hurricane Ike in 2008. “Data from the U.S. Energy Information Administration show that weather-related outages have increased significantly since 1992” [14, p. 7].

In addition to weather, other external forces create power outages. Falling tree branches, for example, are another important cause of power disruption [21]. Animals coming into contact with power lines, such as large birds, are also important culprits in power outages in the United States [16]. Furthermore, human-error incidents cause power outages. Training is essential for technicians and staff to battle outages with proper maintenance procedures [7].

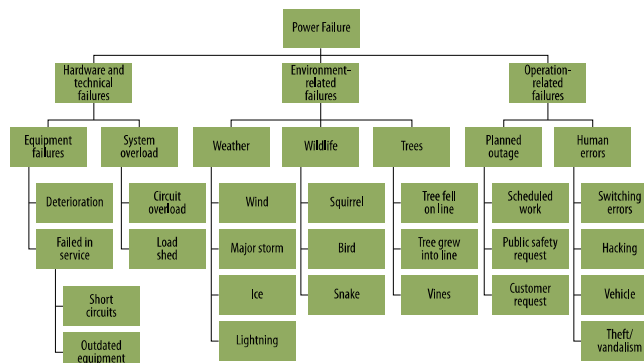


Figure 3. Causes of Power Failure.

Interrupted power supply is no longer a mere inconvenience. As the duration and spatial extent of electricity-system outages increase, costs and inconvenience grow. Critical social services—such as medical care, police and other emergency services, and communications systems—depend on electricity functioning at a minimum. Such failures can bring about catastrophic outcomes; lives can be lost. Grid reliability is an area of research that will help to better explain the causes of outages and aid in prescribing interventions to improve the reliability of the Smart Grid. This report explores Geographic Information Systems (GIS) to correlate population density and power outages in Georgia. This study aims to address whether power outages align with population density.

III. DATA SELECTION AND ACQUISITION

A. Power-Outage Data

The Electric Power Research Institute (EPRI) data repository includes the primary datasets we used to conduct this analysis [22]. The data sets include data from advanced

metering systems, Supervisory Control and Data Acquisition (SCADA) systems, GIS, Outage-Management Systems (OMS), Distribution Management Systems (DMS), asset-management systems, work-management systems, customer-information systems, and intelligent electronic device databases. Access to datasets was provided as part of EPRI's data-mining initiative, an initiative that provides a test bed for data exploration and innovation and seeks to solve major challenges faced by the utility industry [22].

When combined with clever analytic techniques, data provide the potential to transition to a smarter world, where the prevention of power outages may become a true reality, not merely a prediction. The SCADA/OMS/DMS archives at a power utility offer the required data to identify parts of the system that contribute most to overall system downtime. An OMS, for example, provides the data needed to calculate measurements of system reliability. OMS also provides historical data that can be mined to find common causes, failures, and damage. Because OMS has become more integrated with other operational systems such as GIS on the utility side, analysis has become more feasible, allowing researchers to aim to improve grid reliability.

B. Population Data

The U.S. Census Bureau's 2010 Decennial Census data at census-block geography is the population data source. The Research and Analytics Division of the Atlanta Regional Commission using U.S. Census Bureau Topology Integrated Geographic Encoding and Referencing/Line files developed this layer. Polygon features in Census_2010_Blocks_GA are subsets of Census_Blockgroups and Census_Tracts. A link to this data source is available here [23].

IV. TOOLS AND METHODOLOGY

We used the following tools to analyze and process data and explore trends and patterns.

1. ArcGIS, a scalable and secure software-as-a-service program hosted by the Environmental Systems Research Institute (ESRI), can process data and visualize the results. The ArcGIS Spatial Statistics toolbox provides predesigned statistical tools to analyze spatial distributions and identify patterns, processes, and relationships [24]. Specifically, we used the following tools on the ArcGIS platform.
 - ArcMap ModelBuilder: Provided by ArcGIS to create, edit, and manage models. ModelBuilder (Figure 4) can be viewed as a visual programming language for building workflows that string together sequences of geoprocessing tools [25]. We designed three models with ArcMap ModelBuilder to spatially join the 48 map layers of weather data from GaSDI and the Georgia GIS Clearinghouse website with the outage map layer [26].
 - Optimized Hot Spot Analysis Tool: Provided by ArcGIS, the optimized hotspot analysis tool can be useful to identify statistically significant hot and cold spots of outages using the Getis-Ord G_i^* statistic, which returns

a z -score for each feature in the dataset. For statistically significant positive z -scores, a larger z -score implies more intense clustering of high values (i.e., a hot spot). For statistically significant negative z -scores, a smaller z -score implies more intense clustering of low values (i.e., a cold spot). The Hot Spot Analysis tool calculates the Getis-Ord G_i^* statistic for each feature in a dataset. The resultant z -score tells where features with either high or low values cluster spatially. This tool works by looking at each feature in the context of neighboring features. A feature with a high value is interesting, but may not be a statistically significant hot spot. To be a statistically significant hot spot, a feature has a high value and is surrounded by other high-value features. The local sum for a feature and its neighbors is compared proportionally to the sum of all features; when the local sum is much different from the expected local sum, and that difference is too large to be the result of random chance, a statistically significant z -score results [27]. Because hot-spot areas are statistically significant, the end visualization is less subjective [27] (Figure 5).

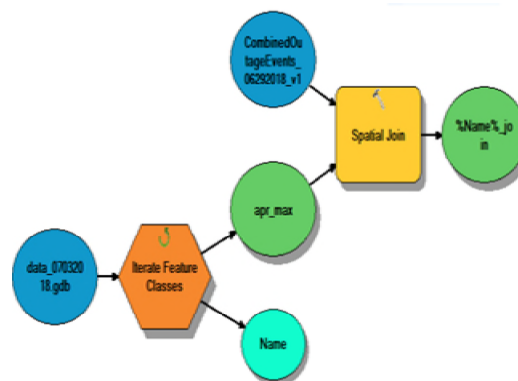


Figure 4. ArcMap ModelBuilder: Spatially Join Outages With Weather

2. GeoDa: a free software package that conducts spatial data analysis, geovisualization, spatial autocorrelation, and spatial modeling. GeoDa has powerful capabilities to perform spatial analysis, multivariate exploratory data analysis, and global and local spatial autocorrelation. It also performs basic linear regression [28].

The project methodology can be divided into seven steps:

1. Load data files from EPRI's Data Repository [22] to ArcGIS.
 - Created a folder (geodata set) and set up local projection to use Georgia's projection system.
 - Imported the data files from EPRI's data repository into the geodata set.
 - Imported basemaps (layers, maps, counties, tracks, roads, etc.) into the geodata set. Sources for Georgia shapefiles follow:
 - Roads shapefile <https://catalog.data.gov/dataset/tiger-line-shapefile-2013-state-georgia-primary-and-secondary-roads-state-based-shapefile>
 - County shapefile <https://www.census.gov/cgi-bin/geo/shapefiles/index.php?year=2010&layergroup=Counties+%28and+equivalent%29>

- Considering the enormous volume of data, a geodatabase to run more efficiently.

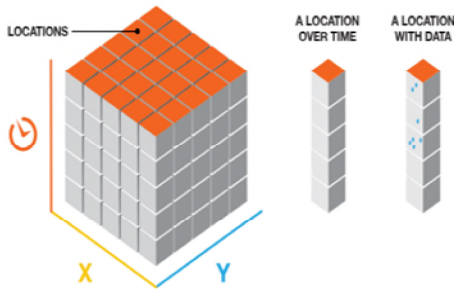


Figure 5. Emerging Hot Spot Analysis Tool [29]

2. Changed the projection of all maps to the World Geodetic System 1984 projection system. This step was necessary to perform calculations using ESRI or Google Earth tools.
 - Used Arc toolbox project (data management tools: Projection & Transformation) to change the projection.
3. Cleaned the outage-events map layer to exclude records that do not have a location (longitude and latitude).
4. Defined and created a study area for the project. Study areas are geographic boundaries to define the extent of analysis. They are typically created when starting a project to ensure the data are confined to a specified area. Only layers in the study area are considered in an analysis, so a study area can enhance processing time. Researchers use two methods or tools to create a smaller subset of data from a larger data set.
 - One way is to select a portion of an existing shape file and create a new layer file from it (or export that to a new shape file) using the ArcGIS select-by-location tool.
 - The other way is to clip an existing shape file using another polygon-shaped file (like using a cookie cutter) to create a new clipped version of the original shape file—ArcGIS Clip (analysis) tool (Figures 6 and 7).

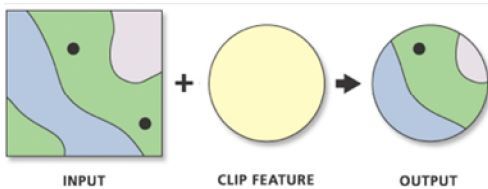


Figure 6. Clip Tool [30]

5. Selected data by block where population and power outage events intersect. This step ensures elimination of the impact of missing data.
6. Ran optimized hot-spot analysis to generate a map (Figure 8) of statistically noteworthy hot and cold spots of population using the Getis-Ord G_i^* statistic.

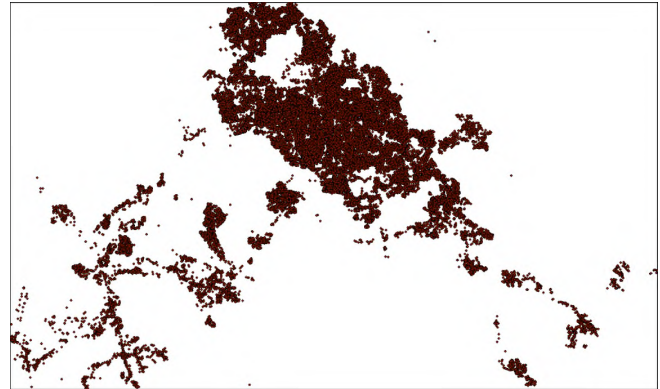


Figure 7. Clip (Analysis) Tool Output Map Layer

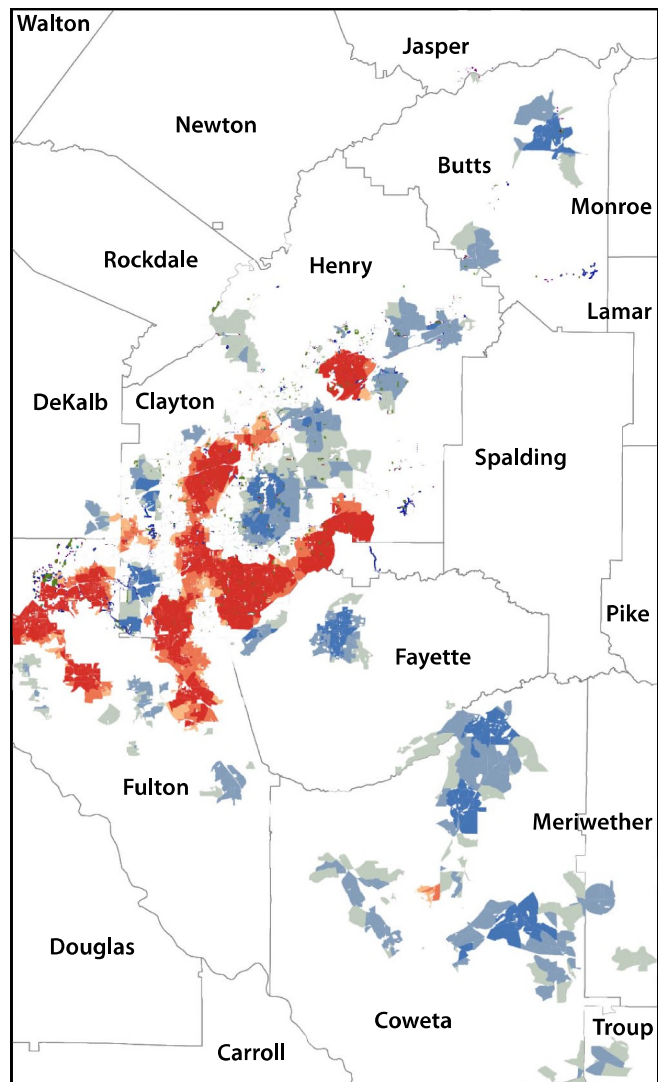


Figure 8. Population 2010 Census Data—Optimized Hot Spot Analysis

7. The final step is to investigate where population hot spots fall compared to the locations of optimized hot spots of power outage (Figure 9) and draw a conclusion.

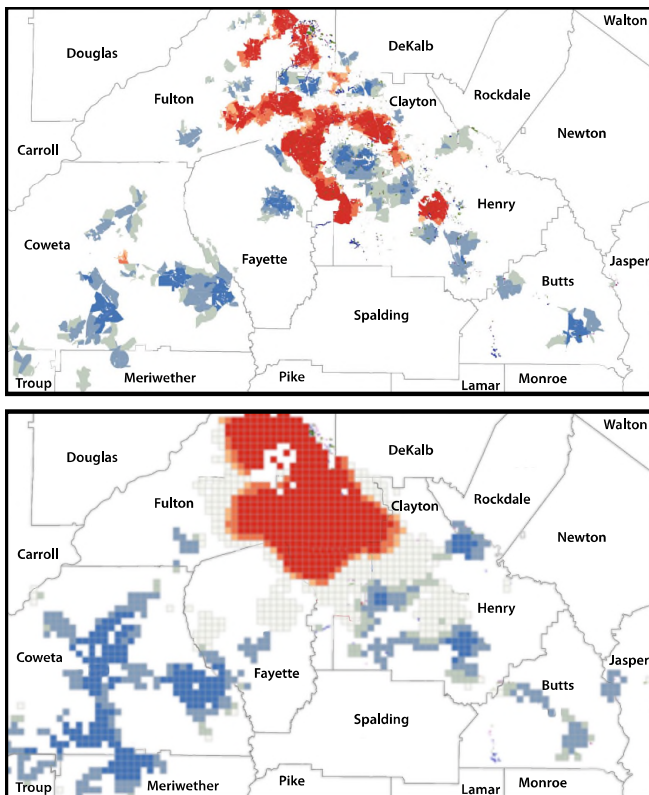


Figure 9. Population Hot Spots Compared to the Power Outage Hot Spots

V. RESULTS & DISCUSSION

From a visual comparison of the two maps, the majority of population hot spots fall in one big area of hot spots in Clayton and Fulton Counties where power outages are statistically significant. The only exception is the population hot spot in Henry County and south Clayton County where no statistically significant outages occurred (Figure 10).



Figure 10. Population Hot Spots Outside Statistically Significant Outage Areas

It appears that, due to the Underground (UG) structures used there, these population hot spots do not show statistically significant outages. UGs contributed to lessening the number of power-outage events so this high-population area is not an outage hot spot (Figure 11).



Figure 11. Underground Structures in Henry and South Clayton Counties

The GIS data has a field (CONSTRUCTION_TYPE) that helps identify UG versus Overhead (OH) assets in the DMI data. Also, the OMS of work-management data contains a field (srv loc) that specifies if the location is OH or UG.

VI. CONCLUSION

This study aimed to address how location analytics enhance understanding of power outages. To answer the research question, we explored GIS and aimed to identify a correlation between population density and power outages in Georgia. Initial investigation, using ArcMap software as a visualization tool, revealed areas where an association emerged between power-outage events and population density.

The GIS model presented in this study can help advance smart-grid reliability by, for example, revealing a root cause of power failure, defining a solution for a blackout through data, or implementing a solution with continuous monitoring and management. In this study, we show the novel use of location analytics to enhance power-outage understanding.

Future research should include analysis in ArcGIS Pro, which is ESRI’s next-generation desktop GIS product that provides professional 2D and 3D mapping and added tools to advanced visualization, analytics, and imaging.

From this research, we conclude that GIS offers a solution to analyze the electric-grid distribution system. Our model provides evidence that GIS can perform the analysis to investigate power-failure events and their causes. If additional funds and data become available, researchers can expand on this analysis, build on ArcMap source code, and create a custom solution for the utility industry to control and forecast power outages. GIS can be a main resource to assist electronic inspection systems, to lower the duration of customer outages, to improve crew-response time, and to reduce labor and overtime costs.

REFERENCES

- [1] K. LaCommare and J. Eto. *Understanding the cost of power interruptions to U.S. electricity consumers*. [Online, retrieved April 2019]. Available from <https://emp.lbl.gov/sites/all/files/lbnl-55718.pdf>
- [2] J. Eto. *The national cost of power interruptions to electricity consumers—A revised update*. [Online, retrieved April 2019]. Available from <http://grouper.ieee.org/groups/td/dist/sd/doc/2017-01-10%20National%20Cost%20of%20Power%20Interruptions%20to%20Electricity%20Customers%20-%20Eto.pdf>
- [3] President's Council of Economic Advisers and the U.S. Department of Energy's Office of Electricity Delivery and Energy Reliability, with assistance from the White House Office of Science and Technology. *Economic benefits of increasing electric grid resilience to weather outages*. [Online, retrieved April 2019]. Available from http://energy.gov/sites/prod/files/2013/08/f2/GridResiliencyReport_FINAL.pdf
- [4] J. Porter. (2018, June 12). *The \$306 billion question: How to make outage management better?* [Online, retrieved April 2019]. Available from <https://www.elp.com/Electric-Light-Power-Newsletter/articles/2018/06/the-306-billion-question-how-to-make-outage-management-better.html>
- [5] American Society of Civil Engineers. *2009 infrastructure fact sheet*. [Online, retrieved April 2019]. Available from http://www.infrastructurereportcard.org/2009/sites/default/files/RC2009_rail.pdf
- [6] D. Stone. It's the electric grid, stupid. September 9, 2011 [Online, retrieved April 2019]. Available from <http://www.thedailybeast.com/articles/2011/09/09/major-power-outage-shows-weakness-of-aging-electric-infrastructure.html>
- [7] K. Chayanam. *Analysis of telecommunications power outages due to power loss*. [Online, retrieved April 2019]. Available from https://etd.ohiolink.edu/!etd.send_file?accession=ohiou1125024491&disposition=inline
- [8] Westar Energy. *What causes power outages?* [Online, retrieved April 2019]. Available from <https://www.westarenergy.com/outage-causes>
- [9] Rocky Mountain Power. *Key causes of power outages*. [Online, retrieved April 2019]. Available from <https://www.rockymountainpower.net/ed/po/or/kcoco.html>
- [10] Diesel Service and Supply. *The many causes of power failures*. [Online, retrieved April 2019]. Available from http://www.dieselserviceandsupply.com/Causes_of_Power_Failures.aspx
- [11] R. Miller. *How to prevent downtime due to human error*. [Online, retrieved April 2019]. Available from <https://www.datacenterknowledge.com/archives/2010/08/13/how-to-prevent-downtime-due-to-human-error>
- [12] A. Freedman. *Weather and climate disasters cost the U.S. a record \$306 billion in 2017*. [Online, retrieved April 2019]. Available from https://mashable.com/2018/01/08/2017-record-year-billion-dollar-disasters-third-warmest/#92t4_Zb.Hmq7
- [13] Electric Reliability Council of Texas. *ERCOT responds to Hurricane Harvey*. [Online, retrieved April 2019]. Available from <http://www.ercot.com/help/harvey>
- [14] U.S. Energy Information Administration. *Hurricane Irma cut power to nearly two-thirds of Florida's electricity customers*. [Online, retrieved April 2019]. Available from <https://www.eia.gov/todayinenergy/detail.php?id=32992#>
- [15] P. Maloney. *Last year's weather, wildfires heighten utilities' storm hardening efforts*. [Online, retrieved April 2019]. Available from <https://www.utilitydive.com/news/last-years-weather-wildfires-heighten-utilities-storm-hardening-efforts/523666/>
- [16] Eaton's Blackout Tracker. *Power outage annual report*. [Online, retrieved April 2019]. Available from <https://switchon.eaton.com/blackout-tracker>
- [17] Wisconsin Public Service. *Why power outages occur*. [Online, retrieved April 2019]. Available from http://www.wisconsinpublicservice.com/home/power_occur.aspx
- [18] Davies Consulting. *State of distribution reliability regulation in the United States*. [Online, retrieved April 2019]. Available from <https://legalelectric.org/f/2010/04/stateofdistributionreliability-2005.pdf>
- [19] A. Kenward and U. Raja. *Blackout: Extreme weather, climate change and power outages*. [Online, retrieved April 2019]. Available from https://www.eenews.net/assets/2014/04/14/document_ew_01.pdf
- [20] R. J. Campbell. *Weather-related power outages and electric system resiliency*. [Online, retrieved April 2019]. Available from <https://fas.org/sgp/crs/misc/R42696.pdf>
- [21] National Academies of Sciences, Engineering, and Medicine. *Enhancing the resilience of the nation's electricity system*. Washington, DC: The National Academies Press. 2017. doi: 10.17226/24836
- [22] Electric Power Research Institute. EPRI Distribution Modernization Demonstration (DMD) data mining initiative. [Online, retrieved April 2019]. Available from <http://smartgrid.epri.com/DMD-DMI.aspx>
- [23] <https://www.arcgis.com/home/item.html?id=1cdf1cb3d51419299f7d1cc319bf2d3>
- [24] L. Scott, and M. Janikas. "Spatial statistics in ArcGIS," in M. Handbook of applied spatial analysis: Software tools, methods and applications, M. Fischer and A. Getis, Eds. Berlin: Springer-Verlag, pp. 27–41, 2010. doi:10.1007/978-3-642-03647-7
- [25] Environmental Systems Research Institute. *What is ModelBuilder?* [Online, retrieved April 2019]. Available from <http://resources.arcgis.com/en/help/main/10.2/index.html#//002w0000001000000>
- [26] Georgia Spatial Data Infrastructure. *About*. [Online, retrieved April 2019]. Available from <https://www.georgiaspatial.org/gasdi/about>
- [27] Environmental Systems Research Institute. *How hot spot analysis (Getis-Ord Gi*) works*. [Online, retrieved April 2019]. Available from <http://desktop.arcgis.com/en/arcmap/10.3/tools/spatial-statistics-toolbox/h-how-hot-spot-analysis-getis-ord-gi-spatial-stati.htm>
- [28] L. Anselin and S. J. Rey. *Modern spatial econometrics in practice: A guide to GeoDa, GeoDaSpace and PySAL*. Chicago: GeoDa Press, 2014.
- [29] Environmental Systems Research Institute. *Emerging hot spot analysis*. [Online, retrieved April 2019]. Available from <http://pro.arcgis.com/en/pro-app/tool-reference/space-time-pattern-mining/emerginghotspots.htm>
- [30] Environmental Systems Research Institute. *Clip (Analysis)*. [Online, retrieved April 2019]. Available from http://webhelp.esri.com/arcgisdesktop/9.3/index.cfm?TopicName=clip_%28analysis%29

Adversarial Resilience Learning

— Towards Systematic Vulnerability Analysis for Large and Complex Systems

Lars Fischer^{*†}, Jan-Menno Memmen[†], Eric MSP Veith[†], Martin Tröschel[†]

^{*}Universität Oldenburg, [†]OFFIS e.V.

Escherweg 2

26121 Oldenburg, Germany

Email: ^{*}l.fischer@uol.de, [†]{eric.veith,martin.troeschel}@offis.de

Abstract—Cyber-physical systems (CPSs) can be checked using numerous approaches, ranging from algorithmic model checking for a complete coverage of a finite-state system to extensive simulation, after which the system’s state is compared with defined invariants. However, modern CPSs are confronted with an increased amount of stochastic inputs, from volatile energy sources in power grids to broad user participation stemming from markets. The search space for a complete cover of a CPS becomes too large, while contracts cannot be formulated anymore considering the potentially erratic behavior of a user, or even in the face of a cyber attack. At the same time, the goal of resilience critical infrastructure cannot be eschewed, but the integration of user behavior and even non-checkable artificial intelligence algorithms is mandated, even required to meet, e.g., the goal to satisfy 80% of the gross power consumption from renewable energy sources by 2050. The concept of Adversarial Resilience Learning (ARL) formulates a new approach to CPS checking and resilient operation. It defines two agent classes, attacker and defender agents. The goal of the attacker is to de-stabilize the CPS, whereas the defender works to maintain a stable operational state. The quintessence of ARL lies in the attacker training the defender on a model of the CPS; as such, it is not a zero-sum game, but the learning of a resilient operation strategy for a CPS. This paper introduces the concept and the nomenclature of ARL, and, based on it, the description of experimental setups and results of a preliminary implementation of ARL in simulated power systems.

Keywords—agent systems; reinforcement learning; adversarial control; resilience; power grid

I. INTRODUCTION

Current newspapers are full of horrific tales of “cyber-attackers” threatening our energy systems; the December 2015 Ukraine power grid cyberattack is a particularly notable one [1], [2], which has seen a continuation in 2017 [3]. And, if not for the notorious “evil state” actor, it is the ongoing digitization necessary to enable increasing renewable and volatile energy generation that threatens our energy supply and thus the stability of our society. While the main approach seems to be to patch-up the detected vulnerabilities of protocols, software and controller devices, our approach is to research and develop the means to systematically design and test systems that are structurally resilient against failures and attackers alike.

Security in cyber-systems mostly should be concerned with establishing asymmetric control in favour of the operator of a system. In order to achieve this on a structural level at design time, reproducible benchmark tests are required. This is notoriously difficult for intelligent adversaries whose primary abilities are adaption and creativity. Thus, testing methods

nowadays are either reproducible, but insufficiently model an attacker; or they involve unreproducible human elements. Reinforcement Learning (RL) may be useful to provide at least some adaptability of reproducible attacker models.

This work takes its motivation and first practical implementation from the power system domain, but the work can directly be applied to all highly complex, critical systems. Systems that may benefit from Adversarial Resilience Learning (ARL) are too complex to be sufficiently described using analytic methods, e.g., because the number of potential states is too large and the behaviour is too complex with too many non-trivial interdependencies. This also includes stochastic external factors, such as the behavior of market actors.

This work introduces ARL, which provides a method to analyze complex interdependent systems with respect to adversarial actors. The foremost motivation is to provide a method for analysis based only on an interface description of an agent’s sensors and actuators in the cyber-physical system (CPS). We expect ARL to identify potentially unknown vulnerabilities. A key part of ARL is to identify the minimal chain of actions required to reproduce a vulnerability; this effectively entails both the ARL nomenclature introduced in the paper as well as careful Design of Experiments (DoE).

The main contribution of this paper is the introduction of a novel structure for training agents competing against each other on a model of a CPS without explicitly perceiving each other’s actions. By setting up RL-based agents in a competitive situation, the learning-complexity is comprised not only of a highly complex system, but also of competing agents, whose changing state, manifested by modified behaviour of the system under consideration, has to be included in the trained model. We assume that this provides a very interesting new problem class for RL, as it introduces a cyclic learning competition.

The paper is structured as follows. First, a brief introduction into related techniques in machine learning and related work for complex system analysis is given in Section II. The paper then defines the concept of ARL in Section III, and introduces its application to adversary testing in power system control in Section IV. The paper is completed by a presentation of lessons learned and results from an early proof-of-concept demonstrator in Section IV-B. It concludes with a discussion and an outlook in Section V.

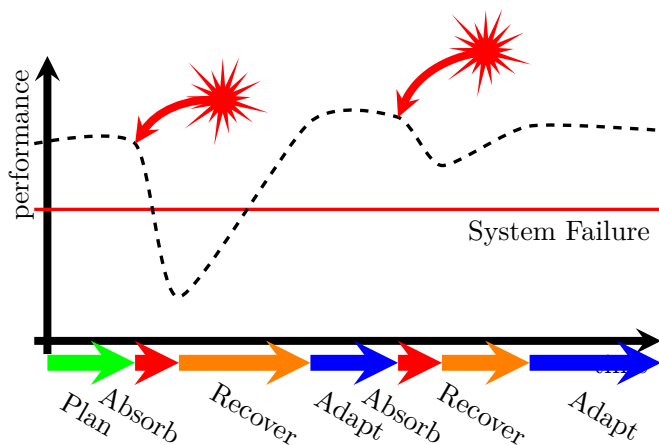


Figure 1. Resilience Process for system performance

II. RELATED WORK

This work aims at exploring the feasibility of improving resilience of complex systems using machine learning to train adaptive agents. The term *resilience* is lacking a coherent and precise definition across fields. Generally, it denotes the ability of a system to withstand unforeseen, rare and potentially catastrophic events, recover from the damage and adapt by improving itself in reaction to these events. Ideally, resilience is increasing monotonously throughout system improvement. A useful simplification is observation of the changing behaviour of system performance as an artefact resulting from resilience processes. Different formalization of resilience processes exist, but most distinguish subprocesses for planning, absorption of damage, recovery (or self-healing) and improvement (or adaptation) [4].

See Figure 1 for an expression of a hypothetical system's performance suffering twice from damaging events. Resilience is modelled as a sequential process: *plan*, *absorb*, *recover*, and *adapt* [5]. As consequence of the first event, the performance of the system is pushed below a *failure threshold*, i.e., the system fails to provide its service. Improvement of the system is then achieved after recovery as the system is able to keep the performance above the failure threshold during the second event.

A. Analysis and Stochastic Modelling

The main distinction of our approach as compared to game theoretic modelling and stochastic analysis is the use of co-simulation and heuristic approaches instead of formal abstraction of complete systems. The underlying assumption is that a system-of-systems is too complex and malicious adversaries are too unpredictable to be sufficiently analyzed.

Traditional analysis of CPSs has either checked for liveness ("something good eventually happens") or safety requirements ("nothing bad ever happens") through mathematical modelling and model checking, using temporal logic, decision trees, or similar devices, or by employing discrete simulations over k timesteps and checking against formulated invariants [6],

through which stochastic effects can be introduced. Complexity has usually been abstracted away by contracts; combining contracts and simulation is still a topic of research [7].

Compared to Attacker-Defender Models, described by, e.g., Brown et al. [8], that aim at analyzing an equilibrium between attackers and defenders in dynamic systems, our work heuristically approaches an estimate of the asymmetry of attacker and defender in these systems. The approach of ARL is structurally similar to the concept of *Stackleberg Competitions* and related applications of stochastic analysis, e.g., pursuit-evasion in differential games [9]. These approaches seem to only be applicable to scenarios that can be restricted to few degrees of freedom. More realistic behaviours of opportunistically acting threat agents within complex system-of-systems leads to an explosion of states in analytic approaches.

Recent surveys seem to support this view. Referenced approaches on power systems by Do et al. [10] provide no details on the used game-theoretic model and use ambiguous terminology of the researched threat scenarios. Approaches in Machine Learning (ML) to tackle complex problems, on the other hand, have been very successful in providing practical solutions.

B. Machine Learning

Artificial Neural Networks (ANNs) are universal function approximators, meaning that they can be used as a statistical model of any Borel-measurable function $\mathbb{R}^n \mapsto \mathbb{R}^m$ with desired non-zero error [11]–[13]. Already the standard Recurrent Neural Network (RNN) has the capacity to approximate any non-linear dynamic system; Siegelmann and Sonntag have shown that RNNs are turing-complete [14]–[16].

In practice, a typical problem for which RNNs, especially structures containing Long-Short Term Memory (LSTM) cells [17] or Gated Recurrent Units (GRUs) [18], [19] are used, is time series prediction. Predicting a time series with an RNN constitutes the instantiation of a (non-linear) dynamic system [20]–[22], i.e., the prediction is the result of the system's behavior, which is, in turn, modeled and approximated by the RNN. Cessac has examined ANNs from the perspective of dynamical systems theory, characterizing also the collective dynamics of neural network models [23].

For ARL, we assume a common model that is used by two distinct agents: while one probes the model for weaknesses in order to find attack vectors, the other monitors the system and, unbeknowing of the presence of the attacker or its actions, works at keeping the system in its nominal state. Through this structure, the notion of ARL assumes that the model—i.e., each agent's environment—is not completely known to the respective agent. Therefore, the usage of RL readily suggests itself. In a setup such as ARL provides, RL is the natural choice for learning algorithms [24]–[26].

Even though in theory, the notion of RL is not tied to ANNs per se [27], the incremental training process makes them suitable for RL in contrast to other structures, such as decision trees, which usually need the full data set for effective training. For training ANNs and RNNs supervisedly, which is

a core task in RL, gradient-decent-based algorithms of the Backpropagation-of-Error family are leading by far [28]–[32], followed by evolutionary algorithms, such as CMA-ES [33]–[35] or REvol [36], [37]. In theory, RNNs have the capacity to simulate arbitrary procedures, given the proper set of parameters; in practice, this training task has proven to be complicated. Neural Turing Machines, such as the Differentiable Neural Computer (DNC) introduced by Graves et al. [38], [39], counter the complexity with a vastly increased addressable memory space and have shown to be able to simulate simple, but complete algorithms like sorting. In theory, DNCs at the core of ARL would make the concept itself transferable to similar CPSs once trained, as well as to allow a variable set of sensors and actuators over time.

However, all optimization methods adapt the ANN to minimize a cost function and not directly to create a model of a problem; this happens only indirectly. As a result, ANNs can still be “foiled,” i.e., made to output widely wrong results in the face of only minor modifications to the input. This effect and how to counter it is the subject of Adversarial Learning (AL) research. Even though seemingly similar by name, ARL should not be confused with AL, as the core problem of ARL is not the quality of sensory inputs, but the unknown CPS being subject to ARL execution. The concept we propose in this paper is related to AL only insofar, as both concepts use two distinct ANNs with conflicting objectives [40].

A second concept that is potentially similar in the name only is that of Generative Adversarial Networks (GANs): With unsupervised learning, the ANN tries to detect patterns in the input data that diverge from the background noise. Unsupervised learning does not use the notion of expected output [41]. In GANs, a modern application of unsupervised learning has emerged. Here, one network, called the generator network, creates solution candidates—i.e., maps a vector of latent variables to the solution space—, which are then evaluated by a second network, the discriminator [42]. Ideally, the results of the training process are virtually indistinguishable from the actual solution space, which is the reason GANs are sometimes called “Turing learning.” The research focus of ARL is not the generation of realistic solution candidates; this is only a potential extension of the attackers and defenders themselves. ARL, however, describes the general concept of two agents influencing a common model but with different sensors (inputs) and actuators (output) and without knowing of each others presence or actions.

The abstract notion of a model can see multiple instantiations; one such instantiation of ARL would be using a power grid as the model considered by both agents. Ernst et al. employ RL for stability control in power grids [43]. In their paper, they design a dynamic brake controller to damp large oscillations; however, since the reward function is easily well-defined, there is no need for using an ANN for function approximation.

III. ADVERSARIAL RESILIENCE LEARNING

ARL is distinguished from AL by the recurrent structure in which adversary and defender are interacting. While GAN directly connect a generating adversary with a detecting defender, ARL adversary and defender interact only through the system they are using for input and output. In this interaction adversaries are identified as agents inserting disturbances into the system, while defenders provide resilience control.

Definition 1 (Adversarial Resilience Learning (informal)). ARL is an experimental structure comprised of two disjoint groups of agents and a system or simulated system. The agents are distinguished as attacker and defender by adhering to conflicting optimization objectives. Both groups of agents receive their input from a, potentially overlapping, set of measurements from the system. They influence the system through two disjunct sets of outputs connected to controls in the simulated system.

A. Fundamental Notation and Model

The basic abstract scenario using ARL consists of two competing agents and a system model. Each of the three elements resembles a state transition. In order to establish a sound formal base, a definition of notation and processes of ARL is provided here. A summary of notations used is given in Table I.

ARL consists of a set of agents, where each agent has a model, denoted by \mathcal{A} , and a model of a system, \mathcal{M} . The agent model \mathcal{A} serves as a “blue-print” for the actual behavior of a running system; similarly, \mathcal{M} denotes a static model of a world. An index identifies a particular agent model, e.g., \mathcal{A}_A denotes the category of attacker models, \mathcal{A}_Ω serves to denote the category of defender models. At run-time, the models are instantiated. We denote instances of a model with lower-case letters a , where the superscript denotes a particular state of the model, such as $a^{(t)}$, with t commonly referring a point in simulation time. In the same vein, $m^{(t)}$ denotes an instance of a world model at t .

Each agent tries to maximize its rewards by approximating the agent-specific performance function,

$$p_a \left(m^{(t)} \right) . \quad (1)$$

For an agent, the performance function $p_a(\cdot)$ is equal to its reward function in RL terminology. However, the notion of the *performance* function lets us decouple agent behavior from the desired/intended or undesired performance of the world, denoted by

$$p \left(m^{(t)} \right) , \quad (2)$$

as the difference between the world’s current performance to its nominal performance, p^* .

Agents are categorized through their performance function, an agent model is identified as attacker model \mathcal{A}_A if his reward function p_a behaves inverse to the systems performance. The opposite is true for agents from \mathcal{A}_Ω . Thus, we can define:

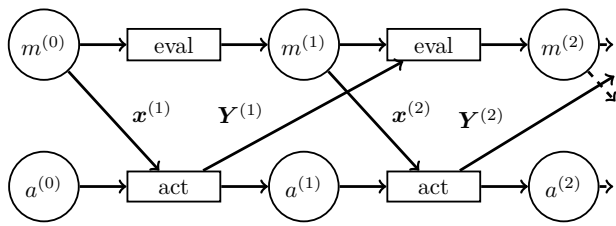


Figure 2. ARL sequence of execution

Definition 2 (Attacker and Defender Classes). For all times t and model instances $m \in \mathcal{M}$, the following provides a classification rule for attackers and defenders:

$$\begin{aligned} a \in \mathcal{A}_A &\Rightarrow p_a(m^{(t)}) \approx p(m^{(t)}), \\ a \in \mathcal{A}_\Omega &\Rightarrow p_a(m^{(t)}) \sim p(m^{(t)}). \end{aligned} \quad (3)$$

The performance of an agent is tightly coupled to an agent's view of its environment, which can change over time as an agent gains control over more sensors (or loses it). Thus, each $p_a(\cdot)$ can only be defined in terms of the agent's sensory inputs. The portion of the state of a system instance an agent a can observe is denoted by

$$\mathbf{x}_a^{(t)} = \psi_a(m^{(t)}). \quad (4)$$

The agent can act by approximating its reward function $p_a(\cdot)$. This approximation is the agent's activation of its internal dynamic system approximator $\text{act}(\cdot)$; implemented through, e.g., an RNN or DNC, expressed in a mapping such that

$$\text{act}_a : (a_t, \mathbf{x}_a^{(t)}) \mapsto (a^{(t+1)}, \mathbf{Y}_a^{(t)}), \quad (5)$$

where we assume that an agent can choose not to act, just as in a classical RL approach, and where \mathbf{y} denotes the probabilities of an agent's action policy, i.e., $\forall y_1, \dots, y_i, \dots, y_n, y_i \in [0; 1]$ denotes the probability that the agent uses its i th actuator. In ARL, $\mathbf{Y}_a^{(t)}$ denotes a matrix, in which the aforementioned \mathbf{y} constitutes the first column vector, and all other elements are set points of the agent's actuators. Each agent defines an action policy for controlling its actuators.

However, this direct mapping of each y_i to an actuator constitutes only the simplest case. In general, an action policy takes on a form that is suitable for the whole action search space, such as a policy network steering a monte carlo tree search as has been shown in [44]. Thus, an agent is acting through the evaluation and application of its system approximator. This happens for each agent individually. In brief, the systems behavior is heavily influenced by the set of all actuators that can be controlled by the respective agents. Thus, an agent does not simply perceive a model (or a part thereof), but the state of the model as the result of all agents acting upon it. Thus, an agent does not simply create an internal representation of a dynamic system, but of a dynamical system-of-systems.

TABLE I. ARL NOTATION.

Symbol	Description
m of \mathcal{M}	An instance of a system model
a of \mathcal{A}	An instance of an agent model
$\mathcal{A}_A, \mathcal{A}_\Omega$	Attacker model, defender model (Definition 2)
$p(\cdot) \in \mathbb{R}_+$	Performance function
p^*, p^f	Reference performance of normal operation, of failure threshold
$p(m^{(t)})$	Overall performance of a system instance m at time t , (2)
$p_a(m^{(t)})$	Performance with respect to the objectives of agent instance a at t given the system instance m , (1)
$\psi_a(m^{(t)})$	Observation function mapping a system model to the inputs available to agent a , (4)
$\mathbf{x}_a^{(t)}$	Inputs to agent a at t , (4)
$\mathbf{Y}_a^{(t)}$	Actions y of a at t , (5)

Finally, the simulator evaluates the actions of all agents applied to the world model at t , $m^{(t)}$. This is represented by the evaluation mapping,

$$\text{eval} : (\mathbf{Y}^{(t)}, m^{(t)}) \mapsto m^{(t+1)}. \quad (6)$$

Note that if the activation vectors of the participating agents consider a disjoint set of controllers, i.e., the actions application is commutative, the transition of the world state from $m^{(t)}$ to $m^{(t+1)}$ is the result of an aggregation of all agents' actions $\mathbf{Y}^{(t)}$. Non-commutative application of actions is out of scope of this work.

B. Formal Definition

Using the notation introduced here and summarized for reference in Table I, we define the concept of ARL as model and connection setup with transition process in the following way.

A setup in ARL is comprised of agents a_1, a_2, \dots, a_n instantiated from a models $\mathcal{A} \in \{\mathcal{A} \cup \Omega\}$ with $|\mathcal{A}| > 0$ and $|\Omega| > 0$. Each agent is related to a set of inputs \mathbf{X}_a and a set of outputs \mathbf{Y}_a . Further, the setup requires a world model \mathcal{M} that provides a set of sensors \mathbf{X}_m and controls \mathbf{Y}_m .

The central process of ARL is the dynamic system-of-systems view of a set of agents a_0, a_1, \dots, a_n acting upon a shared instance of a world model. Activation functions $\text{act}_a(\cdot)$ of agents and application $\text{eval}(\cdot)$ of agent agents to a world model form a cyclic sequence of activation and application that transforms the states of model and agents into a sequence of states as shown in Figure 2.

An experiment of ARL is the execution of this sequence. The resulting data of an experiment is the sequence of states and outputs as well as the initial setup $m^{(0)}, \mathbf{a}^{(0)}$. The vector of evaluations, i.e., states and outputs, $[\text{eval}_a^{(1)}, \dots, \text{eval}_a^{(t)}, \dots, \text{eval}_a^{(n)}] \forall a$, contains the minimal chain of actions necessary to exploit a CPS, iff this is the final result of an ARL execution. Thus, we can finally strive to formalize the idea by collecting all components in a single scenario:

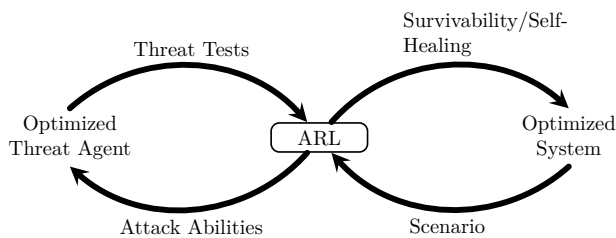


Figure 3. Optimization Objectives

Definition 3 (Adversarial Resilience Learning Scenario). Any experimental setup is comprised of agent instances a of \mathcal{A} of two opposing classes, \mathcal{A} and Ω , and a system model \mathcal{M} , as well as, for each agent instance a , a reward function $p_a(m^{(t)})$, a mapping of observable states $x_a^{(t)}$ and action matrices $Y_a^{(t)}$.

Thus, ARL is the application of RL, as introduced in Section II-B, to iteratively improve the internal decision structure that determines the behaviour of an agent's $act_a(\cdot)$. The output of ARL then is, depending on the experimenters objectives, an observation of the performance of the system model \mathcal{M} or a set of agents trained towards the defined objectives.

C. Optimization Problem Statement

This section describes possible optimization problems that provide the motivation for ARL.

ARL resembles a closed-loop control situation with (at least) two conflicting controls. Herein are distinguished two different optimization objectives that provide different uses of ARL. The different uses, as depicted in Figure 3, improve different elements to achieve either an improved threat test, or a more resilient system. The primary distinction is between evolving parameters of ANN in order to optimize individual agents or step-wise advancing the structure of the system model. Our concept itself is oblivious to the algorithms used for optimization.

1) *System Optimization*: The primary objective is to find the inherent control asymmetry of a given control system to finally recommend system designs that favor the defender over the attacker. In control theory this could be expressed as a system, where, for all possible sequences of actions by the attacker for a given system model \mathcal{M} , there is at least one corresponding sequence of actions for the defender, and the resulting performance of the system will never drop below a given failure threshold. This requirement can be relaxed by defining a finite measure of failure that may be acceptable, for example during an initiation phase.

The objectives of defender and attacker in control scenarios are focused on system states measured by a model performance function (2), as formally given in Definition 2. In general, we call an agent *defender* if its objective is to keep the performance at least above the failure threshold. We denote an agent as *attacker* if it aims at pushing the performance below an expression for a failure threshold, as seen in Figure 1.

We denote the objective of asymmetry—favouring defence of a system—given a candidate system model instance m and defender agent a_Ω as:

$$p^f < p(m^{(t)}) \text{ for all } t > t^{(0)}. \quad (7)$$

Hence, given any attacker, there exists an (optimal) defender a_Ω^* that ensures that the system performance never falls below a failure threshold p^f . To account for a learning period, we allow for a finite initialization time until $t^{(0)}$. Note that this potentially also excludes black starts. For fully initialized agents competing in a black-start scenario, (7) must hold for all t .

Improvement is achieved by evolutionary changes to the system model \mathcal{M} , improved defensive agent models \mathcal{A} or training of defensive agents a_Ω , as discussed in the following section.

2) *Agent Training*: Training of threat agents aims at improving attack abilities, including the identification of previously unknown attack vectors, in order to provide testing capabilities. Improved threat tests allow to define test requirements for system designs that improve systems resilience against security threats. One objective is to train threat agents that can be used as benchmarks for future system designs.

An agent's objective is implemented through a *reward function* that is used within a RL process that successively improves the agent's behaviour towards that objective.

One particularly surprising success of RL algorithms has been the identification of solutions unthought-of by experts, especially if applied to zero-information initial states. A two-agent, conflicting-objectives game only one potential learning structure usable with ARL. But the concept allows potentially for all combinations of one-or-many zero-information RL agents and static or even human-controlled competition.

IV. APPLICATION TO POWER SYSTEMS

Applied to power systems, the performance function is expressed as a diversion from a specified range of acceptable state values. Such state values include voltage, but can also be frequency response in dynamic simulation. The attacker's objective is to force the system to a state where one or more values are outside allowed ranges; its success is measured by the amount and duration of the deviation. The defender has lost the competition if the attacker is able to divert any of the system's parameters beyond the acceptable range. Specific objectives for attackers can vary widely as there are many different parts of a power system that can be affected in order to disrupt service and reduce system performance. Attackers may aim at the demolition of connected machines or components of the transmission and control system. Thus, to strive for a more general specification of objectives, we better consider the objectives of defenders and specify a deviation from these objectives as success for the attackers.

Different specific requirements apply for different parts of the power system, also depending on whether steady-state or dynamic simulation is required. Common parameters

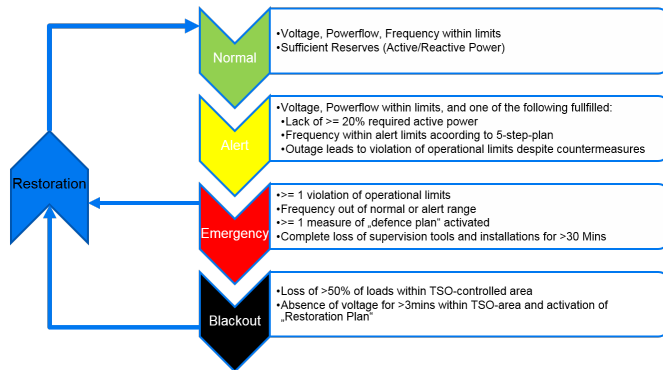


Figure 4. ENTSO-E Operational Phases

to consider are voltage, frequency and frequency response, and real and reactive power. In general, phase synchronicity is more important for high-voltage transmission grids, as asynchronicity leads to harmonics in the power system, with potentially disastrous large power flows between large segments of the grid. For the European transmission grid, the operation guidelines define conditions for four phases: *normal*, *alert*, *emergency*, and *blackout*, as shown in Figure 4.

Similarly operational parameters exist for medium- and low-voltage grids, power generation and connected loads. DIN EN 50160 specifies parameters for the operation of distribution grids: Acceptable voltages range from 0.9 pu to 1.0 pu. It is acceptable, by definition in EN 50160, that voltage drops down to at least 0.85 pu for at most 5% of a week. Frequency must only deviate from the nominal 50 Hz by at most 4% above or 6% for not more than 0.5% of the year, i.e., less than 2 days overall. Normal operation must deviate no more than $\pm 1\%$ [45]. Accordingly, an attacker is successful if any of these values exceeds the defined limits.

Figure 5 shows the refinement of the generic ARL-structure as described in Section III. Both agents interact only through sensors and actuators that influence different controls in the power grid.

In the remainder of this section, we introduce a proof-of-concept implementation of ARL using pandapower [46] for stationary grid simulation and the Keras-RL library [47] for RL algorithms, specifically Deep Q-Learning. First, a brief description of the control scenario is provided, followed by a discussion of the preliminary results.

A. Static Control Scenario

The objective of this proof-of-concept is to show the general feasibility of using (multiple) ANN-heuristics and train them by RL to modify controls in a stationary power system simulation towards their objectives.

The simulation uses a simple medium voltage power grid as model from the grid simulation software pandapower [46]. The grid contains four generators, six loads, and six transformers. We chose to only use voltage as state-indicator and input to the reward of the attacker. The initial configuration of the grid comprises of a stable, healthy state of the grid that would be

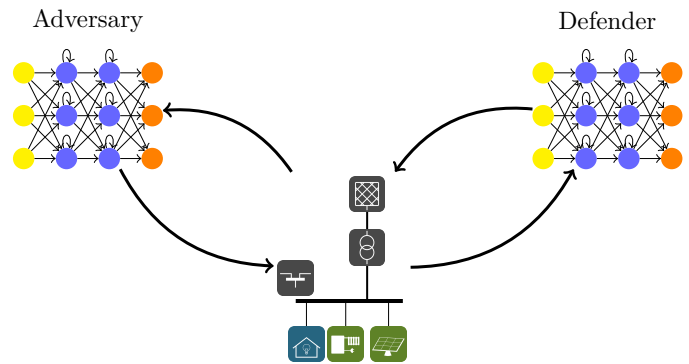


Figure 5. ARL ANN structure

held up constantly if no control actions would be initiated. Actuators in this scenario are: tap positions, reactive power control, and loads and generation levels as represented by the commonly deployed and future automated controls in power systems.

The reward function for the attacker is shown in Figure 7a. Initial trials pointed towards the inverse of a Poisson Density Function centered on the nominal voltage unit. The reward function thus resembles the objective for an attacker, providing only positive rewards if the mean voltage deviates more than 5% from the nominal voltage. The single agent in this demonstration had been assigned direct control of every transformer, generator and load in this scenario.

In terms of optimization from Section III-C, the scenario instantiates m with a single agent $a \in \mathcal{A}_A$ with a parametrized normal distribution,

$$p_a(m^{(t)}) = -1^{[a \in \mathcal{A}_A]} \exp \left[-\frac{(\overline{\psi_a(m^{(t)})} - \mu)^2}{2\sigma^2} \right] - c, \quad (8)$$

where c , μ and σ parametrize the reward curve, $-1^{[a \in \mathcal{A}_A]}$ negates the reward if a is an attacker [48], and $\overline{\psi_a(\cdot)}$ is the arithmetic mean of all inputs. Note that this reward function does not include any information specific to the energy domain. E.g., it treats the difference between 1.0 pu and 0.8 pu similar to a reduction to 0.5 pu, even though this would mean a tremendous success to the attacker compared to a reduction to 0.8 pu. This simplification was done deliberately to verify the general feasibility of the ARL concept without explicitly tying it to the energy domain, but to remain useful to any CPS.

B. Demonstrator

In order to show the general feasibility of the concept, we implemented a demonstrator for RL in power control scenarios. The current implementation uses static simulation in pandapower [46], supporting free configurability of controlled sensors and actuators of multiple agents, selection of ANN-algorithms and -parameters, as well as different logging and output formats.

In order to support documentation and reproducibility, each experiment is specified within a single configuration file. A experimental configuration defines three major simulation components: a grid model, one or more agents, and a collection of result logs that collect results. At the time of writing, the whole demonstrator is refactored to use the mosaik co-simulation framework [49], [50].

The interconnection between agents and grid simulation, i.e., x_a and Y_a respectively, are separately defined for each agent.

The execution of the simulation is round-based. The rounds are advanced in steps according to a defined evaluation order of agents. Agents are sequentially executed, a defined number of steps each. The grid state is evaluated between each consecutive pair of agent evaluation steps. After each step, RL takes place for each agent individually according to its configuration. Current result monitors output the grid states at every node of the grid into a grid-state log. The results are graphically evaluated as is discussed in Section IV-C below.

C. Results

To show the usability of our demonstrator, we pitched two simple agents with inverse reward functions (Figure 7a and Figure 7d) against each other, using the example grid shown in Figure 6a as an arena. Both agents were assigned all voltage sensors as input. The attacker was assigned control of all tap changers, representing a scenario where a vulnerability in one type of controller was exploited. The defender would be granted access to all generators and loads in this scenario. This was a deliberate choice in order to force the defender to develop a strategy that involved all generators and loads; in a reverse scenario, control of the tap changers would allow the defender to act easily against a series of attacker actions and would require a more sophisticated experiment setup involving, e.g., a digital twin in the attacker code for decoupled RL training for a devastating one-shot attack.

Figure 6 shows a late state of the simulation. Seemingly, the attacker gained the upper hand and has been able to increase voltage levels beyond 1.05 pu. The grid representation in Figure 6a shows that especially two central sensors (numbered 4 and 3) are stuck with very high voltage levels, represented by the length of the bars rooted at the nodes, most likely sufficient for the connected loads to shut down or be damaged. The mean voltage level of the system, depicted for steps 1900 to 2000 in Figure 6b, shows that even the lower voltages of other nodes are not sufficient to lower the mean voltage to acceptable levels. Thus, in this example, the attacker has been able to destabilize the grid, despite the efforts of the defender.

Evaluating the two agents in Figure 7 provides no immediately conclusive cause for the loss of the defender. The cumulative number of positive rewards in Figure 7b for the attacker and Figure 7e, show only small differences. These asymmetries might be explained by the order of execution, where the defender always acts in response to the attacker. The current reward for the depicted step in the simulation, depicted in Figure 7a and Figure 7d, shows that the defender

is evaluating a different mean voltage than the attacker. As rewards are calculated after the actions of an agent, thus these graphs show the results of two actions that both improved the performance towards their own objectives.

The effect of the ARL structure of competing agents that is beneficiary for RL algorithms becomes apparent in positive learning curves for both agents (Figure 7b and Figure 7e). In preliminary tests with a lone attacker, the learning process first went through a lengthy phase where only little positive rewards were achieved.

V. CONCLUSION AND FUTURE WORK

This work introduced Adversarial Resilience Learning (ARL), a novel approach to analyze cyber-physical systems (CPSs) through competitive situations in highly-complex systems using self-improving agents. This work is motivated by the need to find better methods to evaluate the behaviour of CPSs under threat of maliciously acting, intelligent threat agents. The main idea is that groups of agents struggle to enforce their objectives against agents with conflicting goals.

Pitching two—or more—Reinforcement Learning (RL) agents with conflicting reward functions against each other may allow to define more realistic tests for adversarial or competitive situations. It harbours the promise of finding novel strategies for both attack and defense, which both can be used to strengthen the resilience of systems during the design and testing phase of a power system or individual components. ARL-based analysis should contribute to building grid structures that are more resilient to attacks and train both artificial and human operators in better handling of security incidents.

Generally, the concept may allow to estimate threat-related indices, for example the maximum amount of control that an adversary may be allowed to gain over a system, which leads to improved and more effective recommendations for security directives and risk mitigations.

The concept of ARL and its ongoing implementation in the ARL-Demonstrator only marks the starting point for in-depth research on structural asymmetries of complex systems and protection against learning threat agents. The demonstrator provides the abilities to further research in a number of interesting directions.

Foremost, this is the analysis of structural resilience of complex systems, especially finding minimum control sets of critical components that provide the most defensive capabilities, or estimates of the structural strength of a system. The integration into our co-simulation framework mosaik opens up the possibility of extending the single system into a whole composition into an interdependent system-of-systems. In the energy domain, the introduction of communications infrastructure (SCADA, CDMA450, etc.) is necessary.

Deeper extensions of the demonstrator itself will involve capabilities of the defender to affect structural changes to the system. This would allow to use RL to identify novel and more resilient structures. The dual ability for threat agents would be the extension of control, i.e., simulation of further compromise

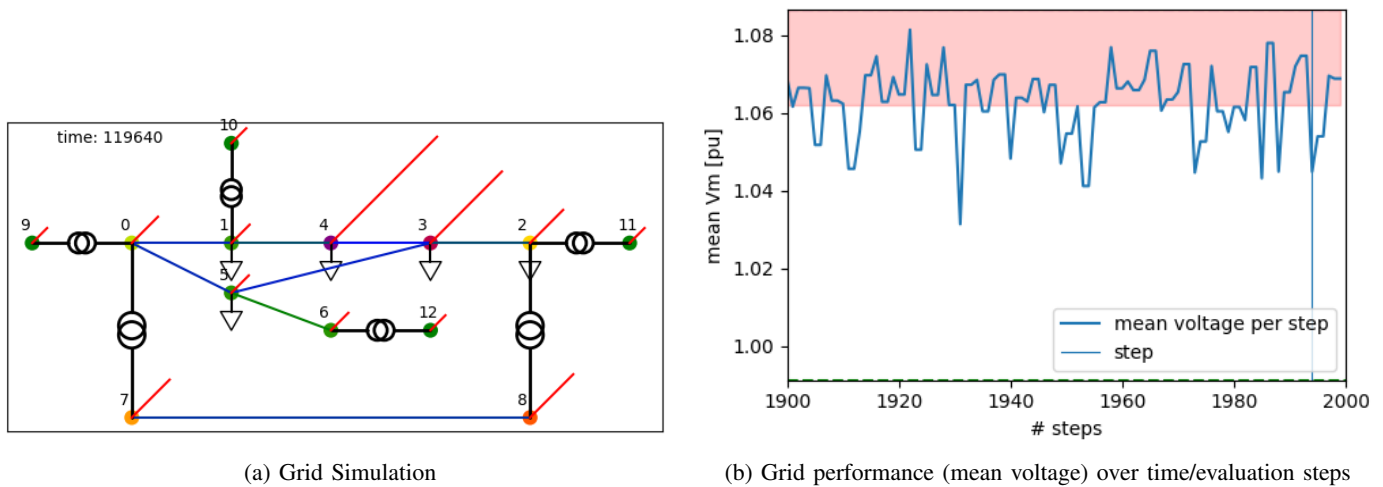


Figure 6. Proof-of-concept ARL grid results

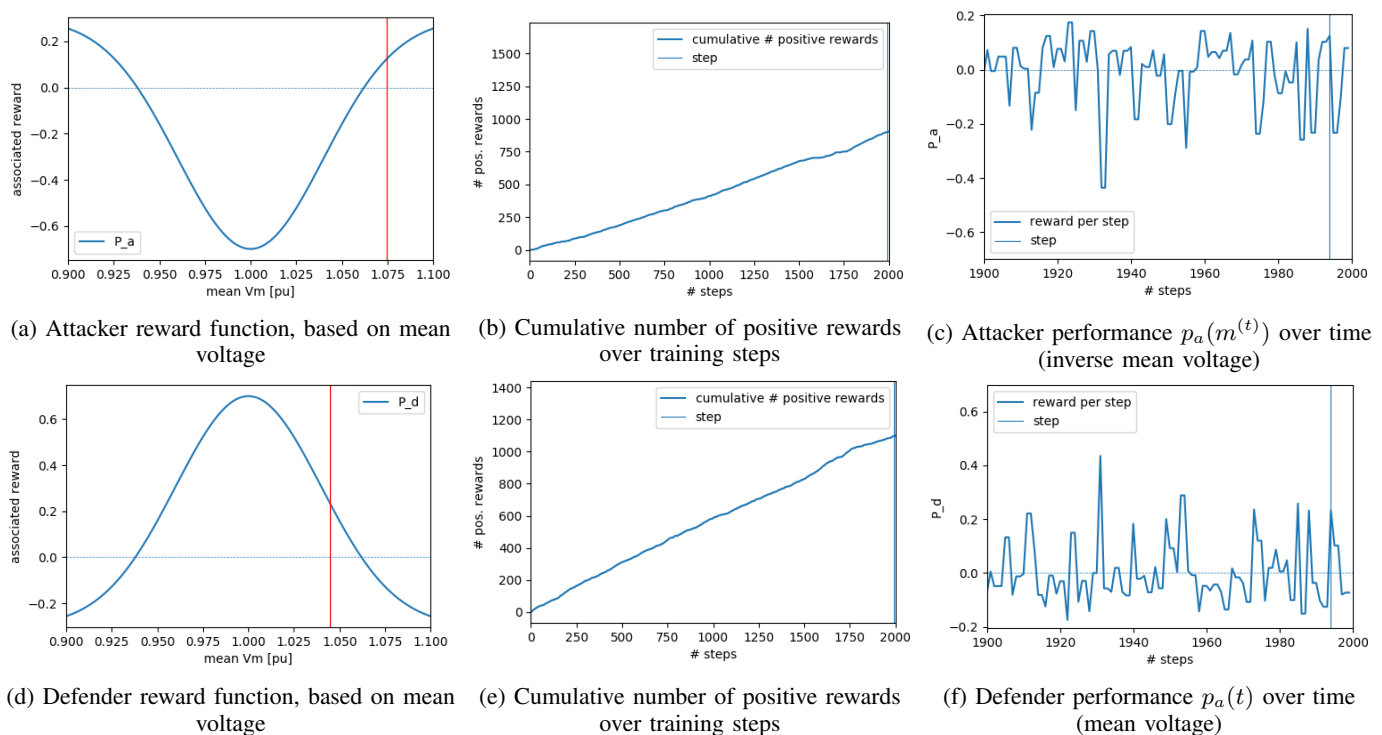


Figure 7. Proof-of-concept ARL agent results

from within a system. Both activities require the introduction of a measure of cost to the demonstrator.

Further, this demonstrator allows to analyze simulated systems from the point of view of threat agents, by pitching the agent against novel security measures, for example simulation of distributed coordinated attacks. Combining this view with multi-domain scenarios would enable analysis of sophisticated, multi-level attack techniques that involve, for example information hiding or emission of misleading information by attacker or defender. That means finding novel ways of attack using a combination of illegal and legal operations and inter-dependencies between different systems. Consequentially, all

these approaches would lead to the development of improved designs and testing methods for highly complex systems.

We can only assume that this finally leads to more resilient designs and defensive adaptable strategies—and, in the end, to improvements for the security of supply, but at this stage of the work, the first results are very satisfying.

VI. ACKNOWLEDGEMENTS

The authors would like to thank Sebastian Lehnhoff for his counsel, strategic advice and for providing extensive compute power for the first experiments conducted with this initial concept.

REFERENCES

- [1] R. M. Lee, M. J. Assante, and T. Conway, "Analysis of the cyber attack on the ukrainian power grid," *Electricity Information Sharing and Analysis Center (E-ISAC)*, 2016.
- [2] N. Beach-Westmoreland, J. Styczynski, and S. Stables, "When the lights went out: Ukraine cybersecurity threat briefing," *Booz Allen Hamilton*, vol. 12, p. 20, 2016.
- [3] A. Prentice, "Ukrainian banks, electricity firm hit by fresh cyber attack," *Reuters*, June, 2017.
- [4] R. Arghandeh, A. Von Meier, L. Mehrmanesh, and L. Mili, "On the definition of cyber-physical resilience in power systems," *Renewable and Sustainable Energy Reviews*, vol. 58, pp. 1060–1069, May, 2016.
- [5] I. Linkov and A. Kott, *Fundamental Concepts of Cyber Resilience: Introduction and Overview*. Cham: Springer International Publishing, 2019, pp. 1–25.
- [6] R. Alur, *Principles of cyber-physical systems*. MIT Press, 2015.
- [7] E. Böde *et al.*, "Design paradigms for multi-layer time coherency in adas and automated driving (multic)," in *FAT-Schriftenreihe 302*, 302nd ed., ser. FAT-Schriftenreihe. Forschungsvereinigung Automobiltechnik e.V. (FAT), October, 2017.
- [8] G. Brown, M. Carlyle, J. Salmerón, and K. Wood, "Defending critical infrastructure," *Interfaces*, vol. 36, no. 6, pp. 530–544, 2006.
- [9] R. Isaacs, *Differential games: a mathematical theory with applications to warfare and pursuit, control and optimization*. John Wiley and Sons, 1965.
- [10] C. T. Do *et al.*, "Game theory for cyber security and privacy," *ACM Comput. Surv.*, vol. 50, no. 2, pp. 30:1–30:37, May, 2017.
- [11] G. Cybenko, "Approximation by superpositions of a sigmoidal function," *Mathematics of control, signals and systems*, vol. 2, no. 4, pp. 303–314, 1989.
- [12] K. Hornik, M. Stinchcombe, and H. White, "Multilayer feedforward networks are universal approximators," *Neural networks*, vol. 2, no. 5, pp. 359–366, 1989.
- [13] I. Goodfellow, Y. Bengio, A. Courville, and Y. Bengio, *Deep learning*. MIT press Cambridge, 2016, vol. 1.
- [14] J. L. Elman, "Finding structure in time," *Cognitive science*, vol. 14, no. 2, pp. 179–211, 1990.
- [15] D. R. Seidl and R. D. Lorenz, "A structure by which a recurrent neural network can approximate a nonlinear dynamic system," in *IJCNN-91-Seattle International Joint Conference on Neural Networks*, vol. ii, Jul 1991, pp. 709–714 vol.2.
- [16] H. T. Siegelmann and E. D. Sontag, "On the computational power of neural nets," *Journal of computer and system sciences*, vol. 50, no. 1, pp. 132–150, 1995.
- [17] S. Hochreiter and J. Schmidhuber, "Long short-term memory," *Neural computation*, vol. 9, no. 8, pp. 1735–1780, 1997.
- [18] K. Cho, B. Van Merriënboer, C. Gulcehre, D. Bahdanau, F. Bougares, H. Schwenk, and Y. Bengio, "Learning phrase representations using rnn encoder-decoder for statistical machine translation," *arXiv preprint arXiv:1406.1078*, 2014.
- [19] J. Chung, C. Gulcehre, K. Cho, and Y. Bengio, "Empirical evaluation of gated recurrent neural networks on sequence modeling," *arXiv preprint arXiv:1412.3555*, 2014.
- [20] H. Tong, *Non-linear time series: a dynamical system approach*. Oxford University Press, 1990.
- [21] A. Basharat and M. Shah, "Time series prediction by chaotic modeling of nonlinear dynamical systems," in *2009 IEEE 12th International Conference on Computer Vision*, Sept 2009, pp. 1941–1948.
- [22] W. Yu, G. Chen, J. Cao, J. Lü, and U. Parlitz, "Parameter identification of dynamical systems from time series," *Physical Review E*, vol. 75, no. 6, p. 067201, 2007.
- [23] B. Cessac, "A view of neural networks as dynamical systems," *International Journal of Bifurcation and Chaos*, vol. 20, no. 06, pp. 1585–1629, 2010.
- [24] L. C. Baird, "Reinforcement learning in continuous time: Advance updating," in *IEEE World Congress on Computational Intelligence, 1994 IEEE International Conference on Neural Networks*, 1994.
- [25] R. S. Sutton and A. G. Barto, "Reinforcement learning: An introduction," 2011.
- [26] M. Lapan, *Deep Reinforcement Learning Hands-On: Apply modern RL methods, with deep Q-networks, value iteration, policy gradients, TRPO, AlphaGo Zero and more*. Packt Publishing Ltd, 2018.
- [27] M. Minsky, "Neural nets and the brain-model problem," *Unpublished doctoral dissertation, Princeton University, NJ*, 1954.
- [28] D. E. Rumelhart, G. E. Hinton, and R. J. Williams, "Learning representations by back-propagating errors," *nature*, vol. 323, no. 6088, p. 533, 1986.
- [29] D. P. Kingma and J. Ba, "Adam: A method for stochastic optimization," *arXiv preprint arXiv:1412.6980*, 2014.
- [30] T. Dozat, "Incorporating nesterov momentum into adam," *Phys. Rev.*, 2016.
- [31] S. Ruder, "An overview of gradient descent optimization algorithms," *arXiv preprint arXiv:1609.04747*, 2016.
- [32] M. P. Cuéllar, M. Delgado, and M. Pegalajar, "An application of non-linear programming to train recurrent neural networks in time series prediction problems," in *Enterprise Information Systems VII*. Springer, 2007, pp. 95–102.
- [33] N. Hansen, "The CMA evolution strategy: a comparing review," in *Towards a new evolutionary computation*. Springer, 2006, pp. 75–102.
- [34] R. Ros and N. Hansen, "A simple modification in cma-es achieving linear time and space complexity," in *International Conference on Parallel Problem Solving from Nature*. Springer, 2008, pp. 296–305.
- [35] N. Hansen, S. D. Müller, and P. Koumoutsakos, "Reducing the time complexity of the derandomized evolution strategy with covariance matrix adaptation (cma-es)," *Evolutionary computation*, vol. 11, no. 1, pp. 1–18, 2003.
- [36] M. Ruppert, E. M. Veith, and B. Steinbach, "An evolutionary training algorithm for artificial neural networks with dynamic offspring spread and implicit gradient information," in *Proceedings of the Sixth International Conference on Emerging Network Intelligence (EMERGING 2014)*. International Academy, Research, and Industry Association (IARIA), 2014.
- [37] E. M. Veith, *Universal Smart Grid Agent for Distributed Power Generation Management*. Logos Verlag Berlin GmbH, 2017, ch. Forecasting Power Demand and Supply, pp. 100–108.
- [38] A. Graves, G. Wayne, and I. Danihelka, "Neural turing machines," *arXiv preprint arXiv:1410.5401*, 2014.
- [39] A. Graves *et al.*, "Hybrid computing using a neural network with dynamic external memory," *Nature*, vol. 538, no. 7626, p. 471, 2016.
- [40] I. J. Goodfellow, J. Shlens, and C. Szegedy, "Explaining and harnessing adversarial examples," in *CoRR*, 2015.
- [41] Z. Ghahramani, "Unsupervised learning," in *Advanced lectures on machine learning*. Springer, 2004, pp. 72–112.
- [42] I. Goodfellow *et al.*, "Generative adversarial nets," in *Advances in neural information processing systems*, 2014, pp. 2672–2680.
- [43] D. Ernst, M. Glavic, and L. Wehenkel, "Power systems stability control: reinforcement learning framework," *IEEE Transactions on Power Systems*, vol. 19, no. 1, pp. 427–435, feb 2004.
- [44] D. Silver *et al.*, "Mastering the game of go without human knowledge," *Nature*, vol. 550, p. 354, 2017.
- [45] "DIN EN 50160:2000-03: Merkmale der Spannung in öffentlichen Elektrizitätsversorgungsnetzen," 2008.
- [46] L. Thurner *et al.*, "pandapower - an open source python tool for convenient modeling, analysis and optimization of electric power systems," *IEEE Transactions on Power Systems*, 2018.
- [47] M. Plappert, "keras-rl," <https://github.com/keras-rl/keras-rl>, 2016, [Retrieved: 2019-04-23].
- [48] K. E. Iverson, "A programming language," in *Proceedings of the May 1-3, 1962, Spring Joint Computer Conference*, ser. AIEE-IRE '62 (Spring). New York, NY, USA: ACM, 1962, pp. 345–351.
- [49] S. Schütte, "Simulation model composition for the large-scale analysis of smart grid control mechanisms," PhD, Carl von Ossietzky University of Oldenburg, 2013.
- [50] S. Lehnhoff *et al.*, "Exchangeability of power flow simulators in smart grid co-simulations with mosaik," in *2015 Workshop on Modeling and Simulation of Cyber-Physical Energy Systems, MSCPES*, 2015.

A Transient Classification System Implementation on an Open Source Distributed Power Quality Network

Charles Dickens

Department of Electrical and
Computer Engineering
University of Hawaii Manoa
Honolulu, Hawaii 96822
Email: dickensc@hawaii.edu

Anthony Christe

Department of Information and
Computer Sciences
University of Hawaii Manoa
Honolulu, Hawaii 96822
Email: achrste@hawaii.edu

Philip Johnson

Department of Information and
Computer Sciences
University of Hawaii Manoa
Honolulu, Hawaii 96822
Email: johnson@hawaii.edu

Abstract—Capturing and classifying Power Quality (PQ) phenomena is important for the smooth functioning of electrical grids. This paper presents methods for classifying the four types of transients (impulsive, arcing, oscillatory, and periodic notching) specified in the IEEE 1159 Power Quality standard. Our methods implement a tractable algorithm, which applies well understood signal processing methods and statistical inference for feature extraction and decision making. We tested our methods on simulated PQ disturbances in order to demonstrate the capabilities of the system. The results of this research include an operational implementation of a transient classifier for Open Power Quality, an open source distributed PQ network. Additional functionality can be easily incorporated into the system to extend the utility of our methods, such as a meta-analysis to capture higher level network wide events.

Keywords—Power quality; power transients; open source; renewable energy.

I. INTRODUCTION

Introducing renewable energy generation to existing electrical grid infrastructures has proven itself to be an engineering challenge. The transition to cleaner energy generation methods such as wind and solar, which are inherently unpredictable, has increased the severity and frequency of problems related to Power Quality (PQ) [1]. For example, sensitive instruments connected to an unstable grid can be potentially de-calibrated or damaged.

A first step to correcting PQ problems is understanding the problem from top to bottom. Electricity supplied by the grid should be continuously monitored to detect and log PQ events. Classification of PQ phenomena can reveal problematic patterns in the system and provide potential explanations for failures that can be understood and resolved.

There is considerable research on classification of PQ [2]–[6]. Current state of the art techniques commonly utilize wavelet transforms for feature extraction and then run the data through a trained neural network or decision tree algorithm. Another approach by Manikandan, Samantaray, and Kamwa [3] decomposes the signal using sparse signal decomposition on an overcomplete hybrid dictionary matrix and then extracts the power disturbance features of the decomposed signal and classifies the transient waveforms using a decision tree algorithm.

In this paper, we present a tractable implementation of a transient classification system for our open source distributed PQ network called Open Power Quality (OPQ). By including this transient detection system in OPQ, we can gather information on both local transients and global transients (i.e., transients from a single source that were detected on multiple, distributed sensors). This information can be used to determine how transients and other PQ signals propagate throughout a power grid. Further, data metrics generated from intermittent renewable sources, weather reports, and user reports can be fused by OPQ with the transient detection results to provide insights on how intermittent renewable energy sources affect the quality of power on the grid.

This paper is structured as follows. Section II explains and justifies the proposed methodology for classifying transients. Section III describes the implementation of the methodology on the OPQ system. Section IV reports the simulated results of the transient detection system. Finally, Section V provides the conclusions.

II. METHODOLOGY

The transients classified with the methodologies discussed in this paper are defined in the IEEE 1159 Draft Recommended Practice for Monitoring Electric Power Quality [7]. Table I summarizes the definition and characteristics of each transient.

TABLE I. TRANSIENT CLASSES

<i>Class</i>	<i>Description</i>
Impulsive	Unidirectional change from the nominal waveform.
Arcing	Bipolar random frequency noise.
Oscillatory	Decaying oscillatory wave.
Periodic Notching	Periodic and strictly negative in power.

We use a decision tree algorithm to classify signals with potential transients. The benefit of this approach is that it minimizes necessary computation. As PQ features are extracted from the signal, the potential classes that it could fall into are narrowed. Computationally expensive analysis can be bypassed if simple features can rule out a class early in the process. Leveraging this idea, the potential transients are checked to see if they fit the classes in the same order as listed in Table I. Once the signal is classified, then additional meta data can be computed that appropriately details the transient.

A. Signal Decomposition

The first task is to decompose the raw signal into the fundamental waveform and the potential transient waveform. In the context of this application, the fundamental waveform is expected to have little to no variation from the standard, which is 60 Hz and 120 Vrms in the U.S. [8]. There is the potential for simultaneous waveform distortion and transient PQ phenomena. However, waveform distortions for frequency phenomena are typically found to only vary by ± 0.1 Hz and for voltage phenomena by 0.11.8 pu [7], whereas the transients that the system is capturing typically have a spectral content between 1 kHz to 5 MHz.

Thus, a simple digital implementation of a 4th order low pass Butterworth filter with a cutoff frequency at 500 Hz is justifiable and practical for this application to extract the fundamental waveform from the raw digital signal. A different filter could be used to achieve similar results. We decided to use a Butterworth filter with these order and cutoff frequencies due to the desirable property that the filter is monotonic in both the passband and stopband, which results in a clean decomposition. Once the fundamental waveform is retrieved, the transient waveform is then obtained by subtracting out the fundamental waveform from the raw signal.

B. Classifying Impulsive Transients

The first step in the decision tree algorithm is to determine whether the transient could be impulsive. We test for impulsive transients first since it is computationally cheapest to verify. As defined by the IEEE 1159 standard, an impulsive transient is a unidirectional change from the nominal condition of the voltage [7]. Therefore, a simple check which ensures that the excitation in the transient waveform is unipolar will qualify the transient to be in the broad category of impulsive transients.

If the transient is impulsive, then arcing and oscillatory transients can be ruled out. Additional cases do need to be accounted for since there is a chance that the transient could also be periodic notching. If the impulsive transient is positive in power, then periodic notching can be ruled out, otherwise it needs to be tested. At this point meta-data detailing the rise and decay time, the peak amplitude, and whether or not the transient causes additional zero crossings in the raw signal can be calculated and recorded with the classification.

C. Classifying Arcing Transients

An arcing transient is a burst of relatively higher frequency noise that is random in frequency content. The arcing transient should have more than ten zero crossings and should not have more than two cycles with same period [7].

Thus, the test for arcing transients can be a verification of more than ten zero crossings and a threshold for randomness in the frequency content. The defined threshold for randomness is whether more than two zero crossings have the same period.

D. Classifying Oscillatory Transients

An oscillatory transient is a bipolar change that typically lasts between a few milliseconds to a quarter cycle of the nominal waveform. It is characterized by its frequency content and decay rate [7].

To determine whether the potential transient fits the oscillatory classification, the system implements an incremental

F-test. The F-test gives a numerical value of the significance of additional variables added to the regression function. The null hypothesis of the test is $H_0 : \beta_3 = \beta_4 = \beta_5 = 0$.

We implement this by first computing a least squares curve fitting of the potential transient waveform and an exponentially decaying sinusoid using gradient descent. The complete model is shown in (1).

$$\hat{y} = \beta_0 + \beta_1 e^{-\beta_2 t} \cos(\beta_3 \cdot 2\pi t + \beta_4) \quad (1)$$

Then, a reduced model is fit using the same least square fitting methods. The reduced model equation is shown in (2).

$$\hat{y} = \beta_0 + \beta_1 e^{-\beta_2 t} \quad (2)$$

Large values of F result in rejection of the null hypothesis and the classification of the transient as oscillatory. The threshold value that F must pass is a design decision and will determine the expected type 1 and type 2 errors of the classification.

We record additional meta-data upon this classification including the decay rate, frequency content, dc offset, and peak amplitude, all of which follow from the results of the curve fitting.

E. Classifying Periodic Notching Transients

A periodic notching transient is a periodic and strictly negative power disruption of the nominal waveform. Therefore, the signal is first verified to be strictly negative in power before further analysis is made. If so, the system moves on to determine whether the potential transient waveform is periodic.

To test for periodicity the auto-correlation of the signal is computed. Auto-correlation highlights the similarity between the signal and its previous values. Our method convolves the first half the transient signal with the original transient. The convolution is only calculated for points where the signals completely overlap. If the potential transient is indeed periodic, then the resulting signal from the convolution will have the same periodicity with peaks that highlight where the signal had the highest correlation.

Our method determines the peaks of the auto-correlation signal by setting a height threshold. Then, it finds the standard deviation of the distance between the peaks, and if this value is less than a defined threshold, the signal is classified as periodic. If so, the period is easily calculated from the auto-correlation signal along with additional meta-data to characterize the transient.

III. IMPLEMENTATION

We implemented and tested these methods using our OPQ system. The OPQ project began in 2012 with the goal of developing and evaluating PQ technology to support improvements to electrical grids, in particular the incorporation of distributed intermittent renewable energy sources.

In general, the OPQ system architecture consists of OPQ Boxes, which are plugged into standard residential outlets to monitor PQ as it is experienced at the point of consumption. These results are communicated over the Internet to OPQ Cloud, a set of cloud-based services that provide end-to-end support for the capture, triggering, analysis, and reporting of

local and global level PQ phenomena. A major design goal of OPQ is to not just report PQ locally for each device, but to look at PQ in an aggregate manner. This is possible because the OPQ cloud services provide a global view of all PQ sensors (OPQ Boxes). Thus, OPQ is able to detect distributed PQ incidents (where multiple distributed sensors sense the same incident) and also observe how PQ incidents propagate through the electrical grid.

The two principle cloud services in OPQ are called Makai and Mauka. The Makai service is responsible for aggregating and processing the measurements generated by the OPQ boxes. Inside Makai, a triggering broker creates a PQ event when it detects a deviation from the nominal waveform in a low fidelity data stream and sends a message to the Mauka system to analyze the event further. The Mauka service performs analysis of high fidelity data and is thus where our transient detection system is located.

Our implementation proceeds as follows.

First, the raw signal is decomposed into its fundamental and potential transient waveform. The fundamental waveform is extracted using a digital implementation of a 4th order low pass Butterworth filter with a cutoff frequency of 500 Hz. The digital filter used is an implementation in the scientific Python library SciPy [9]. The transient waveform is then the raw waveform minus the fundamental waveform.

Our method does not assume that only a single transient exists in a PQ event triggered by the Mauka system. Therefore, before classification, the complete transient waveform is separated into potential windows with individual transients. This is achieved through a sliding window technique with a predefined threshold for a maximum lull. The maximum lull between transients is a design decision that is made with domain knowledge. The transients that are being classified with the system are expected to have a duration on the order of milliseconds.

The sliding window method works by first scanning the transient waveform and finding the first measurement which is above the configuration noise floor. It is common practice to account for potential instrumentation error by defining a noise floor. Measurement deviating from the nominal waveform more than the defined noise floor are considered to be significant and can reasonably be considered to be PQ phenomena and not a faulty measurement. The noise floor in the implementation is defined to be 5% of the nominal voltage.

The first measurement above the noise floor is considered to be the starting point of the transient. Then, the scanning continues until there is a lull in measurements above the noise floor longer than the defined maximum, or the scanning has reached the end of the transient signal. At which point the last significant measurement is defined to be the endpoint of the potential transient. This process is repeated until the end of the transient signal is reached.

Once the start and end points of all of the potential transients are determined, then the classification analysis can begin. Feature extraction and the decision tree structure is described in detail in Section II. Only important implementation notes will be mentioned in the rest of this section.

The multiple non-linear least squares regression required for classification of the oscillatory transient is provided in the SciPy library [9]. The solution to the regression is an

approximation obtained by a gradient descent method. Since the expected characteristics of oscillatory transients are known, the gradient descent method can be seeded to increase the rate at which a local optimum is found.

To classify periodic notching transients, a convolution operation is necessary. The code used to implement this calculation is found in the NumPy library [10].

IV. RESULTS

To test the performance of the proposed methodology, simulated transients were constructed and run through the system. The configuration of the system at the time of these reported results has the sampling rate at 12000 Hz.

First, we created a simulated waveform with an impulsive transient by superimposing an exponentially decaying excitation onto a portion of 6 cycles of a fundamental waveform. This simulated transient has a peak amplitude of 18 volts and decays to the noise floor in $\frac{1}{32}$ cycles. The raw signal is shown in Figure 1.

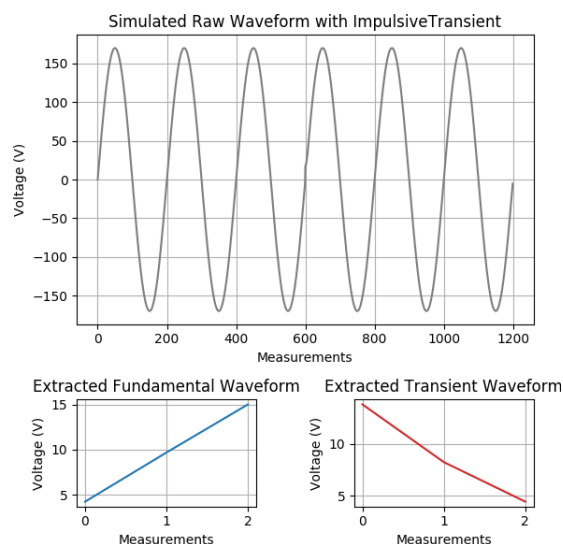


Figure 1. Simulated 60 Hz 120 Vrms sine wave with an impulsive transient. The decomposed fundamental and transient signal are shown in the bottom left and right subfigures, respectively.

Second, we created a simulated waveform with an oscillatory transient by superimposing an exponentially decaying sinusoidal wave with 960 Hz frequency with starting amplitude of 72 volts onto a portion of 6 cycles of a fundamental waveform. The raw signal is shown in Figure 2.

Third, we created a simulated arcing transient by drawing 7 random samples from a uniform random distribution over the support (61, 2401). We then used the random samples to define the frequencies for single cycles of an arcing transient wave. The raw signal is shown in Figure 3.

We simulated a multiple zero crossing transient by superimposing three single sawtooth cycles in positions of the fundamental waveform near a zero crossing. The single sawtooth cycle has an amplitude of a 72 volts and a period of 10 samples. The raw signal is shown in Figure 4.

Finally, we created a simulated waveform with a periodic notching transient by superimposing a sawtooth waveform with

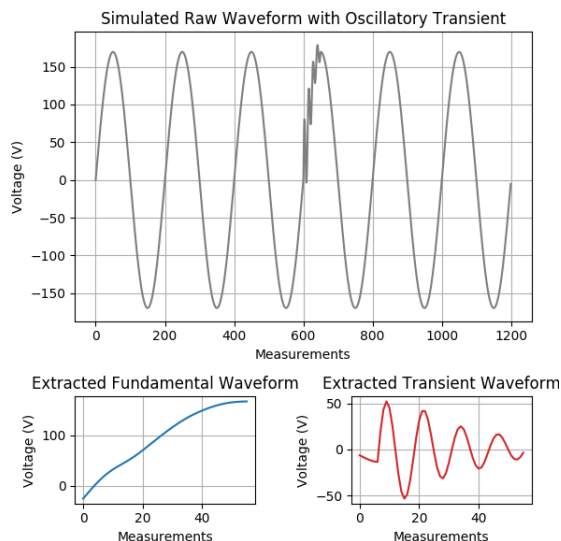


Figure 2. Simulated 60 Hz 120 Vrms sine wave with an oscillatory transient. The decomposed fundamental and transient signal are shown in the bottom left and right subfigures, respectively.

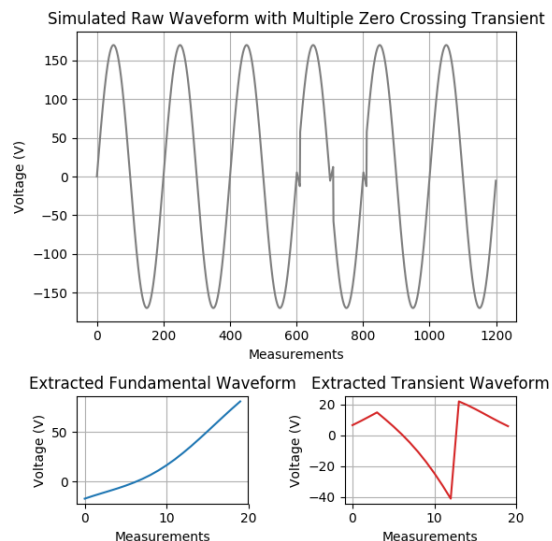


Figure 4. Simulated 60 Hz 120 Vrms sine wave with multiple impulsive transients which cause additional zero crossings in the raw waveform. The first decomposed fundamental and transient signal are shown in the bottom left and right subfigures, respectively.

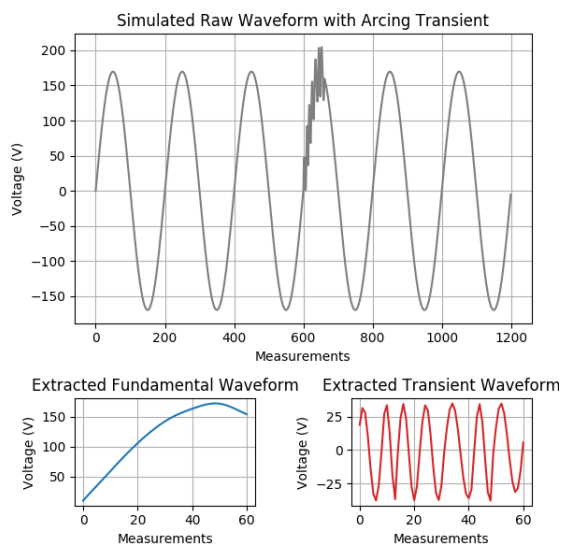


Figure 3. Simulated 60 Hz 120 Vrms sine wave with an arcing transient. The decomposed fundamental and transient signal are shown in the bottom left and right subfigures, respectively.

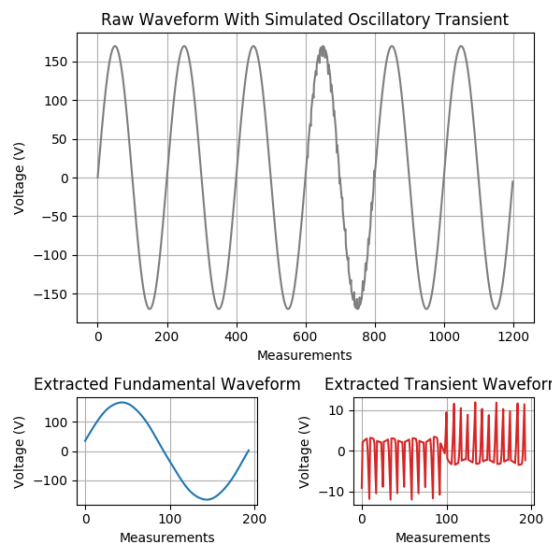


Figure 5. Simulated 60 Hz 120 Vrms sine wave with a periodic notching transient. The decomposed fundamental and transient signal are shown in the bottom left and right subfigures, respectively.

a frequency of 1440 Hz and amplitude of 18 volts for a single fundamental cycle, i.e., 24 notches per cycle for one cycle. We determined the polarity of the notching transient by the fundamental signal since notching is defined to be strictly negative in power. The raw signal is shown in Figure 5.

Figures 1, 2, 3, 5 show the raw simulated waveforms with impulsive, oscillatory, arcing, and periodic notching transients, respectively, all starting near the 600th measurement. The two subfigures show the extracted fundamental waveform and transient waveform detected by the system. These simulated waveforms were all correctly classified by the system using our methods.

V. CONCLUSION AND FUTURE WORK

This paper presents an implementation of a transient detection system using OPQ, an open source distributed PQ network, which can successfully classify four types of transients as defined in the IEEE 1159 standard. Our method shows promise based upon its ability to correctly classify simulated versions of all four transients.

The most immediate future work is to monitor an electrical grid in real-time to determine how well the methods work on real world transients.

We also hope to add functionality to OPQ that would

enable us to search our historical data for the occurrence of transients and classify them. From this, a meta-analysis for higher level network wide events could lead to clues regarding the sources of these phenomena. This data could provide new insight into our understanding of how intermittent renewable energy sources affect PQ on the grid, helping us to better modernize our grids with larger amounts of distributed renewable energy.

REFERENCES

- [1] R. Toma and M. Gavrilas, "The impact on voltage stability of the integration of renewable energy sources into the electricity grids," in *Proceedings of the 2014 International Conference and Exposition on Electrical and Power Engineering (EPE) October 16–18, 2014, Iasi, Romania*. IEEE, Oct. 2014, ISBN: 978-1-4799-5849-8.
- [2] V. Garrido, J. Rodriquez, and A. Garcia, "Classification of power quality phenomena using intelligent techniques," in *Proceedings of the 2014 IEEE PES Transmission and Distribution Conference and Exposition - Latin America (PES TD-LA) September 10–13, 2014, Medellin, Colombia*. IEEE, 2014, ISBN: 978-1-4799-6251-8.
- [3] M. Manikandan, S. Samantaray, and I. Kamwa, "Detection and Classification of Power Quality Disturbances Using Sparse Signal Decomposition on Hybrid Dictionaries," *IEEE Transactions on Instrumentation and Measurement*, vol. 64, pp. 27–38, Jan. 2015, issue: 1, ISSN: 0018-9456.
- [4] K. Thirumala, A. Umarikar, and T. Jain, "A generalized empirical wavelet transform for classification of power quality disturbances," in *Proceedings of the 2016 IEEE International Conference on Power System Technology (POWERCON) September 28–1 October, 2016, Wollongong, NSW, Australia*. IEEE, 2014, ISBN: 978-1-4673-8848-1.
- [5] M. Valtierra-Rodriguez, R. Romero-Troncoso, R. Osornio-Rios, and A. Perez-Garcia, "Detection and Classification of Single and Combined Power Quality Disturbances Using Neural Networks," *IEEE Transactions on Industrial Electronics*, vol. 61, pp. 2473–2482, May 2014, issue: 5, ISSN: 1557-9948.
- [6] N. Tse, J. Chan, W. Lau, and L. Lai, "Hybrid Wavelet and Hilbert Transform With Frequency-Shifting Decomposition for Power Quality Analysis," *IEEE Transactions on Instrumentation and Measurement*, vol. 61, pp. 3225–3233, Dec. 2012, issue: 12, ISSN: 1557-9662.
- [7] *P1159/D3 Draft Recommended Practice for Monitoring Electric Power Quality*, IEEE, 2018.
- [8] *C84.1-2016, American National Standard for Electric Power Systems and Equipment Voltage Ratings (60 Hz)*, ANSI, 2016.
- [9] E. Jones, T. Oliphant, P. Peterson *et al.*, "SciPy 1.1.0: Open source scientific tools for Python," 2001–, [accessed February 2, 2019]. [Online]. Available: <http://www.scipy.org/>
- [10] T. Oliphant, "NumPy 1.14.5: A guide to NumPy," USA: Trelgol Publishing, 2006–, [accessed February 2, 2019]. [Online]. Available: <http://www.numpy.org/>

An Empirical Study of Power Characterization Approaches for Servers

Yewan Wang*[†], David Nörtershäuser*, Stéphane Le Masson* and Jean-Marc Menaud[†]

*Orange Labs R&D, Lannion, France

Email : firstname.lastname@orange.com

[†]IMT Atlantique, INRIA, LS2N, France

Email : firstname.lastname@imt-atlantique.fr

Abstract—Data centers are energy-hungry facilities. Emerging studies have proposed energy-aware solutions for reducing the power consumption of data centers. Power consumption characterization of servers is an essential part to realize power-aware adaption strategies. Traditional methods adopt accuracy and secure direct measurements by using physical instruments such as wattmeters. Recently, watt-meter free solutions are adopted widely as an economical replacement. These solutions provide power consumption information by making use of self-resources without additional instruments. There are two commonly adopted solutions: 1) standard specifications that provide interface with integrated sensors, such as Intelligent Platform Management Interface (IPMI) and Redfish; 2) Power models based on system activity related indicators. The energy-aware scheduling decisions are made based on the power values obtained, but few works give information about the correctness of the power values while discussing the results or drawing conclusions. In this study, we try to fill up this missing part by evaluating some commonly used, economical ways in obtaining power values. We compare and discuss the reliability, advantages and limitations for the CPU-utilization based power models. The findings highlight the challenges in realizing accurate and reliable power models. We also evaluate the reliability of IPMI and RedFish, in order to give references in choosing appropriate power characterization solutions.

Keywords—Server power model; Inlet temperature; IPMI; RedFish.

I. INTRODUCTION

Cloud data centers are computer facilities formed by hundreds or even thousands of servers. With the increasing demand of cloud services, energy efficiency of servers in data center has become a significant issue. Reliable power characterization approaches are essential for supporting energy-aware solutions. High accuracy power analyses are capable of providing accurate power consumption data. However, limitations like high cost, weak support of integration with Unix systems (which are widely adopted among server platforms) make it unrealistic by using power analyzers in a data center environment. Therefore, some alternative economical solutions that make use of available resources without extra investment are widely adopted. The reliability of these solutions need to be evaluated thoughtfully before applying to different real situations. In this paper, we investigate experimentally two kinds of alternative solutions: 1) Power models based on system activity indicators, such as usage of physical components and Performance Monitoring Counters (PMC); 2) Industrial standard specifications based on integrated sensors, such as: IPMI, Redfish.

The paper is organized as follows: In Section II, we present some previous studies about building power models for PC or server systems. In Section III, we evaluate empirically the power models based on CPU utilization. The server is stressed

with an industrial test tool. Principal components like CPU, memory and storage are stressed at different load levels. Then, in Section IV we evaluate the precision of Redfish and IPMI applied in a new series of IBM servers. The measures of power consumption recorded by Redfish and IPMI are compared with a high-accuracy power analyzer. Conclusions and perspectives are given in Section V.

The major contributions of this paper are:

- We evaluate power models based on CPU-utilization. Thermal influence of inlet temperature is especially discussed.
- We give some suggestions in building accuracy power models according to experiments.
- We discuss the reliability of power data provided by IPMI and Redfish based APIs.

II. POWER MODELS: BACKGROUND AND RELATED WORK

Modeling power consumption of servers is an active area of research. Power models takes advantages of indirect measurements to predict the power consumption of the elements in an IT system, from single components like processors, to the entire machine. Comparing to physical power analyzers, power models have several advantages. In general, it provides an economical way via making use of self-resources. In deeper insight, power models are capable of linking the energy usage data with system activities. That makes it possible to isolate the energy consumed by single process or Virtual Machine (VM). In this case, performance bottlenecks, inefficiency of algorithm are possible to be identified and optimized in a more dedicated way. In practical, power models are easy to integrated with server system, they can be used to help with some power management strategies, such as VM Migration, shut down technologies, etc. Therefore, it is not surprising that there has been a considerable amount of work in the area of power modeling.

A. CPU-Utilization based method

In early stage, power models adopt the utilization of CPU as the only input. One of the most notable study is conducted by Fan et al. [1], whose study has shown that the power consumption of servers can be accurately represented by CPU utilization by using simple linear relationship. The error is validated less than 5% for dynamic system activities. Economou et al. [2] introduced a method called Mantis to model full-system power consumption. The model is built with linear regression based on component utilization metrics: CPU Utilization, off-chip memory accesses, disk and network I/O rates. The model achieves an overall error range from 0% to

15% for two different server systems. Especially, the blade model has errors less than 5% for all cases. After that, with the evolution of manufacturing, server architecture becomes more complex, the accuracy of models based on CPU utilization has been questioned in many ways. Orgerie et al. [3] argued that the relationship between the CPU consumption and its load is not linear. The results of their experiments showed that even applying the same CPU load, they observed three different power consumption values. Hence, they concluded that it is indeed not possible to get a linear function between CPU utilization and power consumption. Zhang et al. [4] validated the linear model for 392 published results, which composed of different kind of servers. They use R-squared values to evaluate their model. R-squared is also known as coefficient of determination. The value of R-squared ranges from 0 to 1, describes the goodness of prediction, the higher the better. The authors show that, among 395 published results, 6.5% (25 kinds of servers) have the R-squared values less than 0.95, which means the CPU utilization is not always correlated significantly with server power usage.

B. PMC based method

Furthermore, researchers try to build power estimation models with performance monitoring counters. PMCs record and store the counts of system-related activities. The principal of models based on PMCs is the selection of several PMCs, which have good correlation with power. The models can be then illustrated by linear, non-linear regression formula, or even by neural network. PMCs based power models usually have better accuracy in comparing with single indicators based model.

Da Costa et al [5] evaluate the power consumption of a PC by using performance counters, then extend the conception to predict the power consumption of single applications. Training data is collected by running several applications and synthetic benchmarks. A small number of optimal variables combinations within 165 different counters are selected for each synthetic benchmark, which has the best regression result with the real power consumption measurements. Then, a global model for the entire PC is derived by including and analyzing the possible candidate variables. The global model has R-squared values greater than 0.94 for all the cases when applied respectively to each benchmark. Even though they did not evaluate the global model with some real applications, their results confirm the feasibility by using PMC to predict the power consumption of the IT systems.

Bircher et al. [6] propose a method to create power models for six subsystems (CPU, memory, chipset, I/O, disk and GPU) by using performance counters within processors. They chose several performance events which are highly correlated to power consumption in subsystem including memory, chipset, IO, disk and processor. Resistors are connected in series with power source to capture the power consumption for each subsystem. Their models are validated by a wide range of workloads and achieved an average error less than 9% for each subsystem. However, they did not mention the model accuracy for the entire system.

Witkowski et al. [7] present a practical approach to estimation power consumption of applications in High Performance Computing (HPC) environment. Their models are represented as regression functions by using only a few variables related

to CPU, motherboard and memory. Variables will be included in the model once the coefficient of determination increases. Some of the original variables are transformed to increase model accuracy. When validated with the same synthetic workloads during training phase, their model reports an average error between 1% and 4% comparing to real measurements. However, the average error is increased to a range of 3% -7% when tested with a real HPC application.

Some state-of-the-art power models provide platform-specific solutions [8] [9], which makes the model more accurate and adaptive in current situation. However, the method used to build the model is also less general and portable, limited to specific conditions. Some other researchers suggest advanced machine learning techniques to improve accuracy of PMC-based models for general use. Some of them point that, the accuracy of model can be greatly increased by removing some irregular outliers of measurements [7] [5].

Cupertino et al. [10] propose to use Artificial Neural Network (ANN), one of the computational intelligence technologies to improve the model accuracy. They compare the Mean Absolut Percentage Error (MAPE) between an ANN model and a traditional capacitive model, and show that the ANN can decrease the MAPE from 5.45% to 1.86%.

Wang et al [11] point out that for a given processor, the usage of PMCs is limited by the available event counters and the maximum number of PMCs that can be read simultaneously. Even more, power models with less PMC can be more flexible and applicable. Based on this fact, the authors have then proposed a power model with only Instruction Per Cycle (IPC) and frequency as inputs. In order to improve the accuracy, running benchmarks will be divided into different categories based on IPC values, then they build the models separately for each category. The authors also develop a tool SPAN to realize run-time power profiling and correlate power dissipation to source code functions. Their power model is validated by using two benchmarks from SPEC2008Cjvm, and achieve absolute error rate of 5.17% and 4.46% respectively. Tool "SPAN" achieve accuracy as high as 97% on average by running FT benchmark from NAS Parallel benchmark suite and synthetic workloads.

Mair et al. [12] present their power estimation model called W-Classifier. The model classifies different workloads into 5 categories by using some power-dominant PMCs: INT, FPU, FPU/cache mixed, INT/cache mixed and memory/idle. They validate W-Classifier with OpenMP multi-threaded benchmarks from NAS Parallel Benchmark suite on all 16 cores. They find that W-Classifier has an average MAE of 6.95% for all benchmarks, while traditional multi-variable model achieves an average MAPE of 40.74%. However, authors admit that W-classifier has difficulty to estimate the power consumption of benchmarks with large range of power variation. They have then proposed to improve the model by adding more kinds of classification categories as further work.

C. Challenges

Obtaining accurate results of consumption behavior at the whole system level or individual component level is not straightforward. The difficulties include but are not limited to the following raisons: 1) Diversity. Physical architecture of server differs very much between manufactures and becomes more complicated from generation to generation, with the

emerging of new features. The availability of PMCs differs among different machines [7]. The problem of the diversity makes the power models less portable between heterogeneous servers in Data centers. 2) Evolution. Evolution of system is somehow rapid and random. Some indicators used to build the original model would be no longer exist with the evolution of computing system. For example, four years after the introduce of Mantis [2] (mentioned in 2.1), John C et al [13] have noticed that, some of the original indicators used by Mantis no longer exist in current systems. 3) Hidden system behaviors. Some component incorporates make optimization without exposing to any of the existing counters, which makes some device behaviors invisible to OS [13]. High precision will be difficult to achieve without being aware of these changes that affect power draw. 4) Variability. Previous studies have given quantitative evidences about the significant variability between identical designed CPU and servers [14]–[17]. Parameter variation, also known as Process, Voltage and Temperature (PVT) variation [18], is responsible for most of the variations. Among them, process and voltage variations are caused by imperfections from fabrication process. Temperature variation comes from fluctuating environments. These variations are inevitable and influential to power consumption. One of our previous study has demonstrated the power consumption variation between identical servers leads from thermal effects [19]. These observations bound the potential accuracy achievable concerning all kinds of power modeling approaches.

All the evidences listed here highlights the challenges in building reliable power models for servers, especially for the modern ones.

III. POWER MODELS BASED ON CPU-UTILIZATION

In this section, we evaluate experimentally the effectiveness of using CPU-utilization as the indicator for building power models. Influence of inlet temperature variation has also been demonstrated by using a test use case.

A. CPU-Utilization based models

The model is built for a Gigabyte mw50-sv0 server, equipped with one Xeon E5-2609v3 processor. Several workloads from Server Efficiency Rating Tool (SERT) [20] are chosen as the test suite. SERT is an industrial standard rating tool for evaluating energy-efficiency for server systems, developed by SPEC committee. It contains a number of micro-workloads, called *worklets* that exercise different components of the Server Under Test (SUT) at different target load levels. (see Table I for details). In this experiment, ten worklets composed of both CPU and memory intensive types are chosen to stress the server. The test suit includes six CPU-intensive tests (Compress, CryptoAES, LU, SOR, Sort and SHA256), one CPU and memory hybrid test (SSJ), and two memory-intensive tests (Flood3 and Capacity3). Consumption at idle state is also measured. Details about the worklets used can be found in Table I [21].

The power consumption data is collected by Yokogawa WT330, a high-accuracy power analyzer, with maximum measurement error less than 1%. CPU utilization is collected by redirecting the information from directory `/proc/cpuinfo`. Data collection frequency is set at 1Hz. At the end of test, box plot from `matplotlib` [22] is used to interpreted the dispersion of power for a given CPU utilization. Box plot is widely

used for displaying statistic distribution, a simplified manner in comparison to a histogram or density plot. For a normal distribution, 50% of the data is within the box. Two short lines beyond the box represent for the minimum and maximum values within 99.3% of the data. Outliers represent for the remaining 0.7% data. The test result is shown in Figure 1. We can see from the figure that the models built from CPU-utilization are not reliable enough. For a fixed CPU-utilization, the server power spreads out between a considerable range, especially for the utilization at 100%. Outliers are caused by the quick changes of system loads. The power ranges are relatively lower at 10%, 50%, 70% and 90%, because of a lack of experimental data at these load levels.

We illustrate then the relationship between CPU-utilization and server power for each worklet by marking with different colors. The result in Figure 2 shows that, for each worklet, server power has a narrow distribution for a specific CPU utilization, which means power consumption can be precisely modeled by CPU utilization during a single workload execution. Moreover, for the worklets from the same "CPU intensive" category, power is proportional to CPU utilization with different parameters. For instance, worklet LU has an obvious different way in increasing power comparing with the other CPU intensive worklets. As further work, we will try to improve the accuracy for CPU utilization based power models by classifying the workloads into different groups with PMCs.

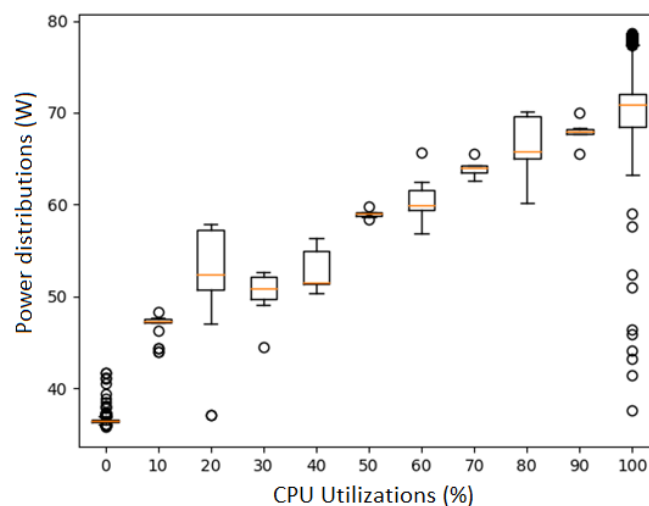


Figure 1. Distribution of power under different CPU-utilization.

B. Influence of ambient temperature: a test use case

Furthermore, we evaluate the influence of inlet temperature to the power consumption of server. The server is placed in a climatic cabin, where we can control the ambient temperature precisely. Inlet temperature is measured by a thermocouple of type K. Test suite SERT is executed three times to the server at 22°C, 35°C and 45°C inlet temperatures respectively. The results of the power consumption of server under different ambient temperatures can be seen in Figure 3. Server power increases with the rise of inlet temperatures. The increment of power is contributed mainly by fans and leakage current of CPU [19]. Unlike power consumption, CPU utilization

TABLE I. TEST SUITE INFORMATION

Worklet	Components	Description	Load Levels
Compress	CPU	Compress and decompress data	100%, 75%, 50%, 25%
CryptoAES	CPU	Encrypts and decrypts data	100%, 75%, 50%, 25%
LU	CPU	LU factorization of dense matrix operations	100%, 75%, 50%, 25%
SOR	CPU	Jacobi Successive Over-relaxation workload	100%, 75%, 50%, 25%
Sort	CPU	Sorts randomized 64-bit integer array	100%, 75%, 50%, 25%
SHA256	CPU	SHA256 hashing transformation and encryption/decryption	100%, 75%, 50%, 25%
SSJ	CPU/Cache/Memory	simulates Online Transaction Processing (OLTP) operations	100%, 87.5%, 75%, 62.5%, 50%, 37.5%, 25%, 12.5%
Flood	Memory	Measures memory bandwidth across four common and important array operations	Full, Half
Capacity	Memory	Exercises Java's XML Validation	Base, Max
Idle	System	No load on SUT	None

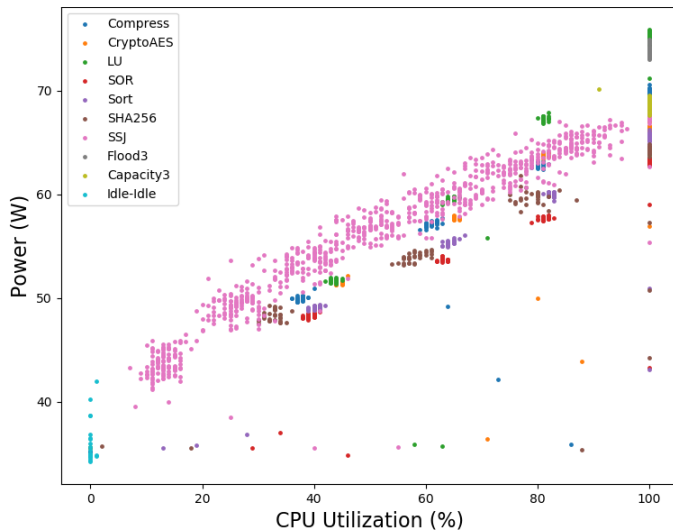


Figure 2. Relationships between CPU-utilization and server power of different worklets.

remains the same under different inlet temperatures as shown by Figure 4. Therefore, as demonstrated by the experiments, there is a risk of losing accuracy without considering variation of ambient temperature in the models.

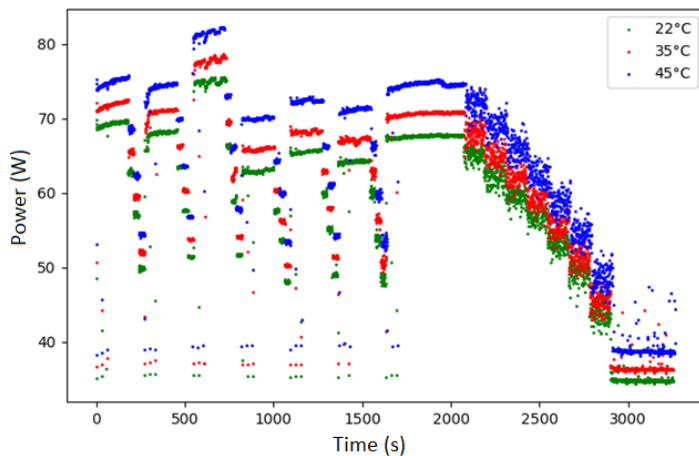


Figure 3. Server power under three different ambient temperatures.

Taking the data sets of worklet SSL as a use case. Function (1) describes a baseline model proposed by [1]. Data set is

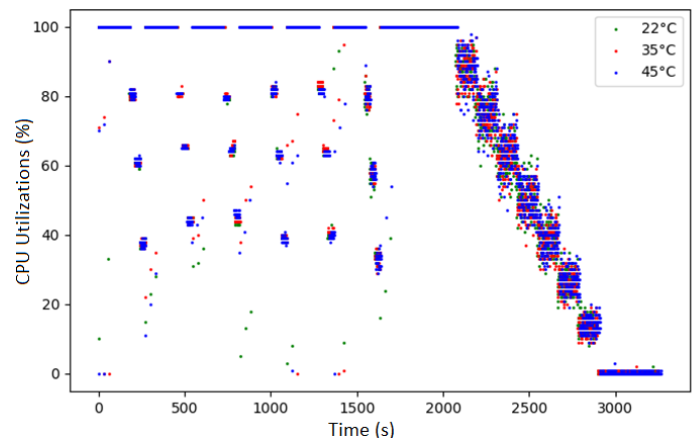


Figure 4. CPU utilization under different inlet temperatures.

collected at 22°C inlet temperature. Estimated power is simply represented by a linear function by using the power values at idle and full load. Beyond the baseline model, $\Delta(T)$ is derived by analyzing the relationship between inlet temperature and power increment for the whole data sets. $\Delta(T)$ can be interpreted by a quadratic equation as shown in function (2). Finally new power model is built by adding $\Delta(T)$ to the baseline model, as shown by (3).

$$P_{estimated} = P_{idle} + U_{cpu\%}(P_{100\%} - P_{idle}) \quad (1)$$

$$\Delta(T) = a_0 + a_1T + a_2T^2 \quad (2)$$

$$P_{estimated} = P_{idle} + U_{cpu\%}(P_{100\%} - P_{idle}) + \Delta(T) \quad (3)$$

Within the formulas, $U_{cpu\%}$ represents CPU utilization in percentage and T is inlet temperature. P_{idle} and $P_{100\%}$ are the average powers (Watt) when server running at idle ($U_{cpu\%} = 0$) and full load ($U_{cpu\%} = 100$). The models are trained and validated with the same data set by using cross validation from function `cross_val_score` from scikit-learn [23], cross validation (cv) generator is set to 4 to realize a 4-fold cross validation. The average MAPEs after CV for model (1) and (3) shown in Table II demonstrate the effectiveness of the updated model (3). The MAPE of baseline model (1) increases dramatically with the inlet temperature rises from 22°C to 45°C.

TABLE II. MAPE OF MODELS AT DIFFERENT INLET TEMPERATURE.

T_{Inlet} ($^{\circ}C$)	22	30	45
Model without Delta (T°)	5.6 %	9.2 %	16.8 %
Model with Delta (T°)	4.6 %	4 %	3.2 %

IV. INDUSTRIAL STANDARD SPECIFICATIONS EVALUATIONS: IPMI & REDFISH

IPMI and Redfish are usually available in modern high performance servers. They can be used to monitor system state information such as power consumption, inlet and exhaust temperatures through specific interfaces. IPMI represents for Intelligent Platform Management Interface, created by Intel, Dell, HP and NEC in 1998. It is a standardized hardware management interface and has been widely implemented on more 200 server vendors nowadays [24]. IPMI is designed to realize system-management independently without passing through OS. Administrators are allowed using IPMI to manage the machine locally or remotely regardless of its state (on or off). Monitoring system status is one of the functionality of IPMI. IPMI can communicate with Baseboard Management Controller (BMC) to retrieve data of certain hardware components (temperature probe, Fans, power supplies, etc.). BMC is a specialized micro controller embedded on the motherboard by the vendors. There are several open source tools supporting IPMI protocol, such as ipmitool, freeipmi, OpenIPMI, etc. Then, with the massive growth in size and complex of Data centers, traditional IPMI is not sufficient to manage the modern scalable data centers anymore. Hence, In 2010, Distributed Management Task Force (DMTF) proposed Redfish to overcome the limitations of IPMI in terms of scalability, performance, simplicity and interoperability [25]. In comparison with IPMI, Redfish is a standard API adopts HTTPS protocol, which is considered more secure than UDP protocol (adopted by IPMI). In addition, Redfish use human readable technologies like JSON and OData, which makes the operations such as request and response more user friendly. However, the work for Redfish hasn't finished and is still a Work in Progress on the website of DMTF [26].

A. IPMI or Redfish: Which is more accurate?

The difference between IPMI and Redfish makes us curious about their actual capabilities of power characterizations. Before implementing specific tool into energy-aware projects, it is better to well aware of the accuracy and limitations of the tool. Therefore, we design and conduct an experiment to evaluate accuracy of power consumption readings from IPMI and Redfish. Their readings are recorded and compared in real time with a high accuracy power analyzer. The experiment is conducted in a prototype modular server from Lenovo Skylake series. Both IPMI and RedFish interfaces are supported. The server equipped with two Xeon Gold 6142@2.6GHz processors, 390GB RAM and 500G SSD. Server is stressed with the same test suite SERT as mentioned in previous experiments, with a total execution time of about 2 hours. The power usage data from IPMI are retrieved by an open source API tool freeipmi [27]. And readings of Redfish are provided by Redfish REST API, through the integrated XClarity Controller introduced by Lenovo. High accuracy power analyzer Yokogawa WT330 is place between server

power supply unit and wall plug to measure and record power consumption data as reference (with maximum measurement error less than 1%). A docker container is developed to redirect and synchronize the readings from three channels to local database by using Network Time Protocol (NTP). Sampling frequency is set to 2 Hz.

We calculate MAPEs for both IPMI and Redfish within three power ranges. The results shown in Table III show that, sensors integrated in servers seem to have different precisions across different power ranges. Otherwise, power readings retrieved from Redfish have better results comparing to IPMI for each ranges. Power consumption has denser variations during lower ranges. After several experiments, we find that, the data collected from Redfish and IPMI is not refreshed instantly. A latency of about 200 ms is observed, which means the power value recorded may come from 200ms ago. The accuracy can be questioned when power varies quickly.

The work presented in this paper give references in choosing power consumption characterization solutions. We suggest that, before applying available economical solutions in an energy-aware scheduling or distribution task, check the precision of the solution and make sure that accuracy is enough for supporting the decision making.

TABLE III. MAPE OF REDFISH & IPMI BETWEEN DIFFERENT POWER RANGES.

Power Ranges (Watt)	Redfish MAPEs (%)	IPMI MAPEs (%)
From 0 to 199	4.1	5.5
From 200 to 399	4.0	4.4
From 400 to 600	1.8	2.3
From 0 to 600	2.9	3.7

V. CONCLUSION

In this paper, we present a deep evaluation about the power models based on CPU utilization. The influence of inlet temperature on models has been especially discussed. According to the analysis, one regression formula by using CPU utilization as the only indicator is not adequate for building reliable power models. First of all, Workloads have different behaviors by using CPU and other hardware resources in server platforms. Therefore, power is observed to have high dispersion for a fixed CPU utilization, especially at full workload (CPU utilization = 100%). At the same time, we also find that, power is well proportional to CPU utilization within the execution of one single workload. Hence, applying workload classifications could be an effective way to improve model accuracy. Moreover, inlet temperature can cause surprising influence on model accuracy. The model reliability can be questioned without including inlet temperature data. In a use case, after including inlet temperature data, we have greatly improved the precision of model outputs while stressing server under three different ambient temperatures. Using industrial specifications, such as IPMI and Redfish is another popular way to get power consumption data for some modern HPC servers. The experiment results show that, the precision of both IPMI and Redfish differs from different power ranges, the higher the better. We blame the loss of precision to the latency during request. Comparing to IPMI, Redfish is observed to have less latency in our experiments.

REFERENCES

- [1] X. Fan, W.-D. Weber, and L. A. Barroso, "Power provisioning for a warehouse-sized computer," in Proceedings of the 34th Annual International Symposium on Computer Architecture, ser. ISCA '07. New York, NY, USA: ACM, 2007, pp. 13–23. [Online]. Available: <http://doi.acm.org/10.1145/1250662.1250665>
- [2] D. Economou, S. Rivoire, C. Kozyrakis, and P. Ranganathan, "Full-system power analysis and modeling for server environments." In Workshop on Modeling Benchmarking and Simulation (MOBS), 2006.
- [3] A. Orgerie, L. Lefvre, and J. Gelas, "Demystifying energy consumption in grids and clouds," in International Conference on Green Computing, Aug 2010, pp. 335–342.
- [4] X. Zhang, J. Lu, X. Qin, and X. Zhao, "A high-level energy consumption model for heterogeneous data centers," Simulation Modelling Practice and Theory, vol. 39, 2013, pp. 41–55, s.I.Energy efficiency in grids and clouds.
- [5] G. Da Costa and H. Hlavacs, "Methodology of measurement for energy consumption of applications," in 2010 11th IEEE/ACM International Conference on Grid Computing, Oct 2010, pp. 290–297.
- [6] W. L. Bircher and L. K. John, "Complete system power estimation using processor performance events," IEEE Transactions on Computers, vol. 61, no. 4, April 2012, pp. 563–577.
- [7] M. Witkowski, A. Oleksiak, T. Piontek, and J. Wglarz, "Practical power consumption estimation for real life hpc applications," Future Generation Computer Systems, vol. 29, no. 1, 2013, pp. 208–217, including Special section: AIRCC-NetCoM 2009 and Special section: Clouds and Service-Oriented Architectures. [Online]. Available: <http://www.sciencedirect.com/science/article/pii/S0167739X12001392>
- [8] A. Lewis, S. Ghosh, and N.-F. Zeng, "Run-time energy consumption estimation based on workload in server systems," in Proceedings of the 2008 Conference on Power Aware Computing and Systems, ser. HotPower'08. Berkeley, CA, USA: USENIX Association, 2008, p. 4. [Online]. Available: <http://dl.acm.org/citation.cfm?id=1855610.1855614>
- [9] R. Basmadjian and H. de Meer, "Evaluating and modeling power consumption of multi-core processors," in Proceedings of the 3rd International Conference on Future Energy Systems: Where Energy, Computing and Communication Meet, ser. e-Energy '12. New York, NY, USA: ACM, 2012, pp. 1–10. [Online]. Available: <http://doi.acm.org/10.1145/2208828.2208840>
- [10] L. F. Cupertino, G. Da Costa, and J.-M. Pierson, "Towards a generic power estimator," Computer Science-Research and Development, vol. 30, no. 2, 2015, pp. 145–153.
- [11] S. Wang, H. Chen, and W. Shi, "Span: A software power analyzer for multicore computer systems," Sustainable Computing: Informatics and Systems, vol. 1, no. 1, 2011, pp. 23–34. [Online]. Available: <http://www.sciencedirect.com/science/article/pii/S221053791000003X>
- [12] J. Mair, Z. Huang, D. Eysers, and H. Zhang, "Pmc-based power modelling with workload classification on multicore systems," in 2014 43rd International Conference on Parallel Processing Workshops, Sep. 2014, pp. 129–138.
- [13] J. C. McCullough et al., "Evaluating the effectiveness of model-based power characterization," in Proceedings of the 2011 USENIX Conference on USENIX Annual Technical Conference, ser. USENIXATC'11. Berkeley, CA, USA: USENIX Association, 2011, p. 12. [Online]. Available: <http://dl.acm.org/citation.cfm?id=2002181.2002193>
- [14] J. von Kistowski et al., "Variations in cpu power consumption," in Proceedings of the 7th ACM/SPEC on International Conference on Performance Engineering, ser. ICPE '16. New York, NY, USA: ACM, 2016, pp. 147–158. [Online]. Available: <http://doi.acm.org/10.1145/2851553.2851567>
- [15] A. Marathe et al., "An empirical survey of performance and energy efficiency variation on intel processors," in Proceedings of the 5th International Workshop on Energy Efficient Supercomputing, ser. E2SC'17. New York, NY, USA: ACM, 2017, pp. 1–8. [Online]. Available: <http://doi.acm.org/10.1145/3149412.3149421>
- [16] B. Acun, P. Miller, and L. V. Kale, "Variation among processors under turbo boost in hpc systems," in Proceedings of the 2016 International Conference on Supercomputing, ser. ICS '16. New York, NY, USA: ACM, 2016, pp. 1–12. [Online]. Available: <http://doi.acm.org/10.1145/2925426.2926289>
- [17] D. Mohammed El Mehdi, G. Olivier, L. Laurant, and M. Jean Christophe, "Your cluster is not power homogeneous: Take care when designing green schedulers!" in 2013 International Green Computing Conference Proceedings, June 2013, pp. 1–10.
- [18] E. Humenay, D. Tarjan, and K. Skadron, "Impact of parameter variations on multi-core chips," Virginia Univ Charlottesville Dept of Computer Science, Tech. Rep., 2006.
- [19] Y. Wang, D. Nörtershäuser, S. Le Masson, and J.-M. Menaud, "Potential effects on server power metering and modeling," Wireless Networks, 2018, pp. 1–8.
- [20] K.-D. Lange and M. G. Tricker, "The design and development of the server efficiency rating tool (sert)," in Proceedings of the 2Nd ACM/SPEC International Conference on Performance Engineering, ser. ICPE '11. New York, NY, USA: ACM, 2011, pp. 145–150. [Online]. Available: <http://doi.acm.org/10.1145/1958746.1958769>
- [21] S. P. Committee. Server efficiency rating tool public design document (latest version). Retrieved: May 2, 2016. [Online]. Available: https://en.wikichip.org/wiki/technology_node (2013)
- [22] J. D. Hunter, "Matplotlib: A 2d graphics environment," Computing In Science & Engineering, vol. 9, no. 3, 2007, pp. 90–95.
- [23] F. Pedregosa, G. Varoquaux, A. Gramfort, V. Michel, B. Thirion, O. Grisel, M. Blondel, P. Prettenhofer, R. Weiss, V. Dubourg, J. Vanderplas, A. Passos, D. Cournapeau, M. Brucher, M. Perrot, and E. Duchesnay, "Scikit-learn: Machine learning in python," Journal of Machine Learning Research, vol. 12, 2011, pp. 2825–2830.
- [24] Intel. Intelligent platform management interface: Ipmi adopters list. Retrieved: Jan 22, 2019. [Online]. Available: <https://www.intel.com/content/www/us/en/servers/ipmi/ipmi-adopters-list.html>
- [25] "Validation of redfish: The scalable platform management standard," in Companion Proceedings of the 10th International Conference on Utility and Cloud Computing, ser. UCC '17 Companion. New York, NY, USA: ACM, 2017, pp. 113–117. [Online]. Available: <http://doi.acm.org/10.1145/3147234.3148136>
- [26] DMTF. Redfish api. Retrieved: Jan 22, 2019. [Online]. Available: <https://www.dmtf.org/standards/redfish>
- [27] F. C. Team. Freeipmi - home. Retrieved: Jan 22, 2019. [Online]. Available: <https://www.gnu.org/software/freeipmi/>

Where Should a Utility Improve Tree Cutting to Reduce the Risk of Vegetation Coming into Contact with Power Lines?

Vivian Sultan
 Claremont Graduate University
 Center For Information Systems & Technology
 Claremont, CA 91711
 Email: vivian.sultan@cgu.edu

Brian Hilton
 Claremont Graduate University
 Center For Information Systems & Technology
 Claremont, CA 91711
 Email: brian.hilton@cgu.edu

Abstract—Utility systems have come under attack from storms, trees, squirrels, fires, and firearms. 2018 was particularly bad for outages from wildfires in California. Fallen trees or tree limbs caused approximately 50% of the total minutes of service interruptions in 2017. In 2018, wildfires burned millions of acres. Regulators have struck back against utility companies, imposing tens of millions of dollars in fines related to wildfires. One issue is that the grid has many poles and wires that are vulnerable to falling trees and flying debris. To reduce the risk of wildfire and keep customers safe, electric utilities need to accelerate their vegetation-management work. The idea is to reduce vegetation below and near power lines that could act as fuel in a wildfire, as an added layer of protection, and to enhance defensible space. This study aimed to address the question, “Where should a utility improve tree cutting and trimming initiatives to foster operational excellence and reduce the risk of vegetation coming into contact with power lines?” To answer the research question, Insights for ArcGIS (a Geographic Information System) was used to build worksheets using a geographic information-systems-based application aimed at resolving current challenges faced by utilities to reduce the risk of power outages. A case study was developed to demonstrate the risk scenario that entails a utility company taking action and preparing for the unexpected. An artifact in Insights for ArcGIS was created using a design-science-research methodology. This research proposes an elegant, interesting, and novel solution to aid in vegetation management. The artifact demonstrates that GIS can play an integral role in the problem resolution.

Keywords—power failure; GIS model; Design-Science-Research; vegetation management.

I. INTRODUCTION AND PROBLEM DEFINITION

The placement of a new automated distribution switch has long-term impacts on the reliability of the circuit in which it is installed [1]. Common placement strategies rely on manual processes and the inherited knowledge of the planning engineer regarding the configuration, past reliability performance, future load growth, planned distributed energy resources, and other protection-related schemes of the circuit being analyzed in order to select a new switch location [2]. Without optimization algorithms to account for the many operating parameters and outage scenarios, the planning engineer may select a less than optimal location. According to Jim Horstman, a utility-industry consultant, a less than optimal placement may lead to less-than-optimal reliability performance and adversely affect customer satisfaction.

The objective of this study was to provide instantiation of a Geographic Information Systems (GIS) model and an analysis framework developed in previous research by the authors of this manuscript. To instantiate is to create a real instance or a particular realization of an abstraction or a process [3]. Therefore, the solution offered in this paper could lead us to a GIS-based application prototype that identifies optimal grid location(s) that need inspection or infrastructure work, as well as detect regions where new components such as distribution switches may provide net benefits to the grid, considering the many operating parameters and outage scenarios.

The Environmental Systems Research Institute [4] defined GIS as a class of tools for seizing, storing, analyzing, and demonstrating data in relation to their positions on the Earth’s surface. Analysts use GIS to view different objects’ locations and study their relationships. Satellite and tabular data can be entered into GIS for a single map display. GIS applications include recognizing site locations, mapping topographies, and developing analytical models to forecast events [4].

Though predictive modeling has existed since the inception of statistics, the penetration of GIS fostered a new approach to forecasting and data analytics. Predictive modeling is a process to determine a mathematical relationship between two or more variables [5]. Future dependent variables can derive if their relationships to independent variables become known. Predictive modeling with GIS has been applied in various sectors such as public health [6] and public-works asset management [7]. GIS is not limited to any specific field; it is only restricted by the availability of geospatial data.

GIS is a catalyst for improving multiple facets of smart grids. For instance, Resch et al. [8] integrated GIS-based modeling into the energy system to address renewable-energy-infrastructure planning. Sultan and Bitar [9] used GIS to optimize the locations of a distributed energy resource such as solar panels. Similarly, Sultan et al. [10] investigated power-grid reliability incidents/power outages and their correlation with infrastructure age by using GIS-based modeling. Therefore, GIS enhances research inquiries in the smart-grid domain. Based on our previous research [9]-[10] we posit GIS can highlight the optimal locations for different components of the electric-power network including the new automated distribution switches. For this

research study, we designed an artifact: a GIS-based solution that resolves current challenges faced by utilities to improve tree cutting and foster operational excellence. Section II presents the study design and methodology. Section III illustrates the design principle. Section IV describes deployment. In Section V, we discuss research evaluation. In Section VI, we offer conclusions.

II. STUDY DESIGN AND METHODOLOGY

The artifact/solution uses a Design-Science-Research (DSR) methodology. Walls, Widmeyer, and El Sawy [11] conceived DSR and laid the foundations and arguments for DSR in behavior-centric information-systems research. March and Smith [12] elucidated DSR further by separating natural science from design science. A decade later, DSR was integrated into the fabric of information-systems research through several seminal publications [3][13]–[16].

Every DSR needs a design principle as guidance. Hence, for this study, we used the principle outlined in Peffers et al. [16]. The principle, collectively called DSR, was also used as a basis for another study [13]. Figure 1 depicts the DSR method.

III. DESIGN PRINCIPLE

The DSR method contains six activities. These activities interact sequentially. In addition, iteration through one or more activities is likely. The DSR method includes four possible entry points that indicate how a DSR project would start.

A. Possible Entry Points

Even though Peffers et al. [16] did not elucidate the four entry points—(1) problem-centered initiation, (2) objective-centered solution initiation, (3) design and development center initiation, and (4) client/context initiation—they did provide four case studies to demonstrate

how each entry point works. Conceptually, researchers could start their research endeavors using any of the entry points, as long as the researchers defined all activities in the design science research method in their entirety.

This research entry point is classified as an objective-centered solution initiation. As noted above, our objective in this research was to reduce the risk of power outages by advancing tree cutting and trimming initiatives. Due to the rapidly changing nature of energy generation, new developments in the electric-power network, the incorporation of distributed energy resources into the grid, and circuit and equipment overloads, grid reliability research has been unable to keep pace. Power outages can be especially tragic in life-support systems in hospitals and nursing homes or systems in synchronization facilities such as airports, train stations, and traffic control. The economic cost of power interruptions to U.S. electricity consumers was \$79 billion annually in damages and lost economic activity [17]. These facts highlight the need to investigate grid reliability, which is the objective of this research and the entry point to initiating an objective-centered solution.

B. Process Guiding Design

In conjunction with the design principle elucidated in the previous section, the research entailed using the process steps in Takeda, Veerkamp, and Yoshikawa’s [18] design cycle to create an artifact/solution. This cycle has five simple steps: awareness of the problem, suggestion, development, evaluation, and conclusion. The Takeda et al. design cycle demonstrates how DSR was embraced as a research paradigm for information-systems research projects [13]. We used the three DSR cycles of relevance, design, and rigor [14] to perform each of the Takeda et al. process steps leading to the final prototype in this paper.

This study aimed to address the following question: “Where should a utility improve tree cutting and trimming-related initiatives to foster operational excellence and reduce

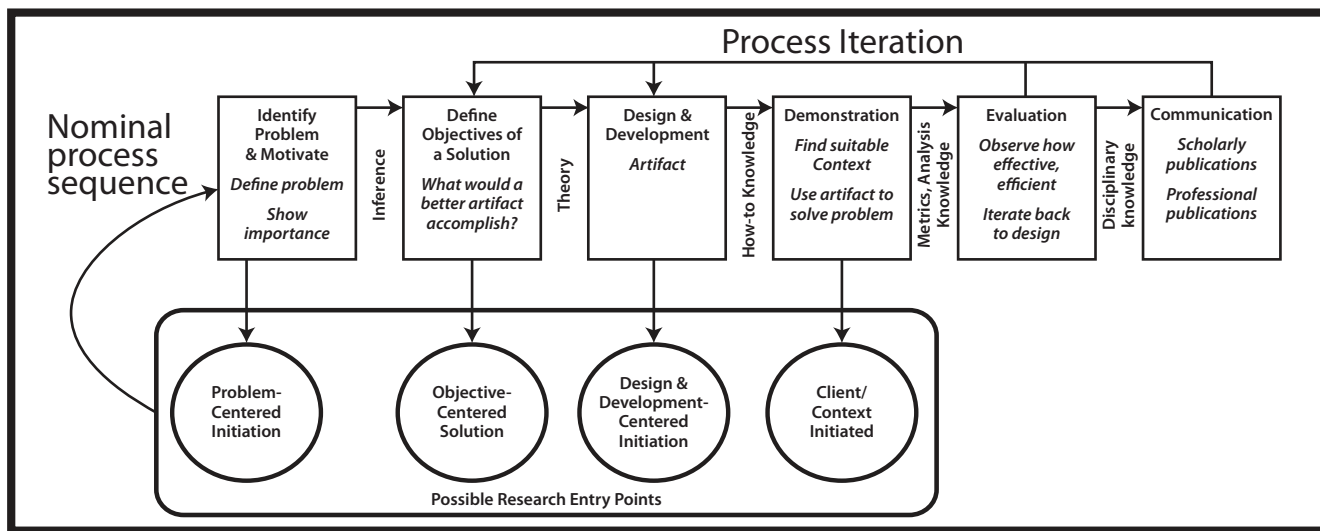


Figure 1. Design science research method [16].

the risk of vegetation coming into contact with power lines?” To answer the research question, we propose a GIS-based application that would be an elegant, interesting, and novel solution to aid in vegetation management. This study illustrates how utilities can address current challenges to improve grid reliability. The artifact demonstrates that GIS can play an integral role in the problem resolution.

We used a scenario-based methodology to evaluate the proposed solution. We extracted case episodes of actual site use by users (described as scenarios) to define the objectives of the target application. The key strength of the scenario-based methodology is its ability to support investigation of phenomena such as power failures that are hard to research by more conventional means. Sugimura and Ishigaki [19] highlighted its potential, for example, to break down an extracted scenario into steps of actions and answer questions about the actions given as check items. To complete the evaluation, we elicited opinions from industry experts regarding the viability of the model. Getting expert feedback is helpful at this phase to see if the instantiation demonstrated the overall usefulness of the intervention.

IV. DEPLOYMENT

One of the newest technologies is Insights for ArcGIS, which is part of the new ArcGIS Enterprise family from the Environmental Systems Research Institute. Insights for ArcGIS can open doors for utilities to expand the use of asset-management data, for example, to support business-related decisions. Insights for ArcGIS has transformed how researchers traditionally performed spatial analysis [20]. It is a web-based, data-analytics application with the

capability to work with interactive maps and charts at the same time.

In this research, we developed a case study to demonstrate the risk scenario/challenge that entails a utility company taking action and preparing for the unexpected.

A. Utilities Case Study/Vegetation Scenario

Utility systems have come under attack from storms, trees, squirrels, fires and firearms and 2018 was particularly bad for outages from wildfires in California. Regulators imposed tens of millions of dollars in fines against utility companies associated with wildfires, including \$37 million for the 2007 Malibu fire; \$14.4 million for the Witch, Rice and Guejito fires in the same year; and \$8.3 million for the 2015 Butte Fire [21]. Many poles and wires in the grid are vulnerable to falling trees and flying debris.

Half of the total minutes of service interruptions in 2017 accrued from fallen trees or tree limbs [22, p. 14]. According to the National Interagency Fire Center, in 2018 more than 48,347 wildfires burned more than 7.3 million acres, as of late September [23]. Figure 2 shows some overall data on the total number of outages caused by weather/falling trees [24].

To reduce the risk of wildfire and keep customers safe, electric utilities need to accelerate their vegetation-management work. Utilities are already working to meet new state vegetation and fire-safety standards. In California, for instance, the new standards require a minimum clearance of 4 feet around power lines in high fire-threat areas with clearances of 12 feet or more at the time of trim to ensure compliance year round [25]. However, accelerated wildfire

2017 (1,159 total outages)	2016 (1,279 total outages)	2015 (1,069 total outages)	2014 (1,081 total outages)
1. California (124)	1. California (116)	1. California (96)	1. California (81)
2. Texas (65)	2. Texas (72)	2. Texas (72)	2. Texas (57)
3. New York (64)	3. Michigan (72)	3. Michigan (43)	3. Pennsylvania (52)
4. Michigan (56)	4. North Carolina (67)	4. Ohio (42)	4. Michigan (49)
5. Pennsylvania (47)	3. Ohio (67)	5. North Carolina (41)	5. Ohio (47)
6. Ohio (42)	5. New York (60)	6. Washington (35)	6. New York (44)
7. Massachusetts (38)	6. Pennsylvania (48)	7. New York (35)	7. North Carolina (41)
8. North Carolina (35)	7. Florida (46)	8. Pennsylvania (34)	8. Georgia (35)
9. Colorado (32)	8. Massachusetts (41)	9. Oklahoma (33)	9. Virginia (32)
9. Virginia (32)	9. Virginia (38)	10. Connecticut (33)	9. Wisconsin (32)

Figure 2. Eaton’s Blackout Tracker [24].

vegetation-management work is still needed to address overhanging branches or limbs. The idea is to reduce vegetation below and near power lines that could act as fuel in a wildfire, as an added layer of protection and to enhance defensible space. Thus, the challenge for an electric utility in this case is, “Where should a utility improve tree cutting and trimming-related initiatives to foster operational excellence and reduce the risk of vegetation coming into contact with power lines?”

B. Insights for ArcGIS Solution

We created an artifact in Insights for ArcGIS using DSR methodology. Insights for ArcGIS workbooks were developed to explore and discover trends and details in a utility company’s data. The workbooks are templates that can be imported from a utility company’s analytics models built in Insights for ArcGIS. Having the data in Insights for ArcGIS provides powerful analysis that can be shared.

In this research, we propose an elegant, interesting, and novel solution to aid in vegetation management, identifying optimal grid location(s) that need inspection or infrastructure work, and detecting regions where new components, such as distribution switches, may provide net benefits, considering the many operating parameters and outage scenarios. Because Insights is so easy to use, everyone at the electric utility, from personnel in the field to the chairman of the board, can take advantage of its capabilities. The following section describes one Insights

worksheet we developed to demonstrate how the proposed solution might address the risk scenario/challenge examined in the previous section.

V. SOLUTION: ARCGIS INSIGHTS VEGETATION SCENARIO INVESTIGATION WORKSHEET

We selected the ArcGIS Insights tool to identify critical locations where a utility company needs to prune trees as an added layer of protection and to enhance defensible space. All relevant data were imported from the supervisory control and data acquisition/Outage-Management System/distribution-management system at a power utility into Insights for ArcGIS.

Page 1: Developed to investigate trees-related outages and the reported right-of-way events shown in Figure 3. This page allows utility personnel to answer the following questions.

1. What is the reported right-of-way event category contributing to the largest count of outage events?
2. What is the reported right-of-way event category contributing to the longest duration of outages?
3. What is the reported tree-related cause contributing to the largest count of customers’ calls?

Page 2: Developed to investigate the relationship between tree-pruning time and outage events shown in Figure 4. This page allows utility personnel to answer the following questions.

1. How many expected pruning staff hours are needed to eliminate vines-caused power outages?

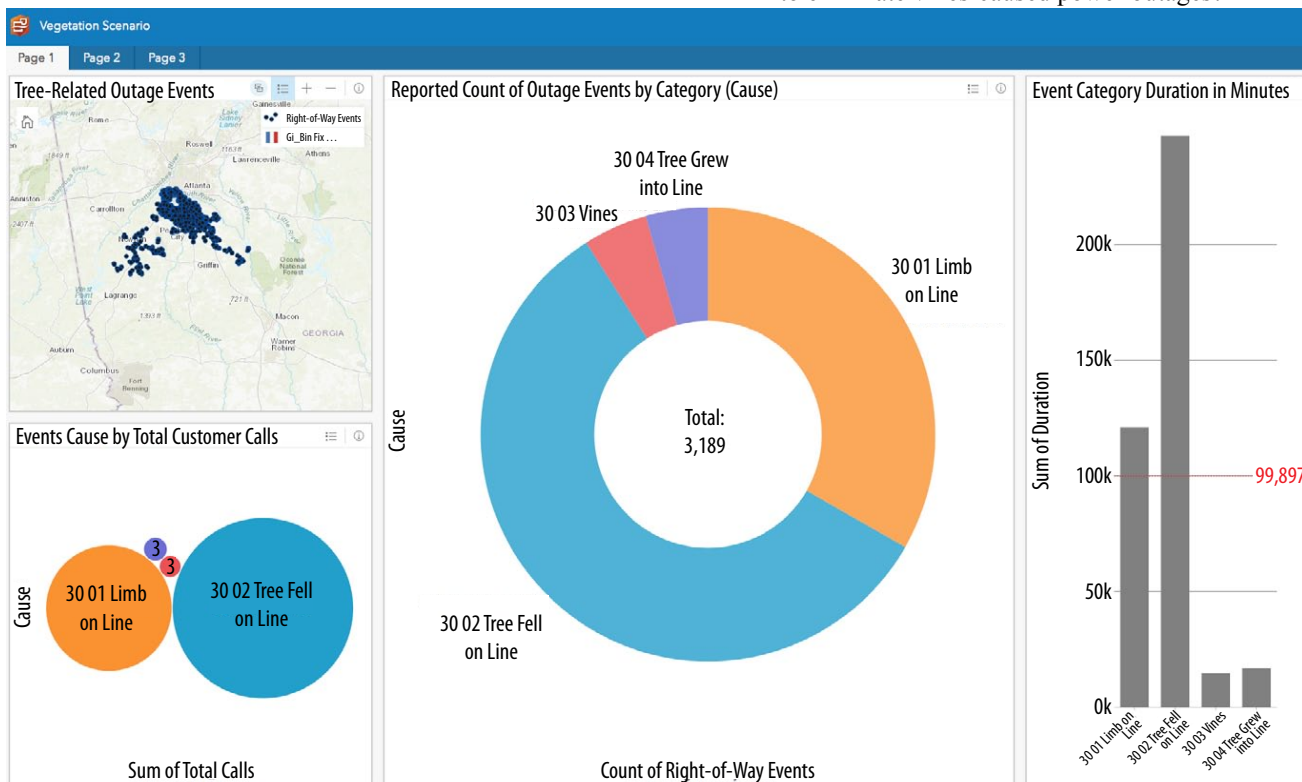


Figure 3. ArcGIS Insights Vegetation scenario investigation Worksheet Page 1

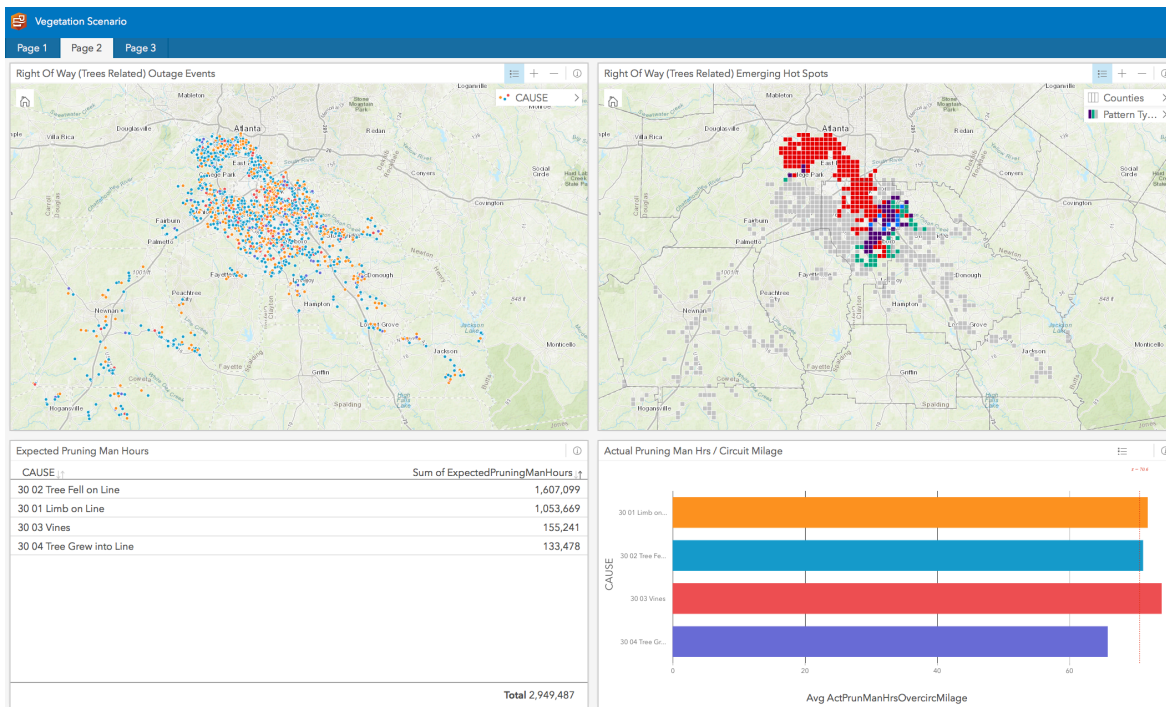


Figure 4. ArcGIS Insights Vegetation scenario investigation Worksheet Pages 2

2. How many pruning staff hours are needed to eliminate which category of right-of-way events?
3. Based on actual pruning staff hours, which category of right-of-way events needs the greatest number of pruning staff hours, on average, to be eliminated?
4. In which counties do you see the consecutive emerging power outage hot spots associated with trees?

Page 3: Developed to investigate tree-related outages optimized and emerging hot spots shown in Figure 5. This page allows utility personnel to answer the following questions.

1. In which counties do you mainly see tree-related outages optimized hot spots?
2. In which counties do you mainly see tree-related outages sporadic emerging hot spots?
3. How many sporadic emerging hot spots do you see?
4. What pattern type of emerging hot spots do you mainly see in the optimized hot spots locations of outages?
5. How many consecutive emerging power-outage hot spots are associated with trees?
6. If you were to send crews (a limited resource) to prune trees, does this map guide you with respect to where you need vegetation management most?

VI. EVALUATION

The proposed solution in this paper brings forth an important contribution to help practitioners identify the

optimal location(s) for the placement of smart-grid interventions while considering many operating parameters, outage scenarios, and potential benefits. The GIS model presented in this study can advance smart-grid reliability by, for example, elucidating the root cause of power failure, defining a solution for a blackout through data, or implementing the solution with continuous monitoring and management.

This study illustrated how Insights for ArcGIS, a GIS-based solution, can be used to perform quick analysis, produce illustrative maps and charts, and share that information with managerial staff on the utility side. Because Insights for ArcGIS is able to record workflows, utility personnel will be able to rerun analysis monthly, whenever inspection budgets become available or whenever a storm is expected to hit the service area.

According to utility industry consultant Horstman, the solution offered here provides useful insights. However, Horstman pointed out that it still needs work because the terms used to describe hot spots, for example, are statistician’s terms, not layperson’s terms. Horstman commented that utilities are becoming more “analytical” and beginning to understand the value of this research.

Doug Dorr, a research program manager at Electric Power Research Institute, confirmed the potential of this application offered by the prototype. According to the program manager,

“ArcGIS Insights worksheets are very easy to use and understand. Other layers like where the lines run and where the customers are located would be an additional useful integration consideration. Utilities would need to do some customization in order to make it truly

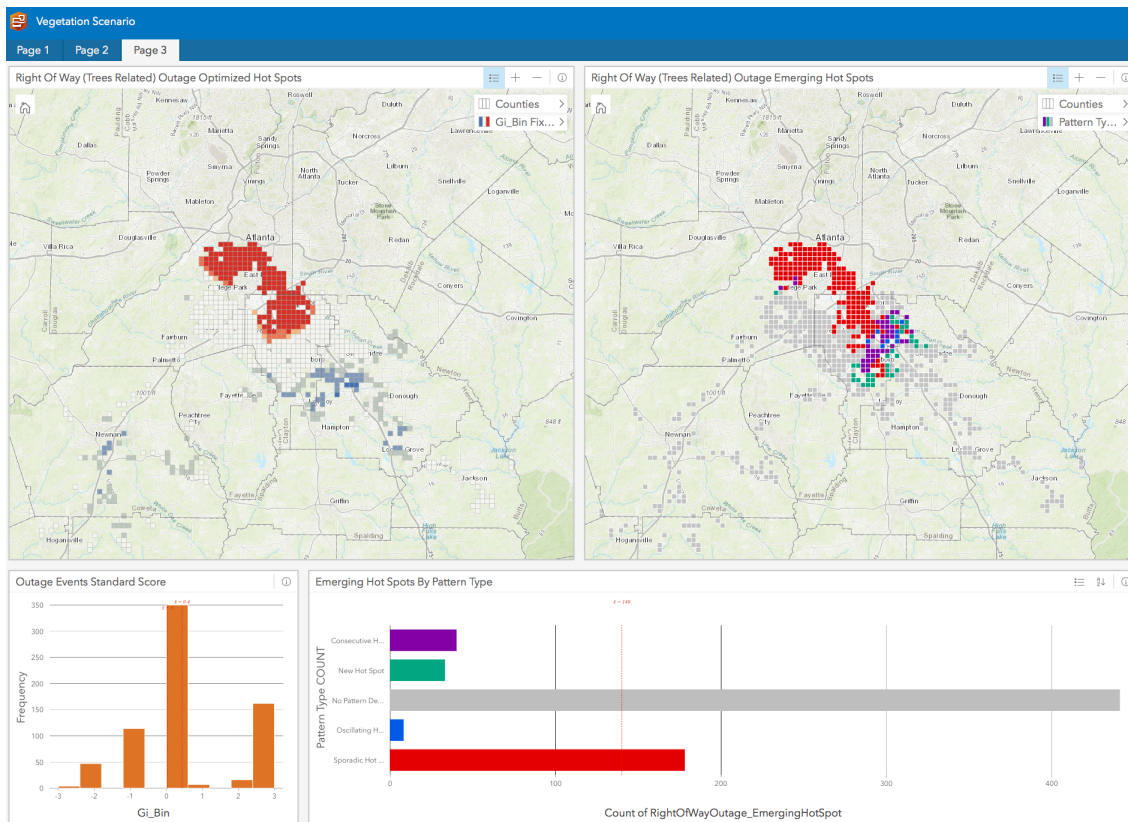


Figure 5. ArcGIS Insights storm scenario investigation Worksheet Page 3

actionable. Visual analytics and the ability to look at data over time is critically important. I really like the hot spots concepts.”

VII. CONCLUSION

This study aimed to answer the question, “Where should a utility improve tree cutting and trimming-related initiatives to foster operational excellence and reduce the risk of vegetation coming into contact with power lines?” To answer the research question, we used Insights for ArcGIS to build worksheets using a GIS-based application aimed at resolving current challenges faced by utilities to reduce the risk of power outages. We developed a case study to demonstrate the risk scenario that entails a utility company taking action and preparing for the unexpected. We created an artifact in Insights for ArcGIS using a DSR methodology. This research proposes an elegant, interesting, and novel solution to aid in vegetation management. The artifact demonstrates that GIS can play an integral role in problem resolution.

REFERENCES

[1] A. Abiri-Jahromi, M. Fotuhi-Firuzabad, M. Parvania, and M. Moseleh, “Optimized sectionalizing switch placement strategy in distribution systems,” *IEEE Trans Power Del*, vol. 27, no. 1, pp. 362–370, 2012.

[2] Electric Power Research Institute. “EPRI data analytics case: Optimal placement of automated distribution switches,” [retrieved: September, 2017] <http://smartgrid.epri.com/doc/DMD-Use-Cases/Optimal Placement of Automated Distribution Switches - Short Version.pdf> 2017

[3] A. Hevner, S. March, J. Park, S. Ram, “Design science in information systems research,” *Manag. Inf. Syst. Q.*, vol. 28, no. 1, pp. 75–105, 2004.

[4] ESRI Environmental Systems Research Institute. *Understanding GIS--The Arc/Info Method* [retrieved November, 2015] <http://www.ciesin.columbia.edu/docs/005-331/005-331.html>, 1992.

[5] D. Dickey, “Introduction to predictive modeling with examples” in *SAS Global Forum Proceedings* [retrieved October, 2015] <http://support.sas.com/resources/papers/proceedings12/337-2012.pdf>, 2012.

[6] A. Idowu, N. Okoronkwo, R. Adagunodo, “Spatial predictive model for malaria in Nigeria,” *J Health Informatics Dev. Ctries.* [retrieved October, 2015] <http://www.jhdc.org/index.php/jhdc/article/view/34>, 2009

[7] D. Totman, *Model Predictions: GIS Helps Public Works Manage Assets*, retrieved October 19, 2015, from <http://americancityandcounty.com/gis-amp-gps/model-predictions-gis-helps-public-works-manage-assets>, 2013.

[8] B. Resch et al. “GIS-based planning and modeling for renewable energy: Challenges and future research avenues,” *ISPRS Int. J. Geo-Inf.*, vol. 3, no. 2, pp. 662–692, 2014.

- [9] V. Sultan and H. Bitar, "Geographic decision support systems to optimize the placement of distributed energy resources," Proc. 22nd AMCIS, San Diego, CA, 2016.
- [10] V. Sultan, A. Alzahrani, H. Bitar, N. Alharbi, "Is California's aging infrastructure the principal contributor to the recent trend of power outage?" Proc. 22nd Annual Cal. GIS Conf., Anaheim, 2016.
- [11] J. G. Walls, G. R. Widmeyer, O. A. El Sawy, "Building an information system design theory for vigilant EIS," Inf. Syst. Res., vol. 3, no. 1, pp. 36–59, 1992.
- [12] S. T. March and G. F. Smith, "Design and natural science research on information technology," Decis. Support Syst., vol. 15, no. 4, pp. 251–266, 1995.
- [13] S. Gregor A. R. and Hevner, "Positioning and presenting design science research for maximum impact," Manag. Inf. Syst. Q, vol. 37, no. 2, pp. 337–356, 2013.
- [14] A. Hevner, "A three-cycle view of design science research," Scand. J. Inform. Syst., vol. 19, no. 2, pp. 87–92, 2007.
- [15] A. R. Hevner and S. Chatterjee, Design Science Research in Information Systems [retrieved September 2018] from http://link.springer.com/chapter/10.1007/978-1-4419-5653-8_2, 2010.
- [16] K. Peffers, T. Tuunanen, M. A. Rothenberger, S. Chatterjee, "A design science research methodology for information systems research," J. Manag. Inform. Syst., vol. 24, no. 3, pp. 45–77, 2007.
- [17] K. LaCommare and J. Eto, J. Understanding the Cost of Power Interruptions to U.S. Electricity Consumers, Berkeley, CA: Lawrence Berkeley National Laboratory, 2004.
- [18] H. Takeda, P. Veerkamp, H. Yoshikawa, "Modeling design process," AI Magazine, vol. 11, no. 4, pp. 37–48, 1990.
- [19] V. S. S. V. M. Sugimura and V. K. Ishigaki, "New web-usability evaluation method: Scenario-based walkthrough," FUJITSU Sci. Tech. J., vol. 41, no. 1, pp. 105–114, 2005.
- [20] ESRI Environmental Systems Research Institute, Insights for ArcGIS [retrieved September 2018] <http://doc.arcgis.com/en/insights/>, 2018.
- [21] California Public Utility Commission, Electric and Fire Related Fines [retrieved September 2018] from http://cpuc.ca.gov/uploadedFiles/CPUC_Public_Website/Content/Safety/Electric_and_Fire_Related_Fines.pdf, no date.
- [22] Pennsylvania Public Utility Commission, Pennsylvania Electric Reliability Report 2017 [retrieved September 2018] http://www.puc.pa.gov/General/publications_reports/pdf/Electric_Service_Reliability2017.pdf, July 2018.
- [23] National Interagency Fire Center, Year-to-Date Statistics, [retrieved September, 2018] <https://www.nifc.gov/fireInfo/nfn.htm>, September 2018.
- [24] Eaton's Blackout Tracker, Power Outage Annual Report, [retrieved July, 2018] <https://switchon.eaton.com/blackout-tracker>, 2017.
- [25] State Board of Forestry and Fire Protection, 2018 Strategic Fire Plan for California [retrieved September 2018] <http://cdfdata.fire.ca.gov/pub/fireplan/fpupload/fpppdf1614.pdf>, August 2018.